Potential therapies and biomarkers for LAMA2-CMD

Potential therapies and biomarkers for LAMA2-CMD:

Does the microRNA hype deliver?

Bernardo Moreira Soares Oliveira

LUND
UNIVERSITY

DOCTORAL DISSERTATION
by due permission of the Faculty of Medicine, Lund University, Sweden.
To be defended at Segerfalk salen, BMC A1, Lund on 2018-09-01 at10:00.

Faculty opponent
Dr. Kanneboyina Nagaraju

Organization: LUND UNIVERSITY	Document name: Doctoral thesis
	Date of issue: 2018-08-10
Author(s): Bernardo Moreira Soares Oliveira	Sponsoring organization: CAPES/CNPq

Title and subtitle: Potential therapies and biomarkers for LAMA2-CMD: does the microRNA hype deliver?

Abstract

Laminin α2 chain-deficient muscular dystrophy, or LAMA2-CMD, is a very severe disease caused by mutations in the LAMA2 gene. Skeletal muscle is the most affected tissue, with patients presenting symptoms such as hypotonia at birth, joint contractures and progressive muscle wasting. Changes in the central nervous system include white matter abnormalities, delayed motor milestones and compromised action potential propagation. To date, there is no cure and most therapeutic interventions aim at alleviating secondary complications. In the last two decades microRNAs (miRNAs) have been explored as biomarkers or therapeutic targets in various diseases. In this thesis we have profiled miRNAs in quadriceps muscle of the dy3K/dy3K mouse model of LAMA2-CMD as an initial screening. We then investigated the effects of genetically removing a pro-fibrotic miRNA, i.e. miR-21, in two mouse models of LAMA2-CMD. We showed that the single deletion of this miRNA is not enough to reduce fibrosis and improve muscle phenotype or function in LAMA2-CMD mouse models. We further explored miRNAs as non-invasive biomarkers of disease progression. Urine miRNAs were profiled at 3 time points representing no symptoms, initial symptoms and severe disease (3, 4 and 6 weeks of age). We found distinct panels of differentially expressed miRNAs at these time points, suggesting that miRNAs can be used as biomarkers for LAMA2-CMD progression. Finally, we explored metabolism as a therapeutic target in a metformin intervention study. We found that metformin treatment improved grip strength in treated dy2J/dy2J mice, despite unaffected muscle weights. Energy efficiency was improved in treated dy2J/dy2J females, which resulted in improved weight gain. Central nucleation decreased in treated dy2J/dy2J mice, which suggests reduced muscle damage. We found a significant reduction of small fibres in dy2J/dy2J females with metformin. White adipose tissue weight increased in treated dy2J/dy2J mice; in contrast, brown adipose tissue weight was reduced in treated dy2J/dy2J males.

Key words: laminin alpha 2, muscular dystrophy, microRNA, fibrosis, metabolism, skeletal muscle

Classification system and/or index terms (if any)

Supplementary bibliographical information		Language: English
ISSN and key title 1652-8220		ISBN 978-91-7619-666-3
Recipient's notes	Number of pages	Price
	Security classification	

Signature Date 2018-07-30

Potential therapies and biomarkers for LAMA2-CMD:

Does the microRNA hype deliver?

Bernardo Moreira Soares Oliveira

LUND
UNIVERSITY

Coverphoto by Bernardo Moreira Soares Oliveira

Faculty of Medicine
Department of experimental medical science

ISBN 978-91-7619-666-3
ISSN 1652-8220

Printed in Sweden by Media-Tryck, Lund University
Lund 2018

To my kin and my friend Masa Ruotniemi (RIP)

Table of contents

Table of contents....8
Acknowledgements....10
List of figures....10
List of articles....11
Abstract....12
Abbreviations....13
Background....15
Skeletal muscle....15
Myogenesis....16
Structure....17
Extracellular matrix....19
Laminin....20
Muscular dystrophies....21
Laminin α2 chain-deficient muscular dystrophy....22
MicroRNAs....25
MiRNAs in myogenesis....26
MiRNAs in dystrophies....29
Methods....33
Histology....33
Polymerase chain reaction (PCR)....33
Next-generation sequencing (NGS)....34
Main research questions....36
Results....37
Article I....37
Article II....37
Article III....38
Article IV....39
Discussion....41

Conclusions.....45
References.....47

Acknowledgements

First and foremost, my kin, for the never-ending support and love. My wife, my partner in crime, there are no words that could thank you. We're finishing another chapter in our 'Book of Adventures' and will soon start another one. With you by my side the sky is the limit. Towards the stars!

Cibely, for introducing me to the group and opening the doors. Thanks for all the supervision and advice! All the best to you and Joan Paul!

All of the Durbeej group, present and past, for the support and patience. It's been a great journey! In special, my mentors Madde and Johan for all the opportunities and help. Tusen tack!

Vahid and Vignesh for keeping the mood lively! All the best in the future.

List of figures

All images used in this thesis are under a Creative Commons licence.

Figure 1A – skeletal muscle macro-structure.
https://cnx.org/contents/bfiqsxdB@3/Skeletal-Muscle

Figures 1B and 2 – laminin and interacting proteins.
http://jcb.rupress.org/content/201/4/499

Figure 3 – miRNA biogenesis.
https://commons.wikimedia.org/wiki/File:MiRNA-biogenesis.jpg

Figure 4 – Next-generation sequencing methods.

https://www.slideshare.net/ueb52/introduction-to-next-generation-sequencing-v2

List of articles

I – Oliveira BMS, Holmberg J and Durbeej M. Profiling skeletal muscle microRNAs and their targets in the *dy^{3K}/dy^{3K}* mouse model of laminin α2 chain-deficient muscular dystrophy (manuscript).

II – Oliveira BMS, Durbeej M and Holmberg J. Absence of microRNA-21 does not reduce muscular dystrophy in mouse models of LAMA2-CMD. PLoS ONE. 2017, 12(8), e0181950.

III – Oliveira BMS, Gawlik KI, Durbeej M and Holmberg J. Exploratory profiling of urine microRNAs in the *dy^{2J}/dy^{2J}* mouse model of LAMA2-CMD: relation to disease progression (submitted).

IV – Fontes-Oliveira CC, Oliveira BMS, Körner Z, Harandi VM and Durbeej M. Effects of metformin on congenital muscular dystrophy type 1A disease progression in mice: a gender impact study (submitted).

Abstract

Laminin α2 chain-deficient muscular dystrophy, or LAMA2-CMD, is a very severe disease caused by mutations in the ***LAMA2*** gene. Skeletal muscle is the most affected tissue, with patients presenting symptoms such as hypotonia at birth, joint contractures and progressive muscle wasting. Changes in the central nervous system include white matter abnormalities, delayed motor milestones and compromised action potential propagation. To date, there is no cure and most therapeutic interventions aim at alleviating secondary complications. In the last two decades microRNAs (miRNAs) have been explored as biomarkers or therapeutic targets in various diseases. In this thesis we have profiled miRNAs in quadriceps muscle of the dy^{3K}/dy^{3K} mouse model of LAMA2-CMD as an initial screening. We then investigated the effects of genetically removing a pro-fibrotic miRNA, i.e. miR-21, in two mouse models of LAMA2-CMD. We showed that the single deletion of this miRNA is not enough to reduce fibrosis and improve muscle phenotype or function in LAMA2-CMD mouse models. We further explored miRNAs as non-invasive biomarkers of disease progression. Urine miRNAs were profiled at 3 time points representing no symptoms, initial symptoms and severe disease (3, 4 and 6 weeks of age). We found distinct panels of differentially expressed miRNAs at these time points, suggesting that miRNAs can be used as biomarkers for LAMA2-CMD progression. Finally, we explored metabolism as a therapeutic target in a metformin intervention study. We found that metformin treatment improved grip strength in treated dy^{2J}/dy^{2J} mice, despite unaffected muscle weights. Energy efficiency was improved in treated dy^{2J}/dy^{2J} females, which resulted in improved weight gain. Central nucleation decreased in treated dy^{2J}/dy^{2J} mice, which suggests reduced muscle damage. We found a significant reduction of small fibres in dy^{2J}/dy^{2J} females with metformin. White adipose tissue weight increased in treated dy^{2J}/dy^{2J} mice; in contrast, brown adipose tissue weight was reduced in treated dy^{2J}/dy^{2J} males.

Abbreviations

BMD – Becker muscular dystrophy

CNS – central nervous system

COPD – Chronic obstructive pulmonary disease

DMD – Duchenne muscular dystrophy

ECM – extracellular matrix

IGF-1 – insulin-like growth factor 1

LAMA2-CMD – laminin α2 chain-deficient muscular dystrophy

LGMD – limb-girdle muscular dystrophy

miR – microRNA (the mature form)

miRNA – microRNA

MRF – muscle regulatory factor

NMJ – neuromuscular junction

SC – satellite cell

TGF-β – transforming growth factor β

Background

Skeletal muscle

Skeletal muscle comprises about 40% of our body weight under normal conditions. It allows us to perform daily activities such as walking and lifting, and it's also responsible for vital functions such as eating, breathing and blood pumping. Skeletal muscle is the main energy consumer in our bodies and therefore plays an important role in metabolic homoeostasis.

Skeletal muscle mass is determined by the balance between muscle breakdown, or catabolism, and muscle build up, or anabolism. These processes are influenced by numerous environmental and physiological cues such as diet, exercise, stress and hormones, for example. These signals can tilt the balance in one direction or the other, resulting in net muscle gain or loss.

Over 70 million people suffer from muscle wasting disease, in one form or another, and this costs the health care industry over $500 billion annually. Yet, there are currently no treatments. These numbers are likely to increase as the elderly proportion increases and age-related muscle wasting (i.e. sarcopenia) becomes more prevalent. Moreover, muscle atrophy isn't an exclusive feature of myodegenerative diseases; it is also a secondary complication of diseases such as cancer cachexia [1], diabetes [2] and COPD [3], for example.

Not only treatments are lacking but also effective ways to assess them. In practice most clinicians resort to muscle biopsies to monitor disease progression, which is invasive, especially for children. They also measure creatine kinase (CK) concentration in blood, a muscle enzyme that leaks into circulation upon muscle damage; it is an indirect measure of muscle breakdown. Unfortunately, CK levels vary with factors such as sex, age, diet and stress, making it an unreliable marker [4]. There is thus a great need for better biomarkers for myopathies.

Myogenesis

The term myogenesis refers to skeletal muscle formation, especially during embryonic development. It is a complex process that depends on timely expression/repression of several genes. Generally speaking, the process involves a) the commitment of pluripotent cells to the myogenic lineage, b) proliferation of these cells followed by differentiation into myotubes and c) fusion of myotubes into myofibres [5; 6].

During the embryonic phase the cells that will give rise to skeletal muscle come from the (paraxial) mesoderm. These cells will form somites, which are parallel bundles of cells that run along the neural tube. The somites start subdividing into sclerotome (which will generate cartilage) and dermomyotome. The latter will be further divided into dermatome (skin) and myotome (muscle). The commitment of myotome cells to become myoblasts is regulated by transcription factors such as myogenic factor 5 (Myf5), myogenin and muscle regulatory factor 4 (MRF4), the main one being myogenic determination protein 1 (MyoD). These factors will initiate the myogenic programme in cells [5; 6].

Myoblasts will proliferate under the influence of MyoD and Myf5. When a sufficient number of cells is reached the myoblasts will exit the cell cycle and start to fuse into myotubes. Myotube formation occurs in two waves: the primary wave consists of embryonic myoblasts that will fuse to form mainly slow-contracting type I fibres; the second wave will have foetal myoblasts fuse to form (mostly) fast-contracting type II fibres. After birth, the number of skeletal muscle fibres is largely set. Therefore, adult skeletal muscle cannot increase fibre number (hyperplasia) but only regulate their size (hypertrophy or atrophy) [5; 6].

Regeneration

In post-natal muscle, especially adult muscle, the process of regeneration resembles that of (embryonic) myogenesis. Post-natal muscle retains stem-like cells that can differentiate into myotubes to aid muscle regeneration. These are called satellite cells (SCs) due to their peripheral position: they are located between the sarcolemma and the basement membrane, normally in a quiescent state. They proliferate in response to muscle damage and migrate to the injury site to fuse into myotubes, providing additional nuclei for transcriptional power [5; 6] .

Structure

Macroscopically, skeletal muscle is formed by fibre bundles surrounded by connective tissue. The latter will have different names depending on location: epimysium surrounds the whole muscle, perimysium covers fibre bundles and endomysium individual muscle fibres (figure 1A). Muscle fibres are the cellular unit of skeletal muscle. They're composed of myofibrils, which are contractile filaments made up mainly of actin and myosin. Other important myofibrillar proteins include titin and nebulin. Myofibrils are in fact a series of sarcomeres, the contractile unit of skeletal muscle. It is the cumulative shortening of sarcomeres that makes muscles contract [7; 8].

The sarcomere is divided into regions according to its interaction with polarised light (figure 1B). The boundaries of the sarcomeres can be seen under the microscope as narrow dense lines, the Z lines (from the German *zwischen*, between). A dense dark band can be observed in the middle of the sarcomere; it's the A band (from anisotropic). Its colour comes from a higher density of thick filaments such as myosin. The area between the A band in one sarcomere and the A band in the adjacent one is called I band (from isotropic). At the very centre of the A band is the M line (from the German *Mittelscheibe*, middle disk). The lighter region in the middle of A bands is the H zone (from the German *heller*, lighter), where thin and thick filaments do not overlap. The width of this region varies with muscle contraction [8] .

In order to contract skeletal muscle needs input from the central nervous system (CNS). Under voluntary contractions this command is generated in the motor cortex and transmitted down the spinal cord. In the anterior horn of the spinal cord the impulse is transmitted to a motor neuron and then passed to muscle cells. Each motor neuron, along with the fibres it innervates, is called a motor unit. The axon terminal and the sarcolemma region adjacent to it constitute the neuromuscular junction (NMJ). This is a specialised interface between neuron and muscle where the action potential is passed from the neuron to the muscle cell [8].

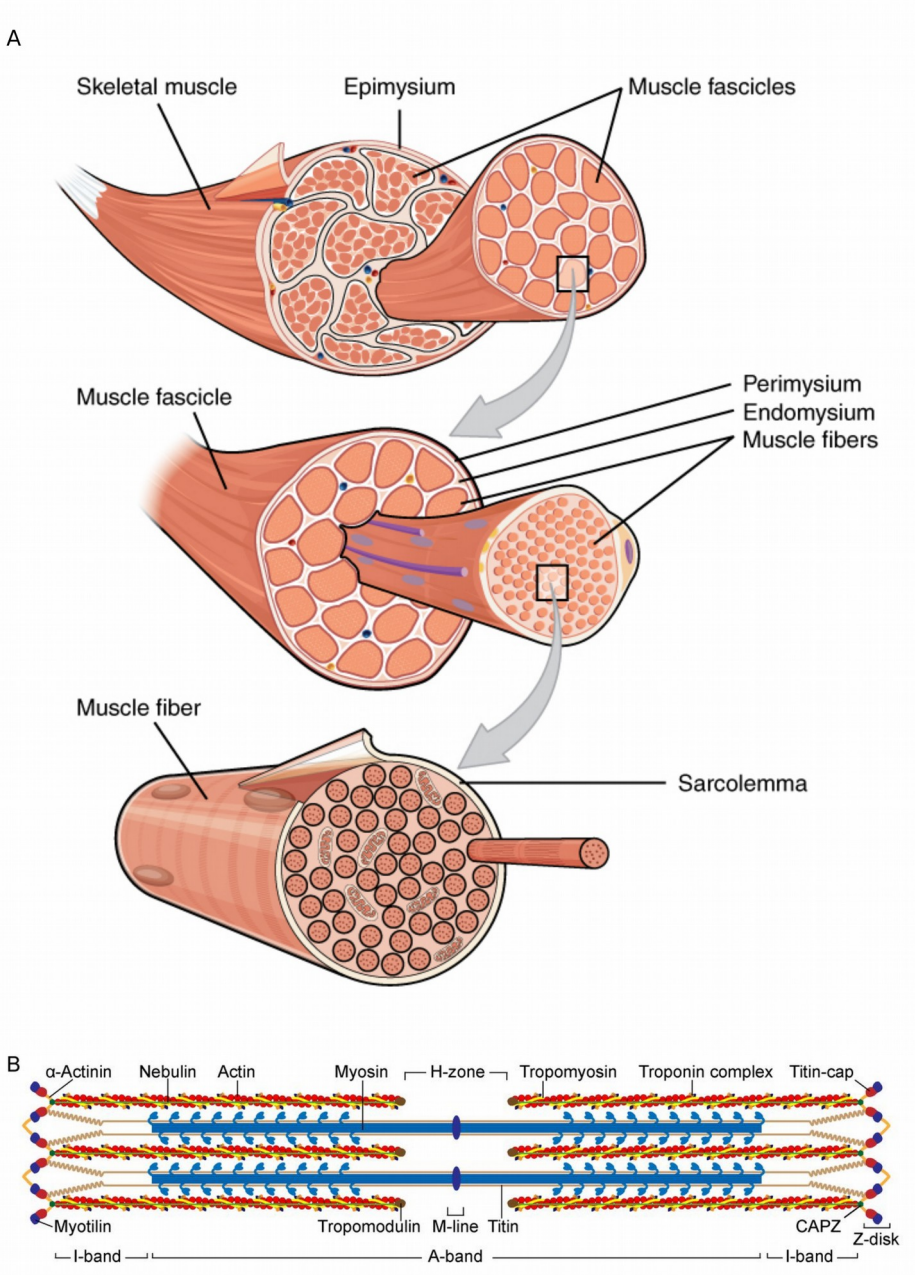

Figure 1.
Skeletal muscle hierarchical structure. A: macro-structure of muscle fibres and surrounding connective tissue. B: structure of the sarcomere, the contractile unit of skeletal muscle.

Extracellular matrix

The extracellular matrix (ECM) is a mesh-like network, composed mainly of polysaccharides and proteins, that provides structural and biochemical support to cells. It provides a scaffold to which cells can adhere and mature, as well as receptors and cytokines to modulate cellular activity. The ECM may store growth factors and cytokines in latent form, as well as proteases to process these into bioactive molecules, a prominent example being TGF-β [9] .

Polysaccharides constitute the ECM foundation where proteins will be inserted. They form coarse structures due to their stiffness and hydrophilicity. Their net negative charge attracts sodium ions that in turn attract water, keeping the cells and tissues hydrated. The main ECM polysaccharide is glycosaminoglycan (GAG) [7].

The most abundant ECM protein is collagen. In skeletal muscle it accounts for one to two percent of the tissue. It is synthesised and exported by fibroblasts as pro-collagen, and subsequently cleaved by ECM proteases. Collagen is composed of 3 tightly packed α chains in a helical structure. So far more than 20 α chains have been discovered, which in turn form approximately 20 collagen types [7; 9].

Basement membrane

The basement membrane (BM) is a specialised region of the ECM: it is a thin sheet that covers cells and separate them from, but also anchor to, the rest of the ECM. The BM is divided into (interior) basal lamina and (exterior) reticular lamina; the former is rich in non-fibrillar collagen, non-collagenous glycoproteins and proteoglycans, whilst the latter contains fibrillar collagen and proteoglycans [10]. The major components of BMs are collagen IV, laminins, heparan sulfate, fibronectin, nidogen and agrin [9; 11; 12] .

The BM has critical roles in mediating cell stability and integrity. Its structural role was described first and is thus better studied. The BM provides much of a muscle’s tensile strength and therefore prevents contraction-induced damage. Furthermore, even in the event of muscle damage the BM serves as a scaffold to support and direct SCs and promote proper muscle architecture [10]. The BM also covers other structures and tissues that

directly interact with skeletal muscle, such as myotendinous junctions and NMJs. For example, the basal lamina spans the cleft between muscle and nerve at the NMJ and keeps this critical structure in proper placement. At myotendinous junctions the basal lamina covers invaginations, increasing the surface area of muscle-tendon interaction and therefore aiding force transmission [7; 9].

Laminin

Laminins are heterotrimers formed by an α, a β and a γ subunit (or chain). Their names come from their composition: e.g. laminin-111 is composed of α1, β1 and γ1 chains. For the most part, their structure resembles a cross, with the β and γ chains protruding laterally and the α one upwards (figure 2). To date, over 15 laminin isoforms have been discovered.

Laminins are the major non-collagenous component of the basement membrane. In particular, laminin-211 is the most abundant isoform in skeletal muscle. Similarly to the ECM, laminins have structural (primary) and biochemical (secondary) roles. Much of the stiffness and tightness of the ECM is due to laminin polymerisation. Both N- (LN) and C-terminal (LG, globular) parts of the protein are crucial to its activity. The LN domain mediates self-assembly and polymerisation, whilst the LG domain binds to cell surface receptors such as integrin α7β1 and α-dystroglycan (figure 2). Thereby, laminins are linked to the intracellular cytoskeleton and transduce extracellular signals to the cytoplasm and hence modulate cellular activity. Laminins are involved in cell adhesion, migration and differentiation. The biological function of laminins is highly dependent on which receptor they interact with. Signalling through integrin α7β1 promotes cell growth and myofibre survival by activating the PI3K/Akt pathway. The lack of laminin α2 and the consequent reduction in Akt signalling stimulate processes involved in muscle atrophy such as apoptosis and the ubiquitin-proteasome system [11]. Less is known about laminin-211 signalling through α- and β-dystroglycan.

The laminin profile in muscle is time- and space-dependent. Some isoforms, such as laminin-111, are only expressed during embryonic stages. Others, are only expressed in specialised regions such as the NMJ (α4, α5 and β5) [9] .

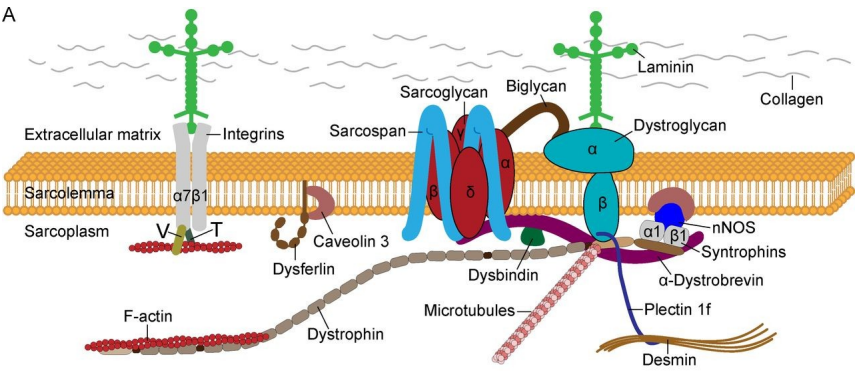

Fig 2.
Laminin and surrounding proteins. The main laminin-interacting proteins are integrins and dystroglycan.

Muscular dystrophies

Muscular dystrophies are a group of more than 50 genetic diseases that affect the neuromuscular system, resulting in progressive muscle loss. Other hallmark features include fibrosis and muscle inflammation. Many muscular dystrophies arise from mutations in genes encoding proteins of the dystrophin-glycoprotein complex (DGC). The DGC is a very large protein complex that sits on the muscle cell membrane (sarcolemma) and works to stabilise it and connect it to the ECM (figure 2). When this connection is faulty, muscle cells become prone to damage or detachment, which ultimately leads to muscle degeneration [13].

The most frequent type of the disease is Duchenne muscular dystrophy (DMD). It is an X-linked illness that affects mostly boys and causes loss of dystrophin, a protein involved in muscle membrane stability. Becker muscular dystrophy (BMD) is a milder variant of DMD due to lower levels of dystrophin or a truncated protein. Mutations in the laminin-interacting sarcoglycan complex lead to limb-girdle muscular dystrophies (LGMD) types 2C, 2D, 2E or 2F, depending on the particular isoform affected. LGMD is in

fact a group of very heterogeneous muscular dystrophies with the common feature that the proximal muscles of trunk and limbs are affected [13-15] .

Laminin α2 chain-deficient muscular dystrophy

Laminin α2 chain-deficient muscular dystrophy (LAMA2-CMD), also called merosin-deficient muscular dystrophy, or MDC1A, is a severe form of the disease caused by mutations in the *LAMA2* gene. Despite being a monogenic defect, the absence of laminin α2 chain leads to multiple complications at the tissue and cellular level. Its symptoms include substantial hypotonia at birth, muscle contractures, progressive muscle atrophy and fibrosis. The lack of laminin α2 chain affects not only skeletal muscle but also the central nervous system. Reported abnormalities include changes in white matter, defective myelination and slower action potential propagation. Thus, LAMA2-CMD, unlike most muscular dystrophies, affects the neuromuscular system as a whole [16].

The lack of proper attachment to the surrounding tissue makes muscle cells prone to contraction-induced detachment: upon muscle contraction the cells detach and undergo apoptosis (programmed cell death). Even cells that do not enter the apoptotic programme suffer detrimental consequences such as increased autophagy and proteasome activity [16-21].

Tissue inflammation and degeneration induce an immune response attracting mainly macrophages to the injury site. Initially, macrophages present a pro-inflammatory phenotype secreting cytokines such as IL-6. They transition into an anti-inflammatory phenotype as the tissue recovers.

Table 1
Most common LAMA2-CMD mouse models.

Mouse model	Mutation	Laminin α2 chain	Severity	Reference
dy/dy	Unknown spontaneous mutation	Reduced levels	Moderate	[22]
dy^{2J}/dy^{2J}	Spontaneous mutation in LN domain	Reduced levels of truncated protein	Mild	[23]
dy^{3K}/dy^{3K}	Knock-out	Complete deficiency	Very severe	[24]

dy^{W}/dy^{W}	Knock-out	Very low levels of truncated protein	Severe	[25]

It is also worth mentioning the *mdx* mouse model of DMD, since it's the most studied mouse model of muscular dystrophy. It has a spontaneous mutation in the dystrophin gene resulting in a premature stop codon on exon 23 [26].

Table 2
Some pre-clinical therapeutic trials for LAMA2-CMD.

Approach	Mouse model	Outcome	Reference
Over-expression of human laminin α2 chain	dy^{W}/dy^{W}	Improved grip strength, fibre CSA normalisation and reduced fibrosis.	[25]
Over-expression of laminin α1 chain	dy^{3K}/dy^{3K}	Improved histology, bodyweight, locomotion, grip strength and lifespan; normalised CK levels.	[27; 28]
Apoptosis suppression	dy^{W}/dy^{W}, dy^{2J}/dy^{2J}	Improved bodyweight, grip strength, CSA distribution and lower serum CK levels.	[17; 29; 30]
Proteasome inhibition	dy^{3K}/dy^{3K}	Moderate improvement in fibre CSA, decreased apoptosis and fibrosis.	[20; 31]
Fibrosis and inflammation suppression	dy^{W}/dy^{W}, dy^{2J}/dy^{2J}	Improved bodyweight, grip strength and locomotion.	[32-34]
Linker proteins	dy^{W}/dy^{W}	Reduced fibrosis, central nucleation and inflammation, improved fibre CSA, myelination and locomotion.	[35; 36]

Fibrosis

Fibrosis is one of the most prominent and deleterious symptoms of LAMA2-CMD (as well as other muscular dystrophies). The progressive replacement of skeletal muscle for fibrous tissue renders it weaker and stiffer.

Fibrosis is (mainly) the result of net increases in collagen synthesis. Repeated degeneration/regeneration cycles lead to inflammation and incomplete ECM remodelling. Increased inflammation and TGF-β signalling in turn lead to excessive synthesis of collagen by fibroblasts, which progressively replaces muscle tissue. The reduced muscular content will need higher activation to meet force demands, making it prone to contraction-induced damage or detachment. The muscular milieu is thus in a feed-forward cycle that promotes fibrosis. Increased TGF-β activity not only promotes fibroblast proliferation but also impairs muscle growth. Myostatin is a TGF-β family member that negatively regulates muscle growth. Its inhibition in *mdx* mice improved histopathology and fibrosis [37; 38]. TGF-β induces fibrosis through canonical, i.e. Smad-mediated, and non-canonical pathways, e.g. MAPK. Another fibrosis-driving mechanism is the TGF-β-related renin-angiotensin system (RAS). Angiotensin (Ang) II is produced from AngI by the angiotensin-converting enzyme (ACE) 1. AngII can activate Smad and MAPK signalling to stimulate fibrosis. The ACE2 enzyme, however, catalyses the conversion of AngI into Ang-1-7, which in turn binds Mas receptors and elicits beneficial responses such as reduced oxidative stress and fibrosis [39].

Different attempts at blocking fibrosis in muscular dystrophies have yielded varying results, *mdx* mice being more responsive than LAMA2-CMD mouse models. Inhibiting TGF-β-related signalling is a clear course of action that has improved the *mdx* phenotype [40] and also LGMD. Ang-1-7 treatment inhibited TGF-β activity and consequently decreased miR-21 levels, which in turn reduced the number of fibroblasts and ECM synthesis [40]. Similarly, blocking angiotensin II receptor type 1 (AT1) in the dy^{W}/dy^{W} mouse model of LAMA2-CMD reduced fibrosis and inflammation, and improved body weight and muscle function [34]. In a similar study, Elbaz et al. [33] found that losartan, an AT1 antagonist, was efficient in reducing fibrosis in dy^{2J}/dy^{2J} mice by repressing TGF-β signalling. Nevo et al. [32] found improved histopathology in dy^{2J}/dy^{2J} mice with fibrosis inhibition. In their study, halofuginone treatment reduced collagen I synthesis by reducing phospho-Smad3 in fibroblasts surrounding centrally nucleated fibres.

Metabolic alterations

A number of metabolic alterations have been described in various muscular dystrophies, including redox unbalance, mitochondrial dysfunction and amino-acid and ion metabolism. Our group has shown altered gene expression and mitochondrial function in LAMA2-CMD patient cells [21].

We have also previously found that a high percentage (~40%) of differentially abundant proteins in dy^{3K}/dy^{3K} muscle are related to metabolism [41; 42] Therefore, metabolic alterations could potentially be disease-driving mechanisms or therapeutic targets. In the present work we assessed if metformin, the most widely used anti-diabetes drug, could improve muscle histology and function in the dy^{2J}/dy^{2J} mouse model of LAMA2-CMD.

MicroRNAs

MicroRNAs (miRNAs) are a class of small non-coding RNAs that have a regulatory role on mRNA translation. They work by base-complementarity to induce mRNA degradation or translation repression; i.e. they are post-transcriptional repressors [43].

MiRNAs are first transcribed in the nucleus as primary miRNAs (pri-miRNA), a multiple stem (or hairpin) loop structure that is hundreds of nucleotides in length. Already in the nucleus these are cleaved into precursor miRNAs (pre-miRNAs) with a single stem loop by a complex whose main components are Drosha and DGCR8. Pre-miRNAs are exported to the cytoplasm by exportin 5, where they're cleaved by DICER, yielding a double-stranded RNA. One of the strands will be incorporated into the RNA-induced silencing complex (RISC) to exert its biological function; this is the mature miRNA. The miRNA serves as a guiding template that drives RISC towards target mRNAs (figure 3). Nucleotides 2-8 on the 5'-end on a mature miRNA are called the seed. This region is the main factor in miRNA target recognition and specificity [43; 44].

Despite their non-coding nature, miRNAs can be located anywhere on the genome. Many miRNAs are within protein-coding regions, usually on introns, and are thus transcribed along with the host gene. MiRNAs located on exons or introns may bypass processing by Drosha/DGCR8 and instead use the spliceosome for cleavage (figure 3). Alternatively, miRNAs are located between genes (intergenic miRNAs) and are regulated by their own promoters. Some miRNAs form clusters (polycistronic miRNAs) and are transcribed together; these include the most prominent skeletal muscle miRNAs, i.e. miR-1, miR-133, miR-206 [43].

Interestingly, miRNAs are also found in extracellular spaces. It's not well-understood how the export process works nor what's the purpose of it. One

clear possibility is that miRNAs are involved in cell-to-cell communication. In support of this, there isn't a direct correlation between the miRNA profiles of different fractions, i.e. intra- and extra-cellular, vesicular [45-47]. For example, some miRNAs are only found in secreted vesicles [48]. Their presence in extracellular space also opens up the possibility of their use as biomarkers. Given the short half-life of RNA, extracellular miRNAs are bound to protein complexes (e.g. HDL or Argonaute) or encapsulated in vesicles of various sizes (e.g. exosomes) for increased stability.

Initial interest in miRNA research was due to their involvement in disease, particularly cancer. Later, they were found to be dysregulated in various diseases, including muscular dystrophies. MiRNAs are ubiquitous regulators of a multitude of cellular processes, making them interesting therapeutic targets.

MiRNAs in myogenesis

Striated muscle has some miRNAs which are semi-specific to it or enriched in the tissue: these are called myomiRs. They are miR-1, miR-133a/b and miR-206, the classical myomiRs, as well as the newcomers miR-208a/b, miR-486 and miR-499. MiRNAs that have a larger than 20-fold expression in skeletal muscle compared to other tissues are termed muscle-specific, whereas lower than 20-fold expression is considered muscle-enriched [43; 49; 50].

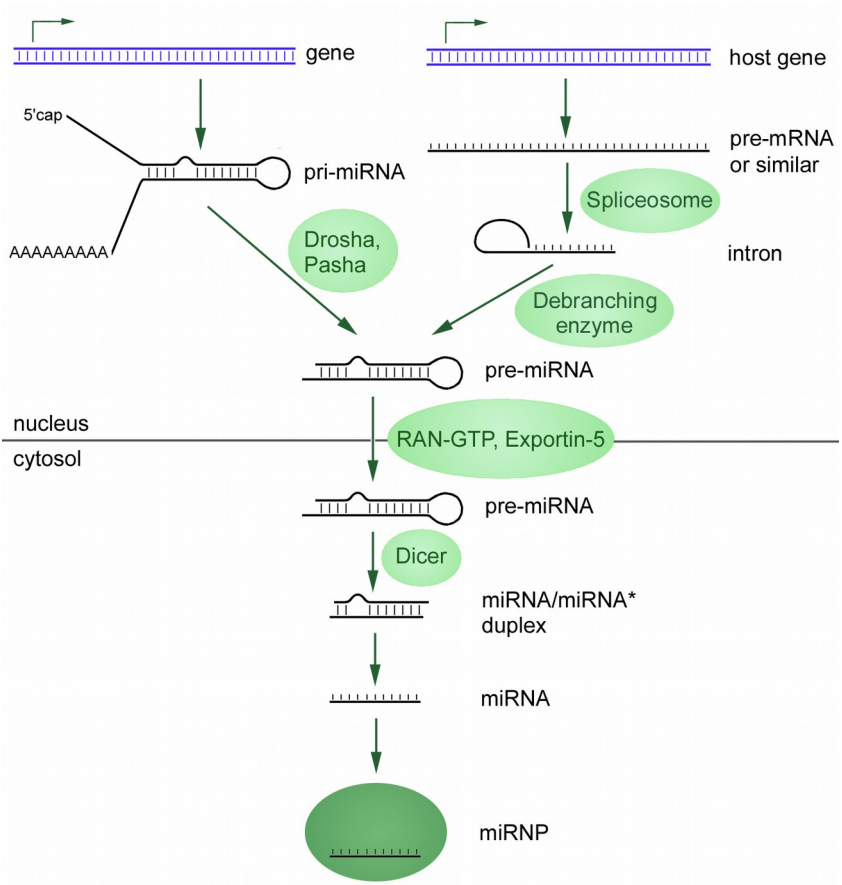

Figure 3.
MiRNA biogenesis. The upper-right branch depicts the alternative route when miRNAs have a host-gene.

MiRNAs influence processes important for myogenesis, i.e. proliferation, differentiation, fusion and migration. MyomiRs, amongst others, help fine-tune and orchestrate myogenesis [49; 51]. They are part of signalling pathways involved in cell survival and growth such as e.g. IGF-1/PI3K/Akt/mTOR, TGF-β and myostatin/FOXO [43; 51-53].

MiR-1, miR-206 and miR-133 are involved in perhaps the most fundamental aspect of myogenesis, i.e. they promote the adoption of myogenic cell lineages during embryogenesis by targeting genes that promote non-muscle cell paths. The expression of these miRNAs is under regulation of MRFs [50]
.

MiR-1 and miR-206 are largely involved in myoblast differentiation. These miRNAs differ in sequence by only four nucleotides in the 3' region, which translates into a great overlap in target-genes. They target Pax3 and Pax7 in progenitor cells to inhibit proliferation and stimulate differentiation [50]. MiR-1 and miR-206 affect myoblast differentiation by targeting HDAC4, a known repressor of muscle genes [50; 54; 55] . MiR-206 accomplishes this by inhibiting SMAD3 induction by TGF-β. They also target cell-cycle regulators such as cyclins and chromatin-remodelling factors. By doing so the miRNAs force cell cycle exit and thus halt proliferation.

The next myomiR, miR-133, is related to the previous two as they form bicistronic clusters: miR-1/miR-133a and miR-206/miR-133b [43; 50]. This means that their expression is related by some common regulatory elements. The role of miR-133 in myogenesis is more controversial, with evidence for the stimulation of both proliferation and differentiation. This suggests that the function of miR-133 may be context-dependent. MiR-133 stimulates proliferation by targeting serum response factor (SRF), an inducer of miR-1 and miR-206. Therefore, by targeting SRF miR-133 represses miR-1 and miR-206 and their anti-proliferative effects. On the other hand, miR-133 may inhibit proliferation by targeting FGFR1, a component of the MAPK pathway. Another MAPK component interacting with miR-133 is p38. It induces miR-133 and miR-1 expression, which in turn target SP1, an inducer of cyclin 1. Once again this has the effect of inducing cell cycle exit and halting proliferation. MiR-133 also interacts with the IGF-1 pathway: the latter induces miR-133a expression via MyoG, which targets IGF1R to down-regulate PI3K/Akt activity, thereby forming a negative feedback loop [50].

MiR-208a/b and miR-499 are encoded in intronic regions of myosin genes and thus play a role in fibre-type specification. MiR-208a is heart-specific and comes from the gene encoding Myh6, a fast myosin isoform. MiR-208b and miR-499, however, come from slow myosin genes (Myh7 and Myh7b, respectively) and are only expressed in slow fibres. These miRNAs have interesting target genes such as MAPK6 and myostatin [50].

MiR-486 is the newest myomiR and thus not so well-studied. Similarly to miR-1 and miR-206, it targets Pax7 to promote differentiation. MiR-486 stimulates PI3K/Akt activity: it directly targets PTEN and FOXO1, both negative regulators of the pathway [50].

MiRNAs in dystrophies

Muscular dystrophies generally arise from mutations in genes encoding DGC proteins. Some of these protein genes may themselves harbour miRNA genes, which could compound the problem. Furthermore, the absence of mRNAs/proteins may disrupt feedback/feed-forward loops that regulate miRNA expression and cellular homoeostasis. Thus, it's no surprise that miRNAs are dysregulated in muscular dystrophies [43; 56-58].

Our group showed that myomiRs, amongst others, are altered in LAMA2-CMD plasma and muscle [59]. A comprehensive study of miRNA expression in 10 types of muscular dystrophy was conducted by Eisenberg et al. [60], although LAMA2-CMD was not included. They showed that most dystrophies were associated with a specific set of dysregulated miRNAs, most of which were up-regulated in disease. This suggests that, despite common phenotypic observations of myofibre degeneration and fibrosis, there are disease-specific mechanisms driving these processes in different muscular dystrophies.

The most deleterious aspect of muscular dystrophies is fibrosis. MiR-21 promotes fibrosis in various diseases and tissues, such as muscle, lung, and kidney [61-64]. It is part of signalling networks involving TGF-β, MAPK and Akt/mTOR that upon stimulation promote fibroblast proliferation and collagen synthesis [65]. Interestingly, similar pathways act in macrophages to keep them in a pro-inflammatory state [66; 67]. Prolonged inflammation compromises the regeneration process thus aiding disease progression. MiR-21 levels are increased in LAMA2-CMD [59] but its genetic deletion does not improve muscle phenotype or function [68]. MiR-29 has the opposite action of miR-21, i.e. anti-fibrotic, and mimicking its activity significantly reduced collagen production in *mdx* myoblasts [63]. TGF-β can also stimulate miR-21 expression in fibroblasts via Smad signalling. TGF-β increases miR-21 levels post-transcriptionally by inducing Drosha activity and the processing of pri-miR-21 into pre-miR-21 [69]. One of miR-21 target genes is phosphatase and tensin homologue (PTEN), which is an inhibitor of Akt. Increased miR-21, therefore, stimulates Akt activity in fibroblasts to promote proliferation or survival.

MiRNAs as biomarkers

MiRNAs have been a hope in the search for biomarkers for muscular diseases. The classical myomiRs were the first proposal due to their higher

levels in patient and *mdx* sera [70-72]. They were thought to leak into circulation due to membrane damage or instability. However, their levels decrease with age and muscle mass, which could make their use difficult. At present it's still hard to interpret a response in the form of higher myomiR levels: does it mean increased muscle mass or necrosis? Zaharieva et al. [72] found that DMD patients with a milder disease course had higher myomiR levels than severe ones, suggesting that these miRNAs may serve as indicators of remaining muscle mass. Li et al. [58] further showed that miR-208 and miR-499 are also increased in serum of DMD patients. Furthermore, miR-133, miR-206, miR-208b and miR-499 were able to distinguish DMD from its milder variant BMD.

Muscular dystrophy patients usually die from cardio-respiratory failure. With this in mind Becker et al. [73] sought to find cardiomyopathy-related miRNA biomarkers. They found, amongst others, increased circulating miR-222, miR-26a and miR-378a in muscular dystrophy patients (DMD and BMD). What's more, these miRNAs were differentially expressed between patients with and without myocardial fibrosis. Another study involving DMD and BMD patients found increased miR-30c and miR-181a in serum [74] . Unlike the classical myomiRs, there was very low correlation between miRNA levels and age, which could make them more stable biomarkers. On the other hand, they found a trend for higher levels of miR-30c with better motor function (in DMD patients).

As we can note, the vast majority of biomarker studies for muscular dystrophies focuses on DMD. To date no study specifically looked for LAMA2-CMD biomarkers. We address this gap in our third article, where we explore urine miRNAs as non-invasive biomarkers of LAMA2-CMD disease progression.

MiRNAs as therapeutic targets

The ubiquitous role of miRNAs as regulators of biological processes also makes them interesting therapeutic targets. In this case, their action can either be blocked or enhanced. Blocking miRNA activity is usually achieved using anti-sense oligonucleotides (antagomiRs) or locked nucleic acids (LNA). These approaches work much like miRNAs themselves, i.e. by complementary-binding their targets and preventing their action; they're said to act as "sponges" that sequester miRNAs and prevent their action. Naturally, another approach is to remove the gene that encodes the miRNA.

One limitation of such method is unforeseen developmental changes. For an extensive review on miRNA inhibition methods see [75].

MiRNA over-expression has mostly been achieved by adeno-associated viral vectors (AAVs). However, system-wide expression is still infeasible due to liver toxicity [76]. Furthermore, AAVs pose a size-limit to the constructs they can deliver. For example dystrophin, the protein absent in DMD, is the largest protein in the human genome, making it unsuitable for AAV transfection [77].

Alexander et al. found that muscle-enriched miR-486 expression is lower in DMD and BMD patients, and its over-expression improves symptoms [78]. The beneficial effects were once again achieved by modulation of the PTEN/Akt pathway: miR-486 targets DOCK3, which in turn increases PTEN levels, an inhibitor of Akt. An interesting possibility that's rarely thought of is that miRNAs could also be exploited as adjunct therapy. For example, Cacchiarelli et al. [79] found that inhibition of miR-31 improved the efficiency of exon-skipping treatment in *mdx* mice. In this context miRNAs wouldn't be the main therapeutic targets but would improve the efficiency of other therapies.

Methods

Histology

Histology is a basic and vital technique in medical science. It allows the inspection of tissues and their properties under the light or electron microscope. Our group makes routine use of this technique to observe muscle fibres and their nuclei by means of haematoxylin and eosin staining (H&E). Haematoxylin binds DNA and colours the nuclei dark blue, which contrasts with the red/pink hues of the other (eosinophilic) structures [80] . We use H&E to assess overall muscle integrity and counting centrally located nuclei (articles II, III and IV).

Polymerase chain reaction (PCR)

Polymerase chain reaction (PCR) is a technique that revolutionised biology. It was developed in the 80's by Kary Mullis and uses the ability of DNA polymerase to extend a nucleotide chain based on complementarity. Given that DNA polymerase can only extend an existing chain, a primer is used as an initial template. Primers are specific to the region that is to be amplified.

PCR works by thermal cycling: 1) denaturation – at 94 °C the DNA strands are separated, 2) annealing – at 54 °C the primers bind the single DNA strands and 3) extension – with the primers in place DNA polymerase can extend the chains. These 3 steps consstitute a single cycle, which will be repeated 30-40 times. Theoretically, every cycle doubles the DNA amount, the end result being millions of copies of the original DNA fragment [81] .

Quantitative PCR (qPCR) monitors the amount (amplification) of DNA during the reaction; it is also called real-time PCR (RT-PCR). However, the acronym RT-PCR usually refers to reverse transcription PCR, which is a

method for cloning regions of interest from their RNA. Thus RT-PCR reverse transcribes RNA into cDNA using reverse transcriptase.

In summary, PCR allows the absolute or relative quantification of gene expression. We have used qPCR in paper II to confirm the absence of miR-21 in relevant groups, as well as TGF-β expression.

Next-generation sequencing (NGS)

The term next-generation sequencing is an umbrella term for a few different technologies that have the aim of deciphering the sequence of nucleotide chains. Like PCR, NGS has revolutionised biomedical science in the last decade, allowing for cheaper and high-throughput experiments to be performed.

Sequencing machines are not yet capable of handling very long fragments, so the samples have to be fractioned into smaller fragments. The size of these will depend on the technology used for sequencing; e.g. Illumina sequencing can handle fragments ~150 nucleotides-long, Ion Torrent ~ 200bp and Roche 454 up to 1kb. Adapters are added after fragmentation; these are used to anchor the DNA templates to slides or beads and also aid the subsequent PCR reaction [82] .

For fragments to be sequenced with confidence, we need many of them. PCR is thus used to amplify the reads. The specifics of the PCR step may vary depending on the type of sequencing, e.g. Ion Torrent uses emulsion PCR. Regardless of that, the goal is to have many copies of a specific DNA template grouped in one place. The (PCR) amplification step is highly related to ‘sequence depth of coverage’ - the term is usually shortened to simply sequence depth or coverage. Sequence depth is the measure of how many times a given base in our sample has been sequenced. To be confident in our sequencing run we need sufficient coverage. The depth of coverage needed is determined by the type of sequencing (RNA-seq, ChIP-seq, miRNA-seq, etc), organism of origin and reference genome, for example [83].

The elongation of the PCR products and detection of incorporated nucleotides differ by manufacturer. Illumina sequencing binds the PCR product to a slide and floods it with nucleotides, DNA polymerase and a terminator which will limit the action of DNA polymerase to one single reaction. The nucleotides are colour-labelled and thus emit a specific signal

when added to the chain. A picture of the slide is taken indicating which nucleotides were added in each position. The terminator is removed and the cycle repeated. Based on the sequence of images (and colours) computers can determine the sequence of a fragment [82].

Roche 454 binds one DNA template per bead for amplification. The beads are then placed in a well with DNA polymerase and buffers. Next, the nucleotides are added sequentially, i.e. first A, then T, C and G, for example. A light signal is emitted when a nucleotide is incorporated, and the signal is proportional to the number of nucleotides added [82].

Differently from the two previous methods, which use optical signals, Ion Torrent/Proton makes use of pH changes to determine the fragment sequence. The addition of nucleotides by DNA polymerase releases a H^+ ion, one per added base. Like Roche 454, the chip is sequentially flooded with known nucleotides, and by measuring the drop in pH we know how many were added [82].

Ion Torrent sequencing was used in articles I and III to profile miRNA expression.

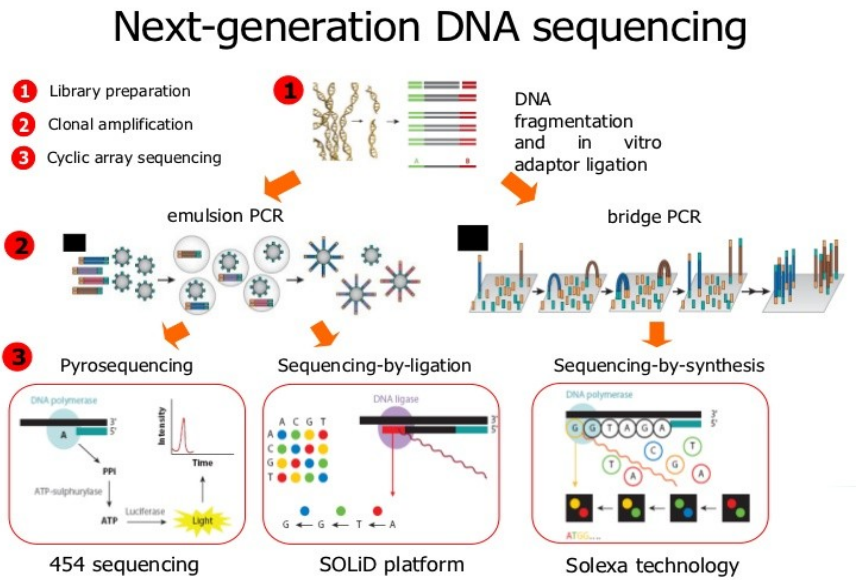

Figure 4.
Overview of some of the most common NGS platforms.

Main research questions

- What is the microRNA profile of laminin α2 chain-deficient muscle?
- Can the absence of pro-fibrotic miR-21 improve muscle phenotype and function in the dy^{3K}/dy^{3K} and dy^{2J}/dy^{2J} mouse models of LAMA2-CMD?
- Are urinary miRNAs potential biomarkers of LAMA2-CMD progression?
- Can metabolism be targeted to improve muscle function and phenotype in LAMA2-CMD mouse models? If so, can metformin be used for this purpose?

Results

Article I

In this work we have used next-generation sequencing to profile miRNAs in *dy^{3K}/dy^{3K}* muscle as an initial screening for our future studies. To make full use of the data we have integrated it with a previous (microarray) mRNA data set [41] from our group to get information about miRNA targets. We found 128 differentially expressed miRNAs in *dy^{3K}/dy^{3K}* muscle compared to wild-type: 70 up- and 58 down-regulated. Of the up-regulated miRNAs, miR-125a, miR-665 and miR-152 had more than 20 down-regulated targets. Conversely, amongst the down-regulated miRNAs with most up-regulated targets we find two myomiRs, namely miR-1a and miR-133a/b, with 17 and 15 targets, respectively. Moreover, expression of several dystromiRs such as miR-1, miR-29c, miR-133, miR-206, miR-223 and miR-499 was dysregulated also in *dy^{3K}/dy^{3K}* skeletal muscle. Furthermore, we also found other miRNAs that are common to various muscle disorders including DMD (e.g. miR-30c, miR-99b, miR-103, miR-125a, miR-195a, miR-214, miR-299a, miR-381, miR-501 and let-7e) [60]. Down-regulated genes targeted by multiple miRNAs include Arhgap28, Maf and S100pbp; and up-regulated targets include Bicc1, Bnc2, Dab2, Dclk1, Enpp1, Prune2 and Sox11. Gene set enrichment analysis of differentially expressed target genes found significant terms which include oxidative phosphorylation, metabolic pathways, protein and RNA metabolism, immunity, etc., in accordance with previous studies in our lab [21; 42], but also, to our knowledge, unrelated terms such as ‘Adrenergic signalling in cardiomyocytes’, and ‘AGE-RAGE signalling in diabetes’.

Article II

Considering the dysregulated miRNA profile observed in the first article and our previous studies, including pro-fibrotic miR-21, we explored the effects of its genetic deletion on skeletal muscle phenotype, function and fibrosis in LAMA2-CMD.

We found no improvement in body weight nor grip strength in either mouse model, despite a very slight reduction in collagen content in dy^{2J}/dy^{2J} double knock-out mice. There was a slight increase in central nucleation in dy^{3K}/dy^{3K} double knock-outs, which suggests increased regeneration; however, we couldn't confirm it with embryonic MHC staining (data not shown). In agreement with the lack of overt improvement, there was no significant change in TGF-β expression.

In summary we showed that the single deletion of miR-21 is not enough to reduce fibrosis in the dy^{2J}/dy^{2J} and dy^{3K}/dy^{3K} mouse models of LAMA2-CMD.

Article III

The lack of reliable biomarkers for myodegenerative diseases has been a limitation in the field for many years. Usually, patients have to undergo blood tests and tissue biopsies, which are invasive, especially for children. We tried to address this problem by exploring urinary miRNAs as reliable and non-invasive biomarkers for LAMA2-CMD. Our results show that already at 3 weeks of age, when no visible symptoms are present, five miRNAs are differentially expressed. At 4 weeks of age, when the first symptoms appear, we found the largest number of dysregulated miRNAs (18 microRNAs) and the only time point with down-regulated genes (in sick mice compared to control); a few muscle-enriched miRNAs are altered. At 6 weeks of age the symptoms are clear and myomiRs are amongst the differentially expressed miRNAs. We found 17 significant miRNAs that also include muscle-enriched and mitomiRs – i.e. mitochondria-related miRNAs.

Interestingly, we observed that male dy^{2J}/dy^{2J} mice have reduced body weight from 3 weeks onwards, compared to WT litter-mates, whilst females only differ at 6 weeks. Muscle function (assessed by grip strength) is lower and central nucleation higher from 4 weeks of age onward. Despite a trend at 4 weeks, collagen content is significantly elevated only at the 6 weeks time point. As expected, CK is higher in dystrophic animals at all time points analysed.

Article IV

A proteomics study performed by our group [42] found that most differentially abundant proteins between dy^{3K}/dy^{3K} and wild-type mice muscle were related to metabolic processes. We therefore chose to explore metabolism as a potential therapeutic target in a metformin intervention study. Six-week-old dy^{2J}/dy^{2J} and WT mice were treated with either metformin or water for 25 days. The analyses were factored on sex due to the different degree of muscle mass between males and females, and different response to disease observed in article III.

We found that metformin treatment improved grip strength in treated dy^{2J}/dy^{2J} compared to untreated, despite unaffected muscle weights. Energy efficiency was improved in treated dy^{2J}/dy^{2J} females, which resulted in increased weight gain in these mice. Central nucleation decreased in both dy^{2J}/dy^{2J} females and males in response to metformin, which suggests reduced muscle damage. We found a significant reduction of small fibres (500-1000 μm^2) in treated dy^{2J}/dy^{2J} females. White adipose tissue weight increased in both dy^{2J}/dy^{2J} females and males; in contrast, brown adipose tissue weight was reduced in dy^{2J}/dy^{2J} males.

Discussion

The main goal of my thesis was to explore potential therapies and biomarkers for LAMA2-CMD, particularly the potential of miRNAs. We've previously shown that miRNAs are dysregulated in LAMA2-CMD, specifically myomiRs, miR-21 and miR-223 [59]. To expand the scope of this analysis we have used miRNA-Seq to profile microRNAs in dy^{3K}/dy^{3K} muscle, which is presented in article I. We detected over 1500 miRNAs in dy^{3K}/dy^{3K} muscle, most of which were expressed at low levels. Of these, 128 were differentially expressed, 70 up- and 58 down-regulated in dystrophic muscle. The up-regulated miRNAs with most repressed target genes were miR-125a, miR-665, miR-152 and miR-501. Arhgap28 (targeted by miR-125a, miR-152 and miR-665) is an actin-interacting protein involved in cell contractility and ECM remodelling [84]. Given that the main function of laminin α2 chain is to connect the actin cytoskeleton of myotubes to the ECM, the repression of Arhgap28 is likely significant for LAMA2-CMD. Basically nothing is known about Maf (targeted by miR-125a, miR-152 and miR-665) in skeletal muscle. In other tissues, however, it interacts with p53 to influence apoptosis and cell cycle progression [85] and p53 has been demonstrated to mediate caspase-activation in LAMA2-CMD [86]. S100pbp (repressed; targeted by miR-125a, miR-501 and miR-665) and Bnc2 (up-regulated; targeted by miR-1a and miR-133a/b) are largely unknown genes except for some involvement in cancers. The function of Bicc1 (targeted by miR-20a and miR-133a/b) in skeletal muscle is mostly unexplored, but it is involved in muscle memory to loading: it was found hypo-methylated after a single bout of resistance exercise and its expression increased in response to reloading [87]. Dab2 (targeted by miR-20a and miR-133a/b) was linked to angiogenesis in facioscapulohumeral muscular dystrophy by interacting with FRG1 (FSHD region gene 1) [88]. More relevant to LAMA2-CMD, Dab2 mediates TGF-β induced fibronectin synthesis in fibroblast-like cell lines by activating JNK [89]. Dclk1 (targeted by miR-1a, miR-20a and miR-133a/b) and Prune2 (targeted by miR-1a, miR-20a, miR-22 and miR-133a/b) are genes involved in various forms of cancer, whilst Enpp1 (targeted by miR-1a, miR-20a, miR-22 and miR-133a/b) affects cardiac and vascular calcification. Sox11

(targeted by miR-1a, miR-22, miR-133a/b and miR-499), besides its involvement in cancers, affects nerve regeneration and CNS development. To better understand the potential role of these target genes we performed gene set enrichment analysis on them. These analyses look for over-represented genes related to a specific function, cellular component or process. Using the KEGG 2016 gene set we found interesting enriched terms such as oxidative phosphorylation, metabolic pathways and cardiac muscle contraction, suggesting that these processes are dysfunctional in LAMA2-CMD. We also found previously LAMA2-CMD-unrelated terms such as 'Adrenergic signalling in cardiomyocytes' and 'AGE-RAGE signalling in diabetes'.

One of our specific goals was to investigate if the genetic deletion of pro-fibrotic miR-21 would reduce fibrosis and improve muscle histology or function in the dy^{2J}/dy^{2J} and dy^{3K}/dy^{3K} mouse models of LAMA2-CMD. To our knowledge, this is the first study to address this question. We have shown that the genetic knock-out of miR-21 is not enough to reduce pathology, most likely due to miRNA redundancy. There are more than 130 miRNAs which share at least 50 targets with miR-21. At the moment miR-21's network in skeletal muscle is largely unknown, which makes it impossible for us to suggest potential candidates that could be taking its place. MicroRNA research still faces limitations such as the lack of validated targets; currently, Tarbase [90] doesn't list any miR-21 validated target in skeletal muscle. Furthermore, we didn't observe any reduction in TGF-β expression, which suggests that the overall inflammation status might be unchanged.

Another factor is different disease-driving mechanisms between LAMA2-CMD and DMD. Earlier studies were performed on the *mdx* mouse model of DMD, which presents a mild dystrophic phenotype compared to human DMD patients and our mouse models, especially the dy^{3K}/dy^{3K}. Furthermore, in DMD the whole DGC is missing from the sarcolemma, which is not the case in LAMA2-CMD. Muscle fibres in DMD are prone to contraction-induced damage whilst LAMA2-CMD leads to contraction-induced detachment. It seems that detachment is a strong signal for cell death and degeneration, leading to fibrosis.

The inability of the single deletion of miR-21 in reducing fibrosis in LAMA2-CMD makes us wonder about the deletion of multiple miRNAs, perhaps clusters or closely related miRNAs. At the moment this is a technical challenge: e.g. AAV vectors have limited capacity for carrying material, either for over-expression or gene editing [76; 77]. Also, genetic deletion of multiple genes may render embryos unviable or have undesired

developmental consequences. One potential limitation of this study is that the absence of miR-21, whilst perhaps beneficial for skeletal muscle fibrosis, could prove to be detrimental for other tissues. In that sense, post-natal RNA interference methods could be more a suitable way to dampen miR-21 activity instead of its complete genetic removal.

The third article explored the potential of urinary miRNAs as biomarkers of disease progression in LAMA2-CMD. We followed disease progression as routinely done with patients, i.e. muscle biopsies for histological inspection and blood concentration of creatine kinase, and also by miRNA sequencing. We found five miRNAs increased in the urine of dy^{2J}/dy^{2J} mice at 3 weeks of age, with no visible symptoms on histological sections. Although uninteresting from a diagnostic perspective, these miRNAs could hint at processes not analysed here, such as initial inflammatory response or immune cell infiltration. At this age, male dy^{2J}/dy^{2J} mice already have lower body weight than WT counterparts. At 4 weeks, with the first visible symptoms, we found the largest number of differentially expressed miRNAs (18 genes). It is also the only time point with down-regulated miRNAs in dy^{2J}/dy^{2J} compared to WT. At this stage dy^{2J}/dy^{2J} mice have increased central nucleation and decreased grip strength. Although there was a trend for higher collagen content in dystrophic animals, it did not reach statistical significance. At the latest time point we also found a large number of dysregulated miRNAs, seventeen genes. Interestingly, one miRNA that was down-regulated at 4 weeks is now up-regulated in dy^{2J}/dy^{2J} mice, namely miR-181a. It may prove to be an interesting candidate for further studies as it changes expression direction from 4 to 6 weeks of age, and it is a muscle-enriched mitochondria-associated miRNA. At 6 weeks of age the pathology is clear on histological sections and many of the differentially expressed miRNAs are either muscle-specific or muscle-enriched; collagen content is significantly higher in dy^{2J}/dy^{2J} mice and grip strength lower. Creatine kinase concentration was higher in dystrophic animals at all time points analysed.

Considering the minimal overlap of differentially expressed miRNAs between the time points analysed we propose that urine miRNAs could be used as biomarkers for LAMA2-CMD. Future studies should confirm our results with an orthogonal method, such as qPCR. Besides, future trials should also try to make use of patient samples, which will present challenges in the form of higher variance and data heterogeneity. One limitation of our study is that we had to pool urine samples for sequencing; it would be

interesting to repeat this study with one sample per subject, which should be possible with patient material.

In article IV we have explored a therapeutic intervention targeting metabolism. To do so we have used the FDA-approved drug metformin, the leading medication against type 2 diabetes. Metformin's mechanisms of action aren't completely understood yet, but it is known to act through AMPK to increase PGC-1α expression and mitochondrial content. It also inhibits gluconeogenesis in the liver and glucose uptake in the intestines; in skeletal muscle and adipose tissue it increases glucose uptake by increasing transport at the membrane [91]. These effects could counteract the decreased mitochondrial content and impaired energetic metabolism observed in patient cells [21].

The improved weight gain observed in treated dy^{2J}/dy^{2J} females seems to stem from non-muscle tissues, specifically, white adipose tissue. The reduction in brown adipose tissue in treated male dy^{2J}/dy^{2J} mice may suggest an effect of metformin on mitochondrial metabolism. Indeed, metformin uptake is substantial in brown adipose tissue, as recently shown by PET/CT [92] (Breining et al. 2018).

It is not clear what the cause of improved grip strength could be given that muscle weights did not change in response to metformin. We could speculate that, if the muscular component is not improved, then perhaps the neural one is. Metformin treatment might have improved motor neuron conductivity or NMJ stability. Future studies should address this possibility. The improved energy efficiency in dy^{2J}/dy^{2J} females might also have delayed fatigue in these mice.

A clear limitation of this study is the age at which treatment began, i.e. 6 weeks. In a clinical setting treatment would ensue as soon as the diagnosis is positive. It is therefore possible that metformin could alter disease progression and delay some of the symptoms.

Conclusions

The main finding of my thesis are:

There is substantial dysregulation in miRNA expression in dy^{3K}/dy^{3K} muscle. This is also highlighted by various target genes being differentially expressed, many of which are related to oxidative metabolism, muscle contraction, RNA, protein and amino-acid metabolism, amongst others. Some of the miRNAs with most target genes are myomiRs miR-1a, miR-133 and miR-499.

By itself, miR-21 knock-out is not enough to reduce fibrosis in LAMA2-CMD. Even in its absence, tissue degeneration is substantial, leading to progressive fibrosis and functional deficit.

MiRNAs are detectable in the urine of the dy^{2J}/dy^{2J} mouse model of LAMA2-CMD. They are potentially dysregulated already at 3 weeks of age, when no symptoms are visible. There is very little overlap in differentially expressed miRNAs throughout disease progression, and we thereby propose that future studies explore their potential.

Metformin yields some positive effects to dy^{2J}/dy^{2J} mice, especially females. Unfortunately, there was no improvement in body or muscle weights, indicating no major impact on skeletal muscle. Central nucleation was reduced in dy^{2J}/dy^{2J} mice with metformin treatment, suggesting reduced muscle degeneration. Most strikingly, metformin treatment improved grip strength in dystrophic mice.

Together, our studies show that LAMA2-CMD is a very difficult disease to tackle. Interventions that were beneficial for other muscular dystrophies show little or no impact on LAMA2-CMD. But not all is lost. Our results suggest that urinary miRNAs can indeed be used as biomarkers. Future studies should benefit from larger sample sizes and patient material. Metabolism-related features have been consistently altered in our recent investigations, indicating that metabolism is a logical therapeutic target to be pursued. Although metformin did not increase body and muscle weights, it might have improved

neural function, leading to the increased grip strength observed. Besides, there are other compounds to be explored, such as anti-oxidant agents.

References

[1] Lee, D. E.; Brown, J. L.; Rosa-Caldwell, M. E.; Blackwell, T. A.; Perry, R. A.; Brown, L. A.; Khatri, B.; Seo, D.; Bottje, W. G.; Washington, T. A.; Wiggs, M. P.; Kong, B.-W. and Greene, N. P. (2017). *Cancer cachexia-induced muscle atrophy: evidence for alterations in microRNAs important for muscle size*, Physiological Genomics 49 : 253-260.

[2] Cetrone, M.; Mele, A. and Tricarico, D. (2014). *Effects of the Antidiabetic Drugs on the Age-Related Atrophy and Sarcopenia Associated with Diabetes Type II.*, Current Diabetes Reviews 10 : 231-237.

[3] Hayot, M.; Rodriguez, J.; Vernus, B.; Carnac, G.; Jean, E.; Allen, D.; Goret, L.; Obert, P.; Candau, R. and Bonnieu, A. (2011). *Myostatin up-regulation is associated with the skeletal muscle response to hypoxic stimuli*, Molecular and Cellular Endocrinology 332 : 38-47.

[4] Zatz, M.; Vainzof, M. and Passos-Bueno, M. R. (2001). *Serum Creatine Kinase in Progressive Muscular Dystrophies*. In: (Ed.), *Muscular Dystrophy*, Springer Nature.

[5] Bentzinger, C. F.; Wang, Y. X. and Rudnicki, M. A. (2012). *Building Muscle: Molecular Regulation of Myogenesis*, Cold Spring Harbor Perspectives in Biology 4 : a008342-a008342.

[6] Fujita, R. and Crist, C. (2018). *Translational Control of the Myogenic Program in Developing, Regenerating, and Diseased Skeletal Muscle*. In: (Ed.), *Current Topics in Developmental Biology*, Elsevier.

[7] Gillies, A. R. and Lieber, R. L. (2011). *Structure and function of the skeletal muscle extracellular matrix*, Muscle & Nerve : n/a-n/a.

[8] de Rezende Pinto, W. B. V.; de Souza, P. V. S. and Oliveira, A. S. B. (2015). *Normal muscle structure, growth, development, and regeneration*, Current Reviews in Musculoskeletal Medicine 8 : 176-181.

[9] Pozzi, A.; Yurchenco, P. D. and Iozzo, R. V. (2017). *The nature and biology of basement membranes*, Matrix Biology 57-58 : 1 - 11.

[10] Sanes, J. R. (2003). *The Basement Membrane/Basal Lamina of Skeletal Muscle*, Journal of Biological Chemistry 278 : 12601-12604.

[11] Holmberg, J. and Durbeej, M. (2013). *Laminin-211 in skeletal muscle function*, Cell Adhesion and Migration 7 : 1-11.

[12] Lowe, J. S. and Anderson, P. G. (2015). *Support Cells and the Extracellular Matrix*. In: (Ed.), *Stevens Lowes Human Histology*, Elsevier.

[13] Durbeej, M. and Campbell, K. P. (2002). *Muscular dystrophies involving the dystrophin–glycoprotein complex and an overview of current mouse models*, Genetics of Disease 12 : 349-361.

[14] Lim, L. E. and Campbell, K. P. (1998). *The sarcoglycan complex in limb–girdle muscular dystrophy*, Current Opinion in Neurology 11 : 443-452.

[15] Murphy, A. P. and Straub, V. (2015). *The Classification, Natural History and Treatment of the Limb Girdle Muscular Dystrophies*, Journal of Neuromuscular Diseases 2 : S7–S19.

[16] Durbeej, M. (2015). *Laminin-upalpha2~Chain-Deficient Congenital Muscular Dystrophy*, Current Topics in Membranes 76 : 31-60.

[17] Girgenrath, M.; Dominov, J. A.; Kostek, C. A. and Miller, J. B. (2004). *Inhibition of apoptosis improves outcome in a model of congenital muscular dystrophy*, The Journal of Clinical Investigation 114 : 1635-1639.

[18] Meinen, S.; Lin, S.; Thurnherr, R.; Erb, M.; Meier, T. and Rüegg, M. A. (2011). *Apoptosis inhibitors and mini-agrin have additive benefits in congenital muscular dystrophy mice*, EMBO Molecular Medicine 3 : 465–479.

[19] Yamauchi, J.; Kumar, A.; Duarte, L.; Mehuron, T. and Girgenrath, M. (2013). *Triggering regeneration and tackling apoptosis: a combinatorial approach to treating congenital muscular dystrophy type 1~A*, Human Molecular Genetics 22 : 4306–4317.

[20] Körner, Z.; Fontes-Oliveira, C. C.; Holmberg, J.; Carmignac, V. and Durbeej, M. (2014). *Bortezomib Partially Improves Laminin a2 Chain-Deficient Muscular Dystrophy*, The American Journal of Pathology 184 : 1518-1528.

[21] Fontes-Oliveira, C. C.; Steinz, M.; Schneiderat, P.; Mulder, H. and Durbeej, M. (2017). *Bioenergetic Impairment in Congenital Muscular Dystrophy Type 1A and Leigh Syndrome Muscle Cells*, Scientific Reports 7 : 45272.

[22] Sunada, Y.; Bernier, S. M.; Kozak, C. A.; Yamada, Y. and Campbell, K. P. (1994). *Deficiency of merosin in dystrophic dy mice and genetic linkage of laminin M chain gene to dy locus.*, Journal of Biological Chemistry 269 : 13729-13732.

[23] Xu, H.; Wu, X.-R.; Wewer, U. M. and Engvall, E. (1994). *Murine muscular dystrophy caused by a mutation in the laminin upalpha2 (Lama2) gene*, Nature Genetics 8 : 297-302.

[24] Miyagoe, Y.; Hanaoka, K.; Nonaka, I.; Hayasaka, M.; Nabeshima, Y.; Arahata, K.; Nabeshima, Y.-i. and Takeda, S. (1997). *Laminin α2 chain-null mutant mice by targeted disruption of the Lama2 gene: a new model of merosin (laminin 2)-deficient congenital muscular dystrophy*, FEBS Letters 415 : 33-39.

[25] Kuang, W.; Xu, H.; Vachon, P. H.; Liu, L.; Loechel, F.; Wewer, U. M. and Engvall, E. (1998). *Merosin-deficient congenital muscular dystrophy. Partial*

genetic correction in two mouse models., The Journal of Clinical Investigation 102 : 844-852.

[26] Manning, J. and O'Malley, D. (2015). *What has the mdx mouse model of duchenne muscular dystrophy contributed to our understanding of this disease?*, Journal of Muscle Research and Cell Motility 36 : 155-167.

[27] Gawlik, K.; Miyagoe-Suzuki, Y.; Ekblom, P.; Takeda, S. and Durbeej, M. (2004). *Laminin α1 chain reduces muscular dystrophy in laminin α2 chain deficient mice*, Human Molecular Genetics 13 : 1775-1784.

[28] Gawlik, K. I. and Durbeej, M. (2010). *TRANSGENIC OVEREXPRESSION OF LAMININ α1 CHAIN IN LAMININ α2 CHAIN–DEFICIENT MICE RESCUES THE DISEASE THROUGHOUT THE LIFESPAN*, Muscle Nerve 42 : 30-37.

[29] Erb, M.; Meinen, S.; Barzaghi, P.; Sumanovski, L. T.; Courdier-Früh, I.; Rüegg, M. A. and Meier, T. (2009). *Omigapil Ameliorates the Pathology of Muscle Dystrophy Caused by Laminin-α2 Deficiency*, Journal of Pharmacology and Experimental Therapeutics 331 : 787-795.

[30] Yu, X. and Zuo, Q. (2013). *MicroRNAs in the regeneration of skeletal muscle~*, Frontiers in Bioscience 18 : 608.

[31] Carmignac, V.; Quéré, R. and Durbeej, M. (2011). *Proteasome inhibition improves the muscle of laminin a2 chain-deficient mice*, Human Molecular Genetics 20 : 541-552.

[32] Nevo, Y.; Halevy, O.; Genin, O.; Moshe, I.; Turgeman, T.; Harel, M.; Biton, E.; Reif, S. and Pines, M. (2010). *Fibrosis inhibition and muscle histopathology improvement in laminin-upalpha2-deficient mice*, Muscle & Nerve 42 : 218-229.

[33] Elbaz, M.; Yanay, N.; Aga-Mizrachi, S.; Brunschwig, Z.; Kassis, I.; Ettinger, K.; Barak, V. and Nevo, Y. (2012). *Losartan, a therapeutic candidate in congenital muscular dystrophy: Studies in the dy2J/dy2J Mouse*, Annals of Neurology 71 : 1531-8249699-708.

[34] Meinen, S.; Lin, S. and Ruegg, M. A. (2012). *Angiotensin II type 1 receptor antagonists alleviate muscle pathology in the mouse model for laminin-α2-deficient congenital muscular dystrophy (MDC1A)*, Skeletal Muscle 2.

[35] Moll, J.; Barzaghi, P.; Lin, S.; Bezakova, G.; Lochmüller, H.; Engvall, E.; Müller, U. and Ruegg, M. A. (2001). *An agrin minigene rescues dystrophic symptoms in a mouse model for congenital muscular dystrophy*, Nature 413 : 302-307.

[36] Reinhard, J. R.; Lin, S.; McKee, K. K.; Meinen, S.; Crosson, S. C.; Sury, M.; Hobbs, S.; Maier, G.; Yurchenco, P. D. and Rüegg, M. A. (2017). *Linker proteins restore basement membrane and correct LAMA2-related muscular dystrophy in mice*, Science Translational Medicine 9.

[37] Li, Z. B.; Kollias, H. D. and Wagner, K. R. (2008). *Myostatin Directly Regulates Skeletal Muscle Fibrosis*, Journal of Biological Chemistry 283 : 19371-19378.

[38] Li, L.; Sarver, A. L.; Alamgir, S. and Subramanian, S. (2012). *Downregulation of microRNAs miR-1, -206 and -29 -stabilizes PAX3 and CCND2 expression in rhabdomyosarcoma*, Laboratory Investigation 92 : 571-583.

[39] Smith, L. R. and Barton, E. R. (2018). *Regulation of fibrosis in muscular dystrophy*, Matrix Biology .

[40] Acuna, M. J.; Pessina, P.; Olguin, H.; Cabrera, D.; Vio, C. P.; Bader, M.; Munoz-Canoves, P.; Santos, R. A.; Cabello-Verrugio, C. and Brandan, E. (2013). *Restoration of muscle strength in dystrophic muscle by angiotensin-1-7 through inhibition of TGF-~ signalling*, Human Molecular Genetics 23 : 1237-1249.

[41] Häger, M.; Bigotti, M. G.; Meszaros, R.; Carmignac, V.; Holmberg, J.; Allamand, V.; Akerlund, M.; Kalamajski, S.; Brancaccio, A.; Mayer, U. and Durbeej, M. (2008). *Cib2 binds integrin alpha7Bbeta1D and is reduced in laminin alpha2 chain-deficient muscular dystrophy*, The Journal of biological chemistry 283 : 24760—24769.

[42] de Oliveira, B. M.; Matsumura, C. Y.; Fontes-Oliveira, C. C.; Gawlik, K. I.; Acosta, H.; Wernhoff, P. and Durbeej, M. (2014). *Quantitative Proteomic Analysis Reveals Metabolic Alterations, Calcium Dysregulation, and Increased Expression of Extracellular Matrix Proteins in Laminin α2 Chain–deficient Muscle*, Mol Cell Proteomics 13 : 3001-3013.

[43] Zacharewicz, E.; Lamon, S. and Russell, A. P. (2013). *MicroRNAs in skeletal muscle and their regulation with exercise, ageing and disease*, Frontiers in Physiology 4.

[44] Bartel, D. P. (2009). *MicroRNAs: Target Recognition and Regulatory Functions*, Cell 136 : 215-233.

[45] Roberts, T. C.; Godfrey, C.; McClorey, G.; Vader, P.; Briggs, D.; Gardiner, C.; Aoki, Y.; Sargent, I.; Morgan, J. E. and Wood, M. J. (2013). *Extracellular microRNAs are dynamic non-vesicular biomarkers of muscle turnover*, Nucleic Acids Research 1.

[46] Matsuzaka, Y.; Tanihata, J.; Komaki, H.; Ishiyama, A.; Oya, Y.; Rüegg, U.; Takeda, S.-i. and Hashido, K. (2016). *Characterization and Functional Analysis of Extracellular Vesicles and Muscle-Abundant miRNAs (miR-1, miR-133a, and miR-206) in C2C12 Myocytes and mdx Mice*, PLOS ONE 11 : e0167811.

[47] Wang, H. and Wang, B. (2016). *Extracellular vesicle microRNAs mediate skeletal muscle myogenesis and disease (Review)*, Biomedical Reports .

[48] Redis, R. S.; Calin, S.; Yang, Y.; You, M. J. and Calin, G. A. (2012). *Cell-to-cell miRNA transfer: From body homeostasis to therapy*, Pharmacology & Therapeutics 136 : 169-174.

[49] Diniz, G. P. and Wang, D. (2016). . In: (Ed.), *Regulation of Skeletal Muscle by microRNAs*, American Cancer Society.

[50] Horak, M.; Novak, J. and Bienertova-Vasku, J. (2016). *Muscle-specific microRNAs in skeletal muscle development*, Developmental Biology 410 : 1-13.

[51] McCarthy, J. J. (2014). *microRNA and skeletal muscle function: novel potential roles in exercise, diseases, and aging*, Frontiers in Physiology 5.

[52] Meyer, S. U.; Sass, S.; Mueller, N. S.; Krebs, S.; Bauersachs, S.; Kaiser, S.; Blum, H.; Thirion, C.; Krause, S.; Theis, F. J. and Pfaffl, M. W. (2015). *Integrative Analysis of MicroRNA and mRNA Data Reveals an Orchestrated Function of MicroRNAs in Skeletal Myocyte Differentiation in Response to TNF-upalpha or IGF1*, PLOS ONE 10 : e0135284.

[53] Meyer, S. U.; Thirion, C.; Polesskaya, A.; Bauersachs, S.; Kaiser, S.; Krause, S. and Pfaffl, M. W. (2015). *TNF-upalpha and IGF1 modify the microRNA signature in skeletal muscle cell differentiation*, Cell Communication and Signaling 13 : 4.

[54] Chen, J.-F.; Mandel, E. M.; Thomson, J. M.; Wu, Q.; Callis, T. E.; Hammond, S. M.; Conlon, F. L. and Wang, D.-Z. (2006). *The role of microRNA-1 and microRNA-133 in skeletal muscle proliferation and differentiation*, Nature Genetics 38 : 228–233.

[55] Goljanek-Whysall, K.; Pais, H.; Rathjen, T.; Sweetman, D.; Dalmay, T. and Münsterberg, A. (2012). *Regulation of multiple target genes by miR-1 and miR-206 is pivotal for C2C12 myoblast differentiation*, Journal of Cell Science 125 : 3590-3600.

[56] Erriquez, D.; Perini, G. and Ferlini, A. (2013). *Non-Coding RNAs in Muscle Dystrophies*, International Journal of Molecular Sciences 14 : 19681–19704.

[57] Morlando, M.; Rosa, A.; Caffarelli, E.; Fatica, A. and Bozzoni, I. (2013). *Non Coding RNA in Muscle Differentiation and Disease*, MicroRNA 2 : 91-101.

[58] Li, X.; Li, Y.; Zhao, L.; Zhang, D.; Yao, X.; Zhang, H.; Wang, Y.-c.; Wang, X.-y.; Xia, H.; Yan, J. and et al. (2014). *Circulating Muscle-specific miRNAs in Duchenne Muscular Dystrophy Patients*, Mol Ther Nucleic Acids 3 : e177.

[59] Holmberg, J.; Alajbegovic, A.; Gawlik, K. I.; Elowsson, L. and Durbeej, M. (2014). *Laminin α2 Chain-Deficiency is Associated with microRNA Deregulation in Skeletal Muscle and Plasma*, Frontiers in Aging Neuroscience 6.

[60] Eisenberg, I.; Eran, A.; Nishino, I.; Moggio, M.; Lamperti, C.; Amato, A. A.; Lidov, H. G.; Kang, P. B.; North, K. N.; Mitrani-Rosenbaum, S.; Flani, K. M.; Neely, L. A.; Whitney, D.; Beggs, A. H.; Kohane, I. S. and Kunkel, L. M. (2007). *Distinctive patterns of microRNA expression in primary muscular disorders*, PNAS 104 : 17016-17021.

[61] Patrick, D. M.; Montgomery, R. L.; Qi, X.; Obad, S.; Kauppinen, S.; Hill, J. A.; van Rooij, E. and Olson, E. N. (2010). *Stress-dependent cardiac remodeling*

occurs in the absence of microRNA-21 in mice, The Journal of Clinical Investigation 120 : 3912-3916.

[62] Ardite, E.; Perdiguero, E.; Vidal, B.; Gutarra, S.; Serrano, A. L. and Muñoz-Cánoves, P. (2012). *PAI-1–regulated miR-21 defines a novel age-associated fibrogenic pathway in muscular dystrophy*, The Journal of Cell Biology 196 : 163-175.

[63] Zanotti, S.; Gibertini, S.; Curcio, M.; Savadori, P.; Pasanisi, B.; Morandi, L.; Cornelio, F.; Mantegazza, R. and Mora, M. (2015). *Opposing roles of miR-21 and miR-29 in the progression of fibrosis in Duchenne muscular dystrophy*, Biochimica et Biophysica Acta 1852 : 1451-1464.

[64] Loboda, A.; Sobczak, M.; Jozkowicz, A. and Dulak, J. (2016). *TGF-β1/Smads and miR-21 in Renal Fibrosis and Inflammation*, Mediators of Inflammation 2016 : 1-12.

[65] Thum, T.; Gross, C.; Fiedler, J.; Fischer, T.; Kissler, S.; Bussen, M.; Galuppo, P.; Just, S.; Rottbauer, W.; Frantz, S.; Castoldi, M.; Soutschek, J.; Koteliansky, V.; Rosenwald, A.; Basson, M. A.; Licht, J. D.; Pena, J. T. R.; Rouhanifard, S. H.; Muckenthaler, M. U.; Tuschl, T.; Martin, G. R.; Bauersachs, J. and Engelhardt, S. (2008). *MicroRNA-21 contributes to myocardial disease by stimulating MAP kinase signalling in fibroblasts*, Nature 456 : 980-984.

[66] Perdiguero, E.; Sousa-Victor, P.; Ruiz-Bonilla, V.; Jard, M.; Caelles, C.; Serrano, A. L. and Muñoz-Cánoves, P. (2011). *p38/MKP-1–regulated AKT coordinates macrophage transitions and resolution of inflammation during tissue repair*, J Cell Biol 195 : 307-322.

[67] Perdiguero, E.; Kharraz, Y.; Serrano, A. L. and Muñoz-Cánoves, P. (2012). *MKP-1 coordinates ordered macrophage-phenotype transitions essential for stem cell-dependent tissue repair*, Cell Cycle 11 : 877-886.

[68] Oliveira, B. M. S.; Durbeej, M. and Holmberg, J. (2017). *Absence of microRNA-21 does not reduce muscular dystrophy in mouse models of LAMA2-CMD*, PLOS ONE 12 : e0181950.

[69] Davis, B. N.; Hilyard, A. C.; Lagna, G. and Hata, A. (2008). *SMAD proteins control DROSHA-mediated microRNA maturation*, Nature 454 : 56-61.

[70] Cacchiarelli, D.; Legnini, I.; Martone, J.; Cazzella, V.; D'Amico, A.; Bertini, E. and Bozzoni, I. (2011). *miRNAs as serum biomarkers for Duchenne muscular dystrophy*, EMBO Molecular Medicine 3 : 258-265.

[71] Mizuno, H.; Nakamura, A.; Aoki, Y.; Ito, N.; Kishi, S.; Yamamoto, K.; Sekiguchi, M.; Takeda, S. and Hashido, K. (2011). *Identification of Muscle-Specific MicroRNAs in Serum of Muscular Dystrophy Animal Models: Promising Novel Blood-Based Markers for Muscular Dystrophy*, PLoS ONE 6 : e18388.

[72] Zaharieva, I. T.; Calissano, M.; Scoto, M.; Preston, M.; Cirak, S.; Feng, L.; Collins, J.; Kole, R.; Guglieri, M.; Straub, V.; Bushby, K.; Ferlini, A.; Morgan,

J. E. and Muntoni, F. (2013). *Dystromirs as Serum Biomarkers for Monitoring the Disease Severity in Duchenne Muscular Dystrophy*, PLoS ONE 8 : e80263.

[73] Becker, S.; Florian, A.; Patrascu, A.; Rösch, S.; Waltenberger, J.; Sechtem, U.; Schwab, M.; Schaeffeler, E. and Yilmaz, A. (2016). *Identification of cardiomyopathy associated circulating miRNA biomarkers in patients with muscular dystrophy using a complementary cardiovascular magnetic resonance and plasma profiling approach*, Journal of Cardiovascular Magnetic Resonance 18.

[74] Llano-Diez, M.; Ortez, C. I.; Gay, J. A.; Álvarez-Cabado, L.; Jou, C.; Medina, J.; Nascimento, A. and Jimenez-Mallebrera, C. (2017). *Digital PCR quantification of miR-30c and miR-181a as serum biomarkers for Duchenne muscular dystrophy*, Neuromuscular Disorders 27 : 15-23.

[75] Beavers, K. R.; Nelson, C. E. and Duvall, C. L. (2015). *MiRNA inhibition in tissue engineering and regenerative medicine*, Advanced Drug Delivery Reviews 88 : 123-137.

[76] Colella, P.; Ronzitti, G. and Mingozzi, F. (2018). *Emerging Issues in AAV-Mediated In~Vivo Gene Therapy*, Molecular Therapy - Methods & Clinical Development 8 : 87-104.

[77] Naso, M. F.; Tomkowicz, B.; Perry, W. L. and Strohl, W. R. (2017). *Adeno-Associated Virus (AAV) as a Vector for Gene Therapy*, BioDrugs 31 : 317-334.

[78] Alexander, M. S.; Casar, J. C.; Motohashi, N.; Vieira, N. M.; Eisenberg, I.; Marshall, J. L.; Gasperini, M. J.; Lek, A.; Myers, J. A.; Estrella, E. A.; Kang, P. B.; Shapiro, F.; Rahimov, F.; Kawahara, G.; Widrick, J. J. and Kunkel, L. M. (2014). *MicroRNA-486-dependent modulation of DOCK3/PTEN/AKT signaling pathways improves muscular dystrophy-associated symptoms*, Journal of Clinical Investigation 124 : 2651-2667.

[79] Cacchiarelli, D.; Incitti, T.; Martone, J.; Cesana, M.; Cazzella, V.; Santini, T.; Sthandier, O. and Bozzoni, I. (2011). *miR-31 modulates dystrophin expression: new implications for Duchenne muscular dystrophy therapy*, EMBO reports 12 : 136-141.

[80] Feldman, A. T. and Wolfe, D. (2014). *Tissue Processing and Hematoxylin and Eosin Staining*. In: (Ed.), *Histopathology*, Springer New York.

[81] Eeles, R. A.; Warren, W. and Stamps, A. (1992). *The PCR revolution*, European Journal of Cancer 28 : 289-293.

[82] Heather, J. M. and Chain, B. (2016). *The sequence of sequencers: The history of sequencing DNA*, Genomics 107 : 1-8.

[83] Muzzey, D.; Evans, E. A. and Lieber, C. (2015). *Understanding the Basics of NGS: From Mechanism to Variant Calling*, Current Genetic Medicine Reports 3 : 158-165.

[84] Yeung, C.-Y. C.; Taylor, S. H.; Garva, R.; Holmes, D. F.; Zeef, L. A.; Soininen, R.; Boot-Handford, R. P. and Kadler, K. E. (2014). *Arhgap28 Is a RhoGAP*

that Inactivates RhoA and Downregulates Stress Fibers, PLoS ONE 9 : e107036.

[85] Hale, T. K.; Myers, C.; Maitra, R.; Kolzau, T.; Nishizawa, M. and Braithwaite, A. W. (2000). *Maf Transcriptionally Activates the Mousep53Promoter and Causes a p53-dependent Cell Death*, Journal of Biological Chemistry 275 : 17991-17999.

[86] Yoon, S.; Beermann, M. L.; Yu, B.; Shao, D.; Bachschmid, M. and Miller, J. B. (2018). *Aberrant Caspase Activation in Laminin-α2-Deficient Human Myogenic Cells is Mediated by p53 and Sirtuin Activity*, Journal of Neuromuscular Diseases 5 : 59-73.

[87] Seaborne, R. A.; Strauss, J.; Cocks, M.; Shepherd, S.; O'Brien, T. D.; van Someren, K. A.; Bell, P. G.; Murgatroyd, C.; Morton, J. P.; Stewart, C. E. and Sharples, A. P. (2018). *Human Skeletal Muscle Possesses an Epigenetic Memory of Hypertrophy*, Scientific Reports 8.

[88] Wuebbles, R. D.; Hanel, M. L. and Jones, P. L. (2009). *FSHD region gene 1 (FRG1) is crucial for angiogenesis linking FRG1 to facioscapulohumeral muscular dystrophy-associated vasculopathy*, Disease Models & Mechanisms 2 : 267-274.

[89] Hocevar, B. A.; Prunier, C. and Howe, P. H. (2005). *Disabled-2 (Dab2) Mediates Transforming Growth Factor upbeta (TGFupbeta)-stimulated Fibronectin Synthesis through TGFupbeta-activated Kinase 1 and Activation of the JNK Pathway*, Journal of Biological Chemistry 280 : 25920-25927.

[90] Vlachos, I. S.; Paraskevopoulou, M. D.; Karagkouni, D.; Georgakilas, G.; Vergoulis, T.; Kanellos, I.; Anastasopoulos, I.-L.; Maniou, S.; Karathanou, K.; Kalfakakou, D.; Fevgas, A.; Dalamagas, T. and Hatzigeorgiou, A. G. (2014). *DIANA-TarBase v7.0: indexing more than half a million experimentally supported miRNA:mRNA interactions*, Nucleic Acids Research 43 : D153-D159.

[91] Viollet, B. and Foretz, M. (2013). *Revisiting the mechanisms of metformin action in the liver*, Annales d'Endocrinologie 74 : 123-129.

[92] Breining, P.; Jensen, J. B.; Sundelin, E. I.; Gormsen, L. C.; Jakobsen, S.; Busk, M.; Rolighed, L.; Bross, P.; Fernandez-Guerra, P.; Markussen, L. K.; Rasmussen, N. E.; Hansen, J. B.; Pedersen, S. B.; Richelsen, B. and Jessen, N. (2018). *Metformin targets brown adipose tissue in vivo and reduces oxygen consumption in vitro*, Diabetes, Obesity and Metabolism .

Profiling skeletal muscle microRNAs and their targets in the *dy^{3K}/dy^{3K}* mouse model of laminin α2 chain-deficient muscular dystrophy

Bernardo Moreira Soares Oliveira*, Johan Holmberg[#], Madeleine Durbeej[#]

Muscle Biology Unit, Department of Experimental Medical Science, Lund University,

Lund, Sweden

[#]Equal contribution

*Corresponding author:

Bernardo Moreira Soares Oliveira
BMC C12
221 84 Lund
SWEDEN
bernardo.moreira_soares_oliveira@med.lu.se,
+46 (0)46 222 06 79

Conflict of interests: the authors declare that no competing interests exist.

Data availability: all data and access information is contained in the article.

Funding:

Anna and Edwin Berger Foundation, Association Française contre les Myopathies, CNPq, Crafoord Foundation, Greta and Johan Kock Foundation, Lars Hierta Foundation, Olle Engkvist Byggmästare Foundation, Royal Physiographic Society in Lund, Swedish Research Council, Thelma Zoéga Foundation, Österlund Foundation

ABSTRACT

Laminin α2 chain-deficient congenital muscular dystrophy, or LAMA2-CMD, is a serious disease for which there is no cure. To gain insight into the molecular mechanisms underlying LAMA2-CMD we previously performed gene expression profiling of laminin α2 chain-deficient dy^{3K}/dy^{3K} mouse limb muscle. For further elucidation of disease mechanisms we have here profiled microRNAs (miRNAs) in skeletal muscle of wild-type and dy^{3K}/dy^{3K} limb muscle. We detected, on average, 1578 miRNAs across samples. One hundred and twenty-eight miRNAs were differentially expressed; 70 up- and 58 down-regulated in dy^{3K}/dy^{3K} muscle compared to wild-type muscle. Around one third of those miRNAs have been shown to be dysregulated in dystrophin-deficient muscular dystrophy. Moreover, we probed the regulatory relationships between differentially regulated mRNAs and miRNAs. Four up- (miR-125a, miR-152, miR-501 and miR-665) and seven down-regulated (miR-133a/b, miR-154, miR-1a, miR-20a, miR-22 and miR-499) miRNAs had target genes that were also differentially expressed in dy^{3K}/dy^{3K} skeletal muscle. Some of the relevant targets include Arhgap28, Maf, Bicc1, Dab2 and Sox11. Finally, enrichment analysis of differentially expressed mRNAs revealed significant pathways relevant for LAMA2-CMD, some that have been described before but also novel. In summary our results may provide better understanding of LAMA2-CMD.

INTRODUCTION

Laminin α2 chain-deficient congenital muscular dystrophy, or LAMA2-CMD, is caused by mutations in the *LAMA2* gene that encodes the extracellular matrix protein laminin α2 chain. LAMA2-CMD can either be very severe if laminin α2 chain is completely deficient or milder if laminin α2 chain is partially missing. Complete deficiency is characterised by profound hypotonia at birth, widespread muscle weakness, proximal joint contractures, scoliosis and delayed motor milestones. In general, children do not acquire independent ambulation and 30% of the patients die in the first decade of life [1]. The dy^{3K}/dy^{3K} mouse is a widely used animal model for LAMA2-CMD with complete laminin α2 chain-deficiency. Dy^{3K}/dy^{3K} mice develop severe muscular dystrophy with a median survival of three weeks and skeletal muscle is characterized by repeated cycles of degeneration/regeneration, massive inflammation and pathological fibrosis [2].

In an attempt to increase our understanding of the molecular mechanisms driving LAMA2-CMD, we previously performed gene expression profiling of mouse dy^{3K}/dy^{3K} limb muscles [3]. The altered gene expression has also been confirmed at the protein level in a more recent proteomic profiling study [4]. From these studies it is evident that many of the differentially expressed genes and proteins are involved in muscle development, metabolic processes, calcium handling and remodelling of extracellular matrix. Although these two studies have identified many genes and proteins in different functional categories that are differently expressed in LAMA2-CMD, the underlying disease mechanisms remain largely unclear. Hence, we decided to investigate microRNAs (miRNAs) in LAMA2-CMD.

MiRNAs are short non-coding RNAs that negatively regulate mRNA translation. MiRNAs are between 18 and 24 nucleotides long and act by base-complementarity to recognise mRNA targets in a cell-specific manner. MiRNAs serve as a guiding template in the RNA-induced silencing complex (RISC), which will bind the target mRNA. Upon binding of the complex, mRNAs are most often destabilised and degraded, or translation is inhibited [5]. Interest in miRNA biology grew substantially after discovery of their involvement in various diseases, including myopathies [6-8]. Our group has previously shown some miRNAs to be dysregulated in LAMA2-CMD [9]. This previous work focused on “dystromiRs”, which have been defined as miRNAs that are differentially expressed in patients with Duchenne muscular dystrophy and/or dystrophic models [10]. Furthermore, we have recently profiled urine miRNA expression in dy^{2J}/dy^{2J} mice (a model that recapitulates the milder form of LAMA2-CMD) and demonstrated unique groups of miRNAs at asymptomatic, initial and established disease [Moreira Soares Oliveira, submitted]. Here, we have

used next-generation sequencing to obtain an extensive profile of miRNAs in skeletal muscle of 3-week-old dy^{3K}/dy^{3K} mice. Moreover, the sequencing results were integrated with a previous mRNA dataset [3] to probe the relationship between miRNA-mRNA and functional annotation was carried out.

MATERIALS AND METHODS

Animal model

Laminin α2 chain-deficient dy^{3K}/dy^{3K} mice have been previously described [11]. Mice were analysed at three weeks of age. Animals were handled in accordance with the animal care guidelines set by the Malmö/Lund (Sweden) ethical committee for animal research (permit number M152-14).

RNA isolation

Total RNA from quadriceps femoris of wild-type (n=5) and dy^{3K}/dy^{3K} (n=5) was extracted with Qiagen miRNeasy Mini Kit following the manufacturer's instructions. The RNA was sent to the Uppsala Genome Centre for high-throughput sequencing on the IonTorrent platform (ThermoFisher Scientific). The raw sequencing data is deposited in the European Nucleotide Archive under accession number PRJEB24388.

Bioinformatics

Reads were received from the sequencing facility in BAM format mapped to the mm10 mouse genome (UCSC genome browser). BAM files were converted to FASTQ using the BEDtools bamtofastq module (2.26.0). Quality assessment of the sequencing run was done with FastQC. Only reads of mature miRNA length, i.e. 18 to 24 nucleotides, were kept for further analyses. Reads were mapped to the mature miRNA reference from miRBase (v 21) using bowtie (1.1.2) [12]. Differential expression analysis was conducted in R (3.2.3) [13] with DESeq2 (1.8.2) [14]. Exploratory data analysis and gene enrichment analyses were perfomed in IPython (6.2.1) [15] with the modules gseapy (0.9.3) [16, 17] and goatools (0.7.11) [18]. MiRNA target prediction was conducted querying Tarbase, a curated database of experimentally validated miRNA targets [19]. The Tarbase subset of Mus musculus and skeletal muscle tissue was used for further analyses. The code and data sets pertaining these analyses can be found at https://gitlab.com/uamoti/muscle_mirna

RESULTS AND DISCUSSION

We used next-generation sequencing to profile and compare the miRNA expression in skeletal muscle of dy^{3K}/dy^{3K} mice with wild-type mice. Dimensionality reduction techniques such as hierarchical clustering, as seen in the heatmap (Figure 1A), and principal component analysis (PCA) (Figure 1B) clearly distinguished the two experimental groups. In total, 1578 miRNAs were detected with mean greater than zero across samples, whilst 640 miRNAs had mean greater than one. This shows that at least 938 miRNAs were expressed at very low levels across samples. One hundred and twenty-eight miRNAs were differentially expressed at 5% significance and absolute log2 fold change greater than or equal to one. Of these, 70 were up-regulated (Table 1) and 58 down-regulated (Table 2) in dy^{3K}/dy^{3K} compared to wild-type muscle. A large majority of the differentially expressed miRNAs have previously been identified in mouse skeletal muscle (http://www.mirbase.org/). Moreover, expression of several dystromiRs [10] such as miR-1, miR-29c, miR-133, miR-206, miR-223 and miR-499 was dysregulated also in dy^{3K}/dy^{3K} skeletal muscle. In agreement with these results, we have by RT-qPCR previously demonstrated altered expression of several of the dystromiRs in dy^{3K}/dy^{3K} and dy^{2J}/dy^{2J} skeletal muscle and plasma [9]. Apart from the dystromiRs we also found other miRNAs that are common to various muscle disorders including Duchenne muscular dystrophy (e.g. miR-30c, miR-99b, miR-103, miR-125a, miR-195a, miR-214, miR-299a, miR-381, miR-501 and let-7e) [20]. Roberts et al., formerly performed a miRNA microarray analysis on dystrophin-deficient *mdx* quadriceps muscle and identified approximately 180 differentially expressed miRNAs [10]. Around 25 of these (not including dystromiRs) were also identified in our screen. Thus, altogether approximately 32% of the dysregulated miRNAs in laminin α2 chain-deficient muscular dystrophy are also dysregulated also in dystrophin-deficient muscular dystrophy. A few miRNAs (not including dystromirs) were also earlier identified in dy^{2J}/dy^{2J} urine (e.g. miR-337, miR-369, miR-376b, miR-475, miR-5100).

We previously conducted a microarray study on skeletal muscle of dy^{3K}/dy^{3K} mice [3]. The two datasets enabled us to look into the reverse relationship between miRNA and mRNA. We found 152 up- and 437 down-regulated genes at the 10% level. Fifty-four up-regulated genes were targeted by 7 down-regulated miRNAs, whilst 73 down-regulated genes were targeted by 4 up-regulated miRNAs (Figure 2). These numbers suggest that a few miRNAs target various mRNAs. Most mRNAs were targeted by one or two miRNAs, with a few genes being targeted by as much as 4 or 5. MiR-1a, miR-133a/b and miR-499 had 17, 15 and 11 up-regulated targets, respectively.

The skeletal muscle subset of Tarbase contains 72 unique miRNAs. From these, 12 are amongst our differentially expressed miRNAs, which combined have 127 unique target genes confirmed in the microarray dataset. We ran pairwise comparisons of target genes amongst the up- and down-

regulated miRNAs and found some overlap, i.e. genes targeted by multiple miRNAs. The targets of up-regulated miRNAs, and thus lower in *dy^{3K}/dy^{3K}* muscle, include Arhgap28 (Rho GTPase-activating protein 28), Maf (avian musculoaponeurotic fibrosarcoma oncogene homologue) and S100pbp (S100P binding protein), whereas targets of down-regulated miRNAs, and therefore elevated in dystrophic muscle, included Bicc1 (BicC family RNA binding protein 1), Bnc2 (basonuclin 2), Dab2 (disabled 2, mitogen-reponsive phosphoprotein), Dclk1 (doublecortin-like kinase 1), Enpp1 (ectonucleotide pyrophosphatase/phosphodiesterase 1), Prune2 (prune homolog 2) and Sox11 (SRY (sex-determining region Y)-box 11). Arhgap28 is an actin-interacting protein involved in cell contractility and extracellular matrix remodelling [21]. Considering that the main function of laminin α2 chain is to connect the actin cytoskeleton of myotubes to the extracellular matrix, the repression of Arhgap28 is likely significant for LAMA2-CMD. Basically nothing is known about Maf in skeletal muscle. In other tissues, however, it interacts with p53 to influence apoptosis and cell cycle progression [22] and p53 has been demonstrated to mediate caspase-activation in LAMA2-CMD [23]. S100pbp and Bnc2 are largely unknown genes except for some involvement in cancers [24, 25]. The function of Bicc1 in skeletal muscle is mostly unexplored, but it is involved in muscle memory to loading: it was found hypo-methylated after a single bout of resistance exercise [26]. Dab2 was linked to angiogenesis in facioscapulohumeral muscular dystrophy by interacting with FRG1 (FSHD region gene 1) [27]. More relevant to LAMA2-CMD, Dab2 mediates TGF-β induced fibronectin synthesis in fibroblast-like cell lines by activating JNK [28]. Dclk1 and Prune2 are genes involved in various forms of cancer [29, 30], whilst Enpp1 affects cardiac and vascular calcification [31]. Sox11, besides its involvement in cancers, affects nerve regeneration and CNS development [32]. Hence, it will now be interesting to analyse the potential function of the novel target genes in LAMA2-CMD in more detail.

Finally, to determine the biological processes or molecular functions associated with the differentially expressed target genes we conducted gene set enrichment analysis on differentially expressed mRNAs. We queried the Enrichr API [17, 33] for KEGG pathways (KEGG 2016 set) and found 12 significantly enriched terms (Table 3). Amongst these are terms that previously have been shown to be relevant for LAMA2-CMD, for example oxidative phosphorylation and metabolic pathways [3, 4, 34] but also terms (e.g. adrenergic and AGE-RAGE signalling) that to our knowledge have not been implicated in LAMA2-CMD.

In summary, we showed that 128 miRNAs are dysregulated in quadriceps muscle of *dy^{3K}/dy^{3K}* mice, of which 78 are up- and 58 are down-regulated. By probing the regulatory relationships between differentially expressed mRNAs and miRNAs we found target genes that potentially are involved in

LAMA2-CMD. In addition, pathway analysis revealed that dysregulated target genes are overrepresented in 12 pathways. Thus, these results may prove valuable for future research into miRNAs and LAMA2-CMD and provide information on disease mechanisms.

REFERENCES

1. Quijano-Roy S, Sparks S, Rutkowski A. LAMA2-Related Muscular Dystrophy. In: Pagon RA, Adam MP, Ardinger HH, Wallace SE, Amemiya A, Bean LJH, et al., editors. GeneReviews(R). Seattle WA: University of Washington, Seattle; 1993.
2. Gawlik KI, Durbeej M. Skeletal muscle laminin and MDC1A: pathogenesis and treatment strategies. Skelet Muscle. 2011;1(1):9.
3. Hager M, Bigotti MG, Meszaros R, Carmignac V, Holmberg J, Allamand V, et al. Cib2 binds integrin alpha7Bbeta1D and is reduced in laminin alpha2 chain-deficient muscular dystrophy. J Biol Chem. 2008;283(36):24760-9.
4. de Oliveira BM, Matsumura CY, Fontes-Oliveira CC, Gawlik KI, Acosta H, Wernhoff P, et al. Quantitative proteomic analysis reveals metabolic alterations, calcium dysregulation, and increased expression of extracellular matrix proteins in laminin alpha2 chain-deficient muscle. Mol Cell Proteomics. 2014;13(11):3001-13.
5. Brown DM, Goljanek-Whysall K. microRNAs: Modulators of the underlying pathophysiology of sarcopenia? Ageing Res Rev. 2015;24(Pt B):263-73.
6. Greco S, Perfetti A, Fasanaro P, Cardani R, Capogrossi MC, Meola G, et al. Deregulated microRNAs in myotonic dystrophy type 2. PLoS One. 2012;7(6):e39732.
7. Dmitriev P, Stankevicins L, Ansseau E, Petrov A, Barat A, Dessen P, et al. Defective regulation of microRNA target genes in myoblasts from facioscapulohumeral dystrophy patients. J Biol Chem. 2013;288(49):34989-5002.
8. Morlando M, Rosa A, Caffarelli E, Fatica A, Bozzoni I. Non coding RNA in muscle differentiation and disease. Microrna. 2013;2(2):91-101.
9. Holmberg J, Alajbegovic A, Gawlik KI, Elowsson L, Durbeej M. Laminin alpha2 Chain-Deficiency is Associated with microRNA Deregulation in Skeletal Muscle and Plasma. Front Aging Neurosci. 2014;6:155.
10. Roberts TC, Blomberg KE, McClorey G, El Andaloussi S, Godfrey C, Betts C, et al. Expression analysis in multiple muscle groups and serum reveals complexity in the microRNA transcriptome of the mdx mouse with implications for therapy. Mol Ther Nucleic Acids. 2012;1:e39.
11. Fukada S, Yamamoto Y, Segawa M, Sakamoto K, Nakajima M, Sato M, et al. CD90-positive cells, an additional cell population, produce laminin alpha2 upon transplantation to dy(3k)/dy(3k) mice. Exp Cell Res. 2008;314(1):193-203.

12. Langmead B, Trapnell C, Pop M, Salzberg SL. Ultrafast and memory-efficient alignment of short DNA sequences to the human genome. Genome Biol. 2009;10(3):R25.
13. Team RC. R: A language and environment for statistical computing 2017. Available from: http://www.R-project.org/.
14. Love MI, Huber W, Anders S. Moderated estimation of fold change and dispersion for RNA-seq data with DESeq2. Genome Biol. 2014;15(12):550.
15. Perez F, Granger BE. IPython: A system for Interactive Scientific Computing. Computing in Science & Engineering. 2007;9:21-9.
16. Subramanian A, Tamayo P, Mootha VK, Mukherjee S, Ebert BL, Gillette MA, et al. Gene set enrichment analysis: a knowledge-based approach for interpreting genome-wide expression profiles. Proc Natl Acad Sci U S A. 2005;102(43):15545-50.
17. Kuleshov MV, Jones MR, Rouillard AD, Fernandez NF, Duan Q, Wang Z, et al. Enrichr: a comprehensive gene set enrichment analysis web server 2016 update. Nucleic Acids Res. 2016;44(W1):W90-7.
18. David DKHTFROBBP-BPFKS 佐建 CMUSGS. tanghaibao/goatools: GOATOOLS v0.7.6 (Version v0.7.6). Zenodo. http://doi.org/10.5281/zenodo.819475. 2017.
19. Vlachos IS, Paraskevopoulou MD, Karagkouni D, Georgakilas G, Vergoulis T, Kanellos I, et al. DIANA-TarBase v7.0: indexing more than half a million experimentally supported miRNA:mRNA interactions. Nucleic Acids Res. 2015;43(Database issue):D153-9.
20. Eisenberg I, Eran A, Nishino I, Moggio M, Lamperti C, Amato AA, et al. Distinctive patterns of microRNA expression in primary muscular disorders. Proc Natl Acad Sci U S A. 2007;104(43):17016-21.
21. Yeung CY, Taylor SH, Garva R, Holmes DF, Zeef LA, Soininen R, et al. Arhgap28 is a RhoGAP that inactivates RhoA and downregulates stress fibers. PLoS One. 2014;9(9):e107036.
22. Hale TK, Myers C, Maitra R, Kolzau T, Nishizawa M, Braithwaite AW. Maf transcriptionally activates the mouse p53 promoter and causes a p53-dependent cell death. J Biol Chem. 2000;275(24):17991-9.
23. Yoon S, Beermann ML, Yu B, Shao D, Bachschmid M, Miller JB. Aberrant Caspase Activation in Laminin-alpha2-Deficient Human Myogenic Cells is Mediated by p53 and Sirtuin Activity. J Neuromuscul Dis. 2018;5(1):59-73.
24. Lines KE, Chelala C, Dmitrovic B, Wijesuriya N, Kocher HM, Marshall JF, et al. S100P-binding protein, S100PBP, mediates adhesion through regulation of cathepsin Z in pancreatic cancer cells. Am J Pathol. 2012;180(4):1485-94.

25. Cesaratto L, Grisard E, Coan M, Zandona L, De Mattia E, Poletto E, et al. BNC2 is a putative tumor suppressor gene in high-grade serous ovarian carcinoma and impacts cell survival after oxidative stress. Cell Death Dis. 2016;7(9):e2374.
26. Seaborne RA, Strauss J, Cocks M, Shepherd S, O'Brien TD, van Someren KA, et al. Human Skeletal Muscle Possesses an Epigenetic Memory of Hypertrophy. Sci Rep. 2018;8(1):1898.
27. Wuebbles RD, Hanel ML, Jones PL. FSHD region gene 1 (FRG1) is crucial for angiogenesis linking FRG1 to facioscapulohumeral muscular dystrophy-associated vasculopathy. Dis Model Mech. 2009;2(5-6):267-74.
28. Hocevar BA, Prunier C, Howe PH. Disabled-2 (Dab2) mediates transforming growth factor beta (TGFbeta)-stimulated fibronectin synthesis through TGFbeta-activated kinase 1 and activation of the JNK pathway. J Biol Chem. 2005;280(27):25920-7.
29. Westphalen CB, Quante M, Wang TC. Functional implication of Dclk1 and Dclk1-expressing cells in cancer. Small GTPases. 2017;8(3):164-71.
30. Salameh A, Lee AK, Cardo-Vila M, Nunes DN, Efstathiou E, Staquicini FI, et al. PRUNE2 is a human prostate cancer suppressor regulated by the intronic long noncoding RNA PCA3. Proc Natl Acad Sci U S A. 2015;112(27):8403-8.
31. Albright RA, Stabach P, Cao W, Kavanagh D, Mullen I, Braddock AA, et al. ENPP1-Fc prevents mortality and vascular calcifications in rodent model of generalized arterial calcification of infancy. Nat Commun. 2015;6:10006.
32. Tsurusaki Y, Koshimizu E, Ohashi H, Phadke S, Kou I, Shiina M, et al. De novo SOX11 mutations cause Coffin-Siris syndrome. Nat Commun. 2014;5:4011.
33. Chen X, Huang Z, Chen D, Yang T, Liu G. MicroRNA-27a is induced by leucine and contributes to leucine-induced proliferation promotion in C2C12 cells. Int J Mol Sci. 2013;14(7):14076-84.
34. Fontes-Oliveira CC, Steinz M, Schneiderat P, Mulder H, Durbeej M. Bioenergetic Impairment in Congenital Muscular Dystrophy Type 1A and Leigh Syndrome Muscle Cells. Sci Rep. 2017;7:45272.

FIGURE LEGENDS

Figure 1. Diagnostic plots. A: heatmap of top-20 mostly expressed miRNAs. B: Principal Component Analysis (PCA) plot shows how well samples grouped based on global gene expression..

Figure 2. Networks of up- (A) and (B) down-regulated miRNAs and their significant target genes. The hue of target genes is mapped to their p-values (darker hues → lower p-values) and the size of miRNAs to the number of targets.

Supplemental Figure 1. MA plot from miRNA-Seq: it shows the relationship between log fold change between two conditions (y axis) and the average expression of these (x axis). Genes significant at the 10% level are coloured red.

FIGURE 1

A

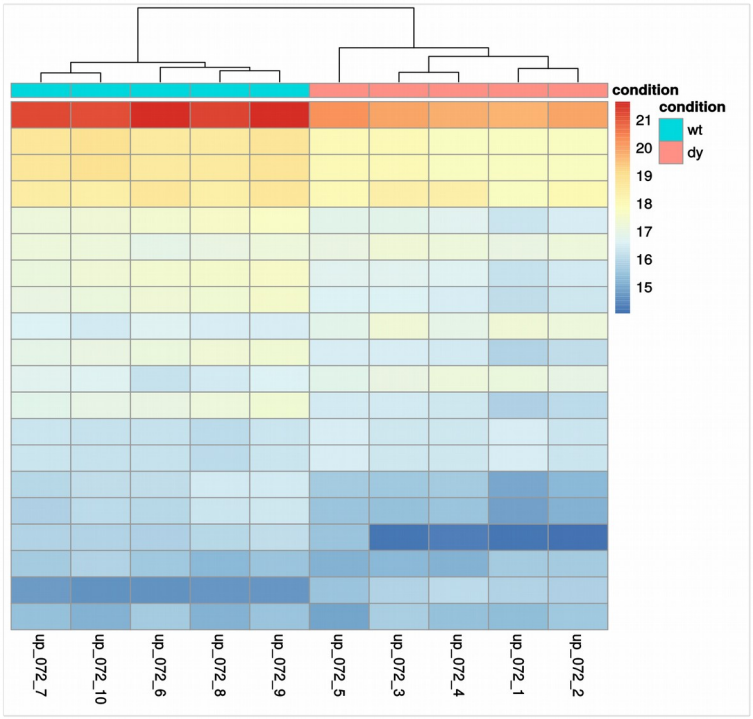
condition
condition
wt
dy
21
20
19
18
17
16
15
up_072_7
up_072_10
up_072_6
up_072_8
up_072_9
up_072_5
up_072_3
up_072_4
up_072_1
up_072_2

B

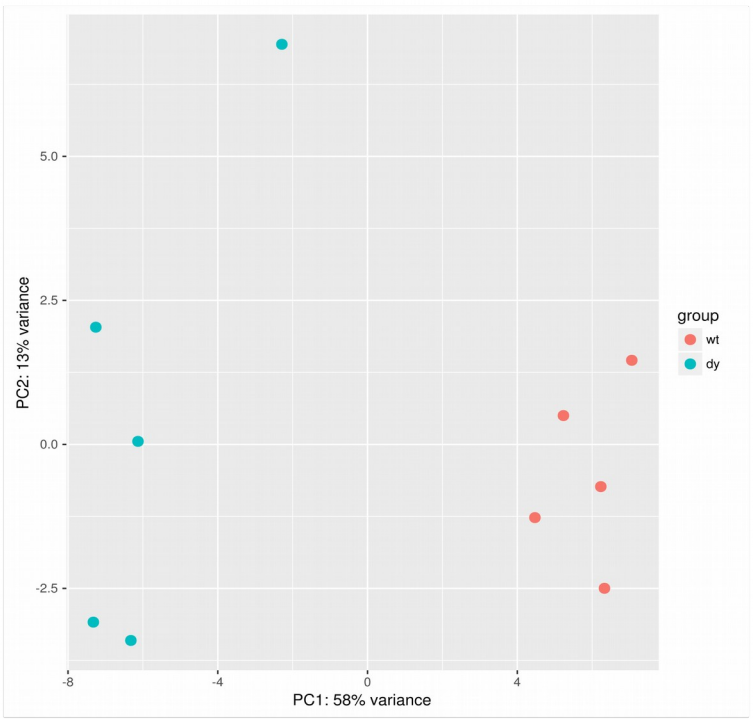
PC2: 13% variance
PC1: 58% variance
5.0
2.5
0.0
-2.5
-8
-4
0
4
group
wt
dy

FIGURE 2

A

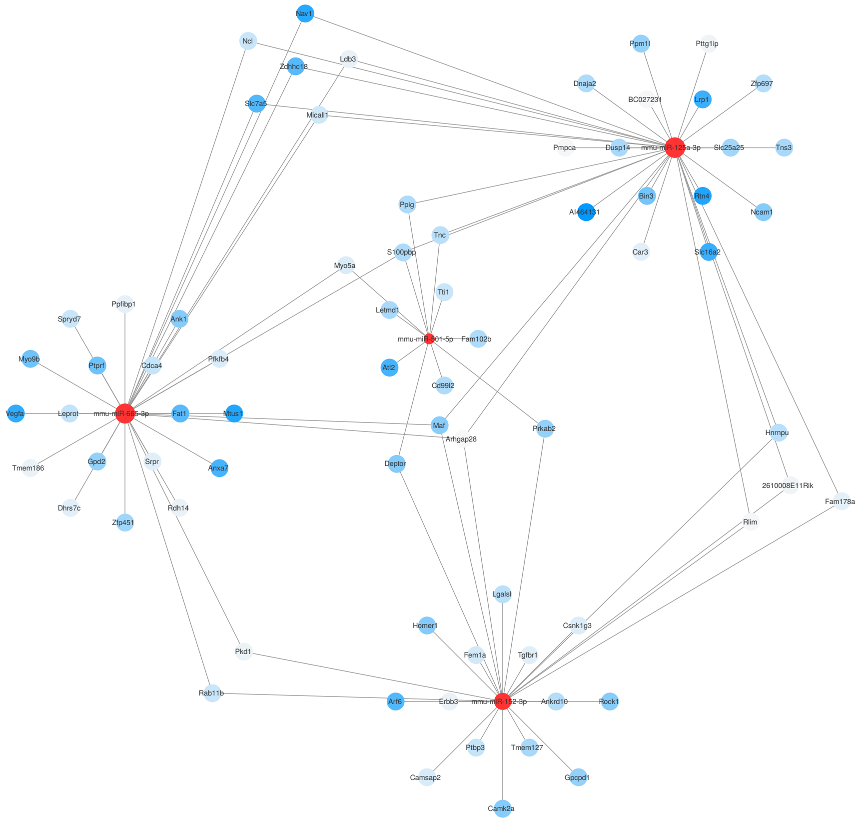
Nav1
Ncl
Ldb3
Zdhhc18
Slc7a5
Micall1
Ppm1l
Pttg1ip
Dnaja2
Zfp697
BC027231
Lrp1
Pmpca
Dusp14
mmu-miR-125a-3p
Slc25a25
Tns3
Ppig
Bin3
Rtn4
AI464131
Ncam1
Tnc
Car3
Slc16a2
S100pbp
Myo5a
Tti1
Letmd1
Fam102b
Atl2
Cd99l2
Ppfibp1
Spryd7
Ank1
Myo9b
Ptprf
Cdca4
Pfkfb4
Vegfa
Leprot
Fat1
Maf
Arhgap28
Prkab2
Hnrnpu
Tmem186
Gpd2
Srpr
Anxa7
Deptor
2610008E11Rik
Fam178a
Dhrs7c
Rdh14
Zfp451
Rlim
Lgalsl
Homer1
Csnk1g3
Fem1a
Tgfbr1
Pkd1
Rab11b
Arl6
Erbb3
mmu-miR-152-3p
Ankrd10
Rock1
Ptbp3
Tmem127
Camsap2
Gpcpd1
Camk2a

B

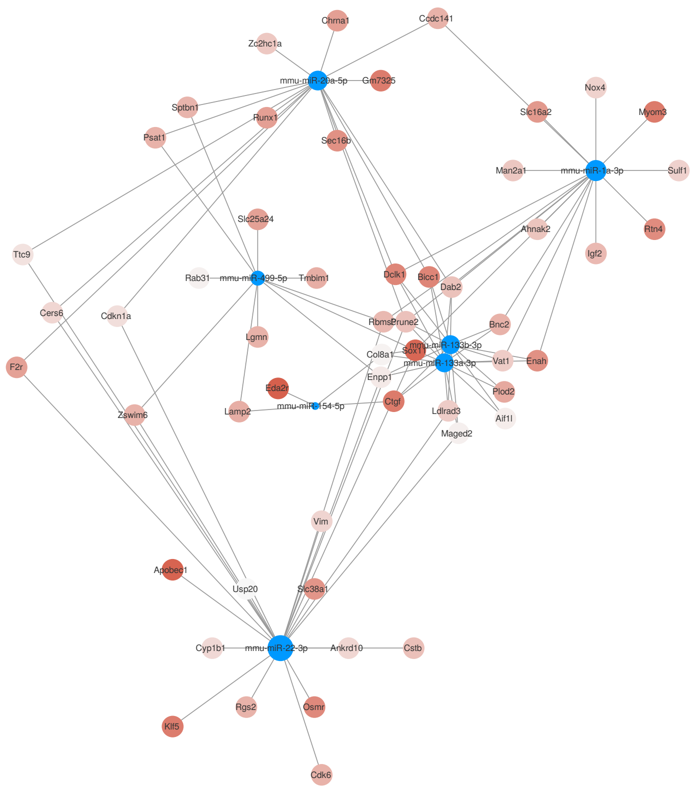
Chrna1
Ccdc141
Zc2hc1a
mmu-miR-26a-5p
Gm7325
Nox4
Sptbn1
Slc16a2
Myom3
Runx1
Psat1
Sec16b
Man2a1
mmu-miR-1a-3p
Sulf1
Slc25a24
Ahnak2
Rtn4
Ttc9
Igf2
Rab31
mmu-miR-499-5p
Tmbim1
Dclk1
Bicc1
Dab2
Cers6
Cdkn1a
Rbms
Prune2
Bnc2
Lgmn
mmu-miR-133b-3p
Col8a1
Sox11
mmu-miR-133a-3p
Vat1
Enah
F2r
Enpp1
Eda2r
Plod2
mmu-miR-154-5p
Ctgf
Zswim6
Lamp2
Ldlrad3
Aif1l
Maged2
Vim
Apobec1
Usp20
Slc38a1
Cyp1b1
mmu-miR-22-3p
Ankrd10
Cstb
Rgs2
Osmr
Klf5
Cdk6

SUP. FIGURE 1

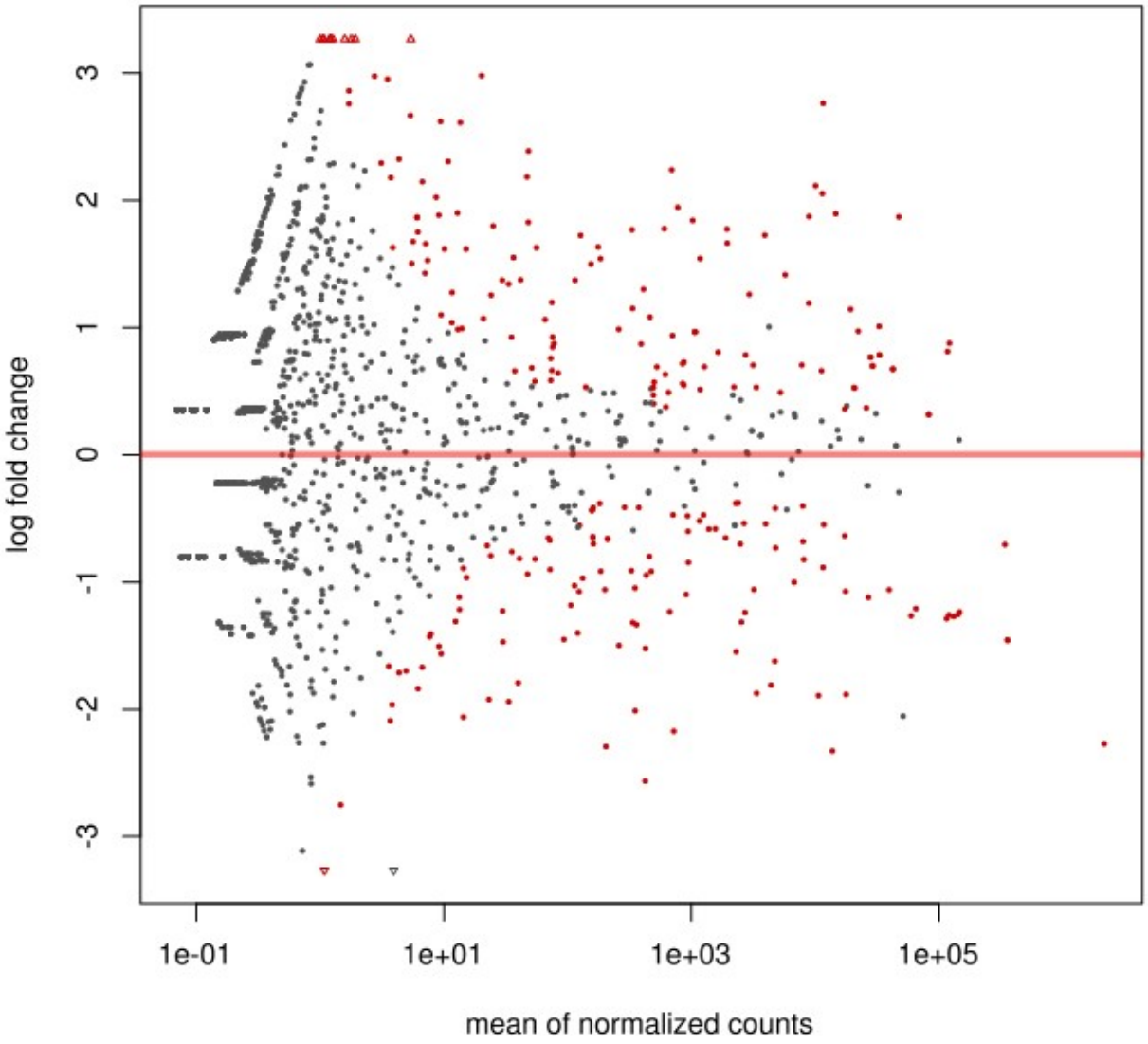
log fold change
3
2
1
0
-1
-2
-3
1e-01
1e+01
1e+03
1e+05
mean of normalized counts

Table 1. Up-regulated miRNAs in dy^{3K}/dy^{3K} skeletal muscle.

miRNA	Base mean	Log2 fold change	P-adjusted
mmu-miR-1188-5p	5,4018	3,2010	0,0000
mmu-miR-485-3p	20,4875	2,7043	0,0000
mmu-miR-223-3p	11743,2337	2,6297	0,0000
mmu-miR-147-5p	1,7908	2,4338	0,0043
mmu-miR-6922-5p	1,5795	2,3449	0,0060
mmu-miR-6394	13,7919	2,3133	0,0000
mmu-miR-673-5p	49,0415	2,2760	0,0000
mmu-miR-2139	9,5531	2,2560	0,0000
mmu-miR-409-3p	703,9058	2,1903	0,0000
mmu-miR-147-3p	3,5683	2,1396	0,0043
mmu-miR-370-3p	47,7388	2,1049	0,0000
mmu-miR-152-3p	10211,8869	2,0658	0,0000
mmu-miR-223-5p	11,0033	2,0453	0,0000
mmu-miR-7116-5p	1,9197	2,0294	0,0223
mmu-miR-214-3p	11569,2852	1,9949	0,0000
mmu-miR-6966-5p	1,2645	1,9771	0,0260
mmu-miR-702-3p	1,2020	1,9005	0,0335
mmu-miR-501-5p	5,4575	1,8969	0,0147
mmu-miR-665-3p	787,8759	1,8880	0,0000
mmu-miR-148b-3p	14869,4111	1,8560	0,0000
mmu-miR-7667-5p	2,8006	1,8543	0,0284
mmu-miR-6985-5p	1,0503	1,8464	0,0381
mmu-miR-142b	6,8106	1,8291	0,0019
mmu-miR-16-5p	48032,7070	1,8390	0,0000
mmu-miR-342-3p	9041,9845	1,8273	0,0000
mmu-miR-470-5p	4,4139	1,7905	0,0126
mmu-miR-142a-3p	1039,6201	1,7687	0,0000
mmu-miR-7676-3p	1,2034	1,7650	0,0495
mmu-miR-449b	8,8074	1,7533	0,0019
mmu-miR-214-5p	1965,0024	1,7331	0,0000
mmu-miR-5100	13,0874	1,7181	0,0003
mmu-miR-6389	336,1398	1,7094	0,0000
mmu-miR-543-3p	613,4066	1,7079	0,0000
mmu-miR-134-5p	3971,3889	1,6892	0,0000
mmu-miR-206-5p	48,8629	1,6887	0,0001
mmu-miR-133b-5p	129,0795	1,6711	0,0000
mmu-miR-376b-3p	1974,8193	1,6402	0,0000
mmu-miR-6371	9,2571	1,6187	0,0060
mmu-miR-3060-3p	6,1818	1,6099	0,0056
mmu-miR-132-3p	179,1053	1,5822	0,0000
mmu-miR-212-3p	56,8246	1,5792	0,0000
mmu-miR-3072-5p	6,1702	1,5737	0,0119
mmu-miR-2137	25,4100	1,5401	0,0109
mmu-miR-140-3p	1191,7496	1,5019	0,0000
mmu-miR-1930-5p	15,3619	1,4913	0,0006
mmu-miR-3473b	37,0728	1,4873	0,0000

mmu-miR-6341	186,8590	1,4757	0,0000
mmu-miR-302b-3p	6,2650	1,4634	0,0248
mmu-miR-449c-5p	10,2891	1,4496	0,0048
mmu-miR-132-5p	7,2425	1,4257	0,0176
mmu-miR-302d-3p	5,7279	1,4115	0,0275
mmu-miR-671-5p	156,6565	1,4093	0,0002
mmu-miR-99b-5p	5799,1860	1,3778	0,0000
mmu-miR-6923-5p	7,5135	1,3495	0,0141
mmu-miR-1936	42,3551	1,3248	0,0000
mmu-miR-5124a	116,6308	1,3002	0,0002
mmu-miR-3061-5p	5,5888	1,2890	0,0344
mmu-miR-142a-5p	33,9146	1,2707	0,0003
mmu-miR-652-5p	30,0790	1,2685	0,0041
mmu-miR-6419	7,1654	1,2294	0,0415
mmu-miR-574-3p	2977,5203	1,2153	0,0000
mmu-miR-380-3p	415,9370	1,1985	0,0079
mmu-miR-671-3p	24,4609	1,1832	0,0015
mmu-miR-667-5p	11,8442	1,1573	0,0189
mmu-miR-125a-3p	75,8170	1,1562	0,0000
mmu-miR-484	9007,9971	1,1469	0,0001
mmu-miR-192-5p	339,7628	1,1156	0,0000
mmu-miR-195a-5p	19570,3444	1,1012	0,0001
mmu-miR-194-5p	468,9640	1,0536	0,0000
mmu-miR-449a-5p	66,7366	1,0041	0,0069

Table 2. Down-regulated miRNAs in dy^{3K}/dy^{3K} skeletal muscle.

miRNA	**Base mean**	**Log2 fold change**	**P-adjusted**
mmu-miR-544-3p	429,4354	-2,5383	0,0000
mmu-miR-365-3p	13964,3498	-2,2392	0,0000
mmu-miR-1a-3p	2189415,2418	-2,2231	0,0000
mmu-miR-499-5p	206,7507	-2,1314	0,0000
mmu-miR-369-3p	731,0826	-2,0163	0,0000
mmu-miR-3544-5p	356,4450	-1,9955	0,0000
mmu-miR-7014-5p	14,6116	-1,8812	0,0001
mmu-miR-22-3p	10780,7092	-1,8636	0,0000
mmu-miR-3966	33,9808	-1,8604	0,0000
mmu-miR-337-3p	17990,3285	-1,8517	0,0000
mmu-miR-544-5p	23,5215	-1,8373	0,0000
mmu-miR-22-5p	3413,1853	-1,7883	0,0000
mmu-miR-154-5p	4456,0922	-1,7849	0,0000
mmu-miR-434-3p	52038,3759	-1,7330	0,0060
mmu-miR-29b-2-5p	40,4434	-1,7239	0,0000
mmu-miR-491-3p	3,7489	-1,5989	0,0335
mmu-miR-539-3p	3,8843	-1,5760	0,0257
mmu-miR-122-5p	6,2803	-1,5629	0,0122
mmu-miR-381-5p	4792,5410	-1,5507	0,0000

mmu-miR-1957b	2331,0350	-1,5161	0,0000
mmu-miR-137-3p	6,7969	-1,4678	0,0104
mmu-miR-29c-5p	263,7817	-1,4602	0,0000
mmu-miR-133b-3p	362138,5578	-1,4472	0,0000
mmu-miR-133a-3p	362336,7811	-1,4472	0,0000
Mmu-miR-540-5p	431,5793	-1,4216	0,0009
mmu-miR-495-5p	94,6648	-1,4128	0,0000
mmu-miR-1249-5p	5,0280	-1,4018	0,0382
mmu-miR-3092-3p	4,4165	-1,3991	0,0422
mmu-miR-300-5p	122,3388	-1,3824	0,0000
mmu-miR-6373	9,6605	-1,3791	0,0163
mmu-miR-3962	30,5328	-1,3513	0,0052
mmu-miR-669d-3p	9,2754	-1,3508	0,0122
mmu-miR-3071-3p	2573,5940	-1,3104	0,0000
mmu-miR-144-3p	365,5291	-1,2966	0,0000
mmu-miR-7115-3p	340,6924	-1,2850	0,0000
mmu-miR-6404	7,9732	-1,2633	0,0217
mmu-let-7e-5p	116836,4346	-1,2622	0,0000
mmu-let-7g-5p	132865,8654	-1,2530	0,0000
mmu-miR-9-3p	7,7953	-1,2530	0,0348
mmu-miR-98-5p	60308,6952	-1,2365	0,0000
mmu-let-7f-5p	144368,2590	-1,2352	0,0000
mmu-let-7c-5p	121757,5853	-1,2343	0,0000
mmu-miR-6382	2748,2424	-1,2215	0,0000
mmu-let-7a-5p	148449,1527	-1,2158	0,0000
mmu-miR-499-3p	12,6173	-1,2116	0,0103
mmu-miR-341-3p	678,4725	-1,1919	0,0002
mmu-miR-493-5p	30,3144	-1,1899	0,0001
mmu-let-7b-5p	65919,8845	-1,1808	0,0000
mmu-miR-9-5p	107,8352	-1,1571	0,0000
mmu-miR-103-2-5p	13,6029	-1,1399	0,0097
mmu-miR-30a-5p	27246,6611	-1,0918	0,0002
mmu-miR-30c-2-3p	125,7143	-1,0689	0,0000
mmu-miR-136-3p	919,0918	-1,0615	0,0013
mmu-miR-299a-5p	40091,4924	-1,0597	0,0000
mmu-miR-29c-3p	17824,7893	-1,0563	0,0000
mmu-miR-664-3p	203,1091	-1,0479	0,0000
mmu-miR-551b-3p	13,5289	-1,0435	0,0251
mmu-miR-20a-5p	3247,1080	-1,0426	0,0000

Table 3. Enriched KEGG terms at the 10% level.

Significant KEGG 2016 terms	**Overlap**	**P-adjusted**
Oxidative phosphorylation	13/133	0,0331
Alzheimer's disease	14/168	0,0418
Metabolic pathways	56/1239	0,0418
Huntington’s disease	15/193	0,0418

Non-alcoholic fatty liver disease	12/151	0,0579
Adrenergic signaling in cardiomyocytes	12/148	0,0579
AGE-RAGE signaling pathway in diabetic complications	9/101	0,0652
Cardiac muscle contraction	8/78	0,0579
Phagosome	12/154	0,0579
Parkinson’s disease	11/142	0,0652
Arginine and proline metabolism	6/50	0,0652
Alanine, aspartate and glutamate metabolism	5/35	0,0652

PLOS ONE

RESEARCH ARTICLE

Absence of microRNA-21 does not reduce muscular dystrophy in mouse models of LAMA2-CMD

Bernardo Moreira Soares Oliveira*, Madeleine Durbeej☯, Johan Holmberg☯

Muscle Biology Unit, Department of Experimental Medical Science, Lund University, Lund, Sweden

☯ These authors contributed equally to this work.
* bernardo.moreira_soares_oliveira@med.lu.se

Citation: Moreira Soares Oliveira B, Durbeej M, Holmberg J (2017) Absence of microRNA-21 does not reduce muscular dystrophy in mouse models of LAMA2-CMD. PLoS ONE 12(8): e0181950. https://doi.org/10.1371/journal.pone.0181950

Editor: Atsushi Asakura, University of Minnesota Medical Center, UNITED STATES

Received: May 5, 2017

Accepted: July 10, 2017

Published: August 3, 2017

Data Availability Statement: All relevant data are within the paper and its Supporting Information file.

Funding: This work was supported by the Conselho Nacional de Desenvolvimento Científico e Tecnológico (cnpq.br) to BO; Association Française contre les Myopathies to JH; Crafoord Foundation to JH; Greta and Johan Kock Foundation to MD; Lars Hierta Foundation to JH; Olle Engkvist Byggmästare Foundation to JH; Royal Physiographic Society in Lund to JH; Swedish

Abstract

MicroRNAs (miRNAs) are short non-coding RNAs that modulate gene expression post-transcriptionally. Current evidence suggests that miR-21 plays a significant role in the progression of fibrosis in muscle diseases. Laminin-deficient congenital muscular dystrophy (LAMA2-CMD) is a severe form of congenital muscular dystrophy caused by mutations in the gene encoding laminin α2 chain. Mouse models dy^{3K}/dy^{3K} and dy^{2J}/dy^{2J}, respectively, adequately mirror severe and milder forms of LAMA2-CMD. Both human and mouse LAMA2-CMD muscles are characterized by extensive fibrosis and considering that fibrosis is the final step that destroys muscle during the disease course, anti-fibrotic therapies may be effective strategies for prevention of LAMA2-CMD. We have previously demonstrated a significant up-regulation of the pro-fibrotic miR-21 in dy^{3K}/dy^{3K} and dy^{2J}/dy^{2J} skeletal muscle. Hence, the objective of this study was to explore if absence of miR-21 reduces fibrogenesis and improves the phenotype of LAMA2-CMD mice. Thus, we generated dy^{3K}/dy^{3K} and dy^{2J}/dy^{2J} mice devoid of miR-21 (dy^{3K}/miR-21 and dy^{2J}/miR-21 mice, respectively). However, the muscular dystrophy phenotype of dy^{3K}/miR-21 and dy^{2J}/miR-21 double knock-out mice was not improved compared to dy^{3K}/dy^{3K} or dy^{2J}/dy^{2J} mice, respectively. Mice displayed the same body weight, dystrophic muscles (with fibrosis) and impaired muscle function. These data indicate that miR-21 may not be involved in the development of fibrosis in LAMA2-CMD.

Introduction

Laminin-deficient congenital muscular dystrophy type 1A (LAMA2-CMD) is a severe form of muscular dystrophy caused by mutations in the *LAMA2* gene encoding the laminin α2 chain that together with laminin β1 and γ1 chains form the heterotrimeric molecule laminin-211. Without this laminin isoform, the muscle cell loses one of its main connections to the extracellular matrix and a series of deleterious events ensue. General symptoms of LAMA2-CMD include muscle wasting and weakness and delayed motor development [1]. Genotype-phenotype studies have established that complete absence of laminin α2 chain leads to a very severe muscular dystrophy (ambulation is typically not achieved) whereas partial deficiency causes a

Research Council to MD; Thelma Zoéga Foundation to JH and Österlund Foundation to MD. The funders had no role in study design, data collection and analysis, decision to publish, or preparation of the manuscript.

Competing interests: The authors have declared that no competing interests exist.

milder limb-girdle-type muscular dystrophy [2; 3] There are several relevant mouse models for LAMA2-CMD recapitulating grave and milder forms of LAMA2-CMD, including the dy^{3K}/dy^{3K} and dy^{2J}/dy^{2J} mouse models. The dy^{3K}/dy^{3K} mouse completely lacks laminin α2 chain and is the most severely affected among all LAMA2-CMD mouse models, with a life span of approximately 3 weeks. The dy^{2J}/dy^{2J} mouse has a moderate muscular dystrophy with a significantly longer survival, because it still expresses laminin α2 chain, albeit a truncated chain that is unable to polymerize [2; 3]. Several preclinical approaches to combat LAMA2-CMD in mice have been tested [2; 3]. Addressing the primary cause of the disease and trying to restore the connection between the muscle cell and the basement membrane has been the most successful line of attack, but translation into the clinics remains cumbersome [3–9] Thus, many efforts have also focused on secondary aspects to mitigate disease progression [10–14]. One of the main traits of LAMA2-CMD (as well as other types of muscular dystrophy) is the build-up of fibrotic tissue, which gradually replaces muscle [15–17]. Fibrotic tissue is less elastic and contractile than skeletal muscle, which consequently leads to decreased muscle function. Thus, attempts to prevent or reduce excessive fibrogenesis are highly desirable.

MicroRNAs (miRNAs) are short non-coding RNAs that modulate gene expression post-transcriptionally. Their mature form is about 22 nucleotides long and they work by complementary binding mRNA. Subsequently, miRNA-bound mRNA can be degraded (most cases) or translation is blocked, making miRNAs negative regulators of translation. MiRNA-21 (miR-21) has been implicated in fibrosis in different tissues [18–20]. It is a powerful mediator of fibrogenesis in the *mdx* mouse model of Duchenne muscular dystrophy [21; 22], with its suppression (by antagomirs for miR-21) leading to improved muscle phenotype whereas its over-expression (by miR-21 mimics) worsened it [22]. Furthermore, it was demonstrated that the miR-21 fibrogenic pathway involves PAI-1/urokinase-type plasminogen activator balance and TGF-β [21; 22]. MiR-21 expression is also stress-responsive, as evidenced by its elevated levels after exercise [23] or heart failure [19; 24]. Furthermore, it interacts with major players in fibrosis and inflammation such as TGF-β, Akt, MAPK, Toll-like receptors and osteopontin [19; 21; 25; 26]. Finally, we have demonstrated that miR-21 expression is significantly augmented in dy^{3K}/dy^{3K} (already at 9 days of age) and dy^{2J}/dy^{2J} muscle [27].

Therefore, the purpose of this study was to investigate if deleting miR-21 genetically in mouse models of LAMA2-CMD reduces fibrogenesis and improves the phenotype. Hence, we generated dy^{3K}/dy^{3K} and dy^{2J}/dy^{2J} mice devoid of miR-21 (dy^{3K}/miR-21 and dy^{2J}/miR-21 mice, respectively) and analyzed the phenotypes.

Materials and methods

Animal models

Laminin α2 chain-deficient dy^{3K}/dy^{3K} mice were previously described [28]. Heterozygous dy^{2J}/dy^{2J} (B6.WK-*Lama*$^{2dy\text{-}2J}$/J) [29; 30] and miR-21 ko (B6;129S6-*Mir21a*^{tm1Yoli}/J) [31] mice were purchased from Jackson Laboratory (Bar Harbor, ME) and bred in the Biomedical Center according to institutional animal care guidelines. Heterozygous dy^{3K}/+ and dy^{2J}/+ mice (healthy carriers of LAMA2-CMD), respectively, were mated with miR-21 ko mice. The resulting dy^{3K}/+:miR-21/+ males and females were mated to generate double knockout mice (dy^{3K}/miR-21), dy^{3K}/dy^{3K} mice, miR-21 ko and wild-type (WT) mice. Similarly, the resulting dy^{2J}/+:miR-21/+ males and females were mated to generate double knockout mice (dy^{2J}/miR-21), dy^{2J}/dy^{2J} mice, miR-21 ko and WT mice. Ear biopsies were used for genotyping. All experimental procedures involving animals were approved by the Malmö/Lund (Sweden) Ethical Committee for Animal Research (ethical permit number: M152-14) in accordance with the guidelines approved by the Swedish Board of Agriculture.

Animal handling and tissue collection. Three-week-old WT, miR-21 ko, dy^{3K}/dy^{3K}, dy^{3K}/miR-21 and 6-week-old WT, miR-21 ko, dy^{2J}/dy^{2J}, dy^{2J}/miR-21 mice were euthanized by CO_2. Quadriceps muscles were dissected for immunohistochemistry and embedded in O.C.T compound (Sakura Finetek, Torrance, CA) prior to freezing in liquid nitrogen or embedded in paraffin. Paraffin embedded specimens were sectioned using microtome (5 μm) (Microm H355, Cellab). Additionally, quadriceps muscles were dissected for hydroxyproline assay and frozen directly in liquid nitrogen.

RNA isolation and quantitative RT-PCR analysis

Total RNA was isolated from quadriceps muscles from 3-week-old WT, miR-21 ko, dy^{3K}/dy^{3K} and dy^{3K}/miR-21 mice and from 6-week-old WT, miR-21 ko, dy^{2J}/dy^{2J} and dy^{2J}/miR-21 mice using miRNeasy Mini Kit (Qiagen, Valencia, CA), including DNA digestion by DNase I following the manufacturer's specifications. Concentration and purity of RNA samples were assessed using NanoDrop 1000 Spectrophotometer (ThermoFisher Scientific, Waltham, MA). For miRNA expression analysis, 10 ng of muscle RNA was reverse transcribed to cDNA using the TaqMan Advanced miRNA cDNA Synthesis Kit (Applied Biosystems, Waltham, MA). For mRNA expression analysis, 50 ng RNA was reverse transcribed to cDNA using the High Capacity cDNA Reverse Transcription Kit (Applied Biosystems, Waltham, MA) according to manufacturer's protocol. The amplification was performed in a LightCycler 480 Real-Time PCR System (Roche Diagnostics, Basel Switzerland) using TaqMan Fast Advanced Master Mix. TaqMan probes detecting mouse miR-21, miR-93 (reference miRNA), TGF-β and Rn18s (reference gene) were used (Applied Biosystems, Waltham, MA). Comparative CT method was used for relative quantitation.

Histology and morphometric analysis

Muscle sections were stained with hematoxylin and eosin [32] or picro sirius red/fast green [27]. Stained cross-sections were scanned using Aperio's Scanscope CS2 (with Scanscope console v.8.2.0.1263, Aperio, Vista, CA) and representative images were created using Aperio software. Centrally nucleated muscle fibers representing regenerating muscle cells and peripherally nucleated normal muscle cells were counted in quadriceps muscles using ImageJ software version 1.43u (NIH, Bethesda, MD). A whole area of each muscle cross section was considered.

Sirius red/fast green quantification. Collagen content was quantified by a colorimetric method as described by Leon and Rojkind (1985) [33]. Briefly, approximately 15 paraffin sections of 15μm were placed in a plastic tube. Paraffin removal was accomplished by immersing the section in the following solutions: 5 min. xylene, 5 min. xylene/ethanol (1:1), 5 min. ethanol, 5 min. ethanol/water (1:1), 5 min. water. The sections were then stained with fast green/sirius red for 30 min. on rotation. The tissue was washed with distilled water until excess dye is removed and the solution is clear. One ml of 0.1 N NaOH was added and the solutions were analyzed for absorbance at 560 nm and 605 nm.

Hydroxyproline assay

Quadriceps muscles were isolated and frozen in liquid nitrogen. Samples were weighed and incubated overnight in 200 μl 12 M HCl at 95˚C. The hydrolyzate (25 μl) was neutralized with 0.6 M NaOH (25 μl) and incubated with 0.056 M chloramine-T reagent (450 μl) at room temperature for 25 min. Erlich's reagent (500 μl) was added to each sample and incubated for 1 hour at 65˚C, followed by cooling on ice. Subsequently, 100 μl (in duplicates) was transferred to a 96-well plate and absorbance was read at 560 nm. Standards from 4-hydroxyproline at

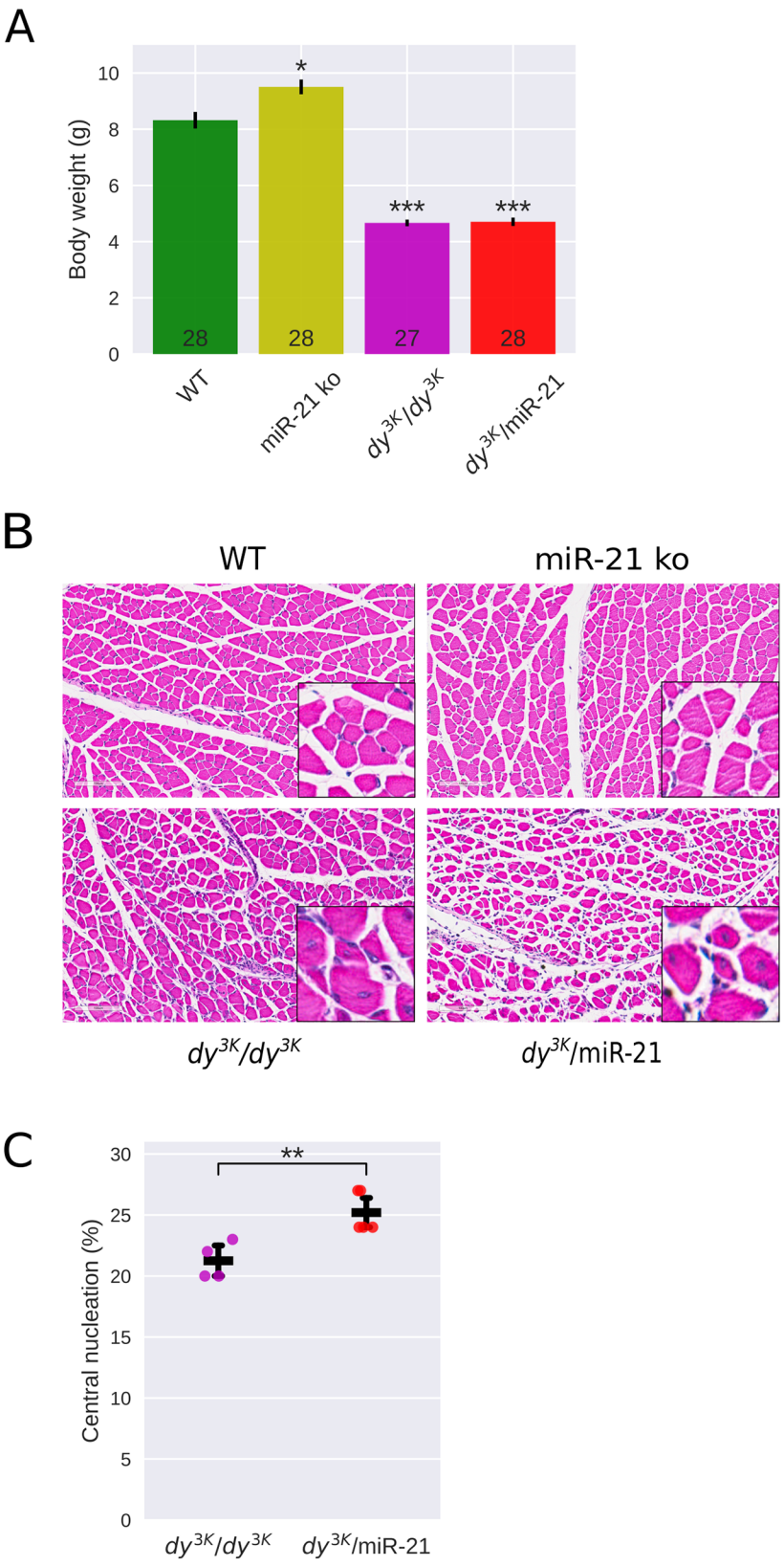

Fig 1. Muscular dystrophy hallmarks are not reduced in 3-week-old *dy^{3K}*/miR-21 mice. A. The body weight is significantly increased in miR-21 ko compared to wild-type (WT) mice but significantly reduced in

dy^{3K}/dy^{3K} and dy^{3K}/miR-21 mice. Notably, there is no significant difference between $dy^{3K}/dy^{3K}$and dy^{3K}/miR-21 mice. **B**. Hematoxylin & eosin staining of quadriceps muscles shows similar muscular dystrophy histopathology in $dy^{3K}/dy^{3K}$and dy^{3K}/miR-21 muscle. **C**. Quantification of centrally nucleated fibers shows significantly increased number of regenerating fibers in dy^{3K}/miR-21 compared to dy^{3K}/dy^{3K} quadriceps muscle. * $p < 0.05$, ** $p < 0.01$, *** $p < 0.001$.

https://doi.org/10.1371/journal.pone.0181950.g001

concentrations (μg/μl); 0, 0.05, 0.1, 0.15, 0.2, 0.25, 0.4 were treated the same way as the samples. Absorbance (A_{560}) of standards was plotted against amount of hydroxyproline (μg) and a linear regression was performed to determine slope and intercept. All absorbance values were subtracted with blank (0 μg/ml hydroxyproline). Content of hydroxyproline in samples was calculated by equation:

$$x(\mu g) = \frac{(A_{560} - y_{intercept})}{slope}$$

Collagen conversion factor = 13.5 [27]. Values are presented as μg collagen/mg muscle.

Grip strength

Forelimb grip strength was measured on a grip-strength meter (Columbus Instruments, Columbus, OH). In short, the mouse was held by the base of the tail and allowed to grasp the flat wire mesh of the pull bar with its forepaws. When the mouse got a good grip it was slowly pulled away by its tail until it released the pull bar. Each mouse was allowed to pull the pull bar five times. The two lowest values were rejected and the mean of the three remaining values was counted. Animals were not subjected to any training prior to the experiment.

Statistical analysis

The analyses were performed in the Ipython environment [34] using the SciPy (v. 0.18.1) [35] and statsmodels packages (v. 0.61). Difference between groups was assessed by one-way analysis of variance. Multiple test correction was done with the Bonferroni method. Significance was set at the 5% level.

Results

The phenotype of dy^{3K}/miR-21 double knock-out mice is not improved compared to dy^{3K}/dy^{3K} single knock-outs

Dy^{3K}/dy^{3K} mice display a very severe muscular dystrophy and have a median life span of approximately 3 weeks [3]. In order to investigate if deletion of miR-21 improves the phenotype of dy^{3K}/dy^{3K} mice, we generated mice (dy^{3K}/miR-21) lacking both laminin α2 chain and miR-21 (by series of breeding; please see Materials and methods for further information). Absence of miR-21 in dy^{3K}/miR-21 muscle was confirmed by RT-PCR (S1 Fig). The overall health of 3-week-old dy^{3K}/miR-21 mice was, however, not improved compared to dy^{3K}/dy^{3K} mice. Dy^{3K}/miR-21 mice exhibited similar decreased survival, growth retardation, muscle wasting, kyphosis and reduced body weight as dy^{3K}/dy^{3K} mice (Fig 1A).

Dy^{3K}/dy^{3K} muscle is characterized by enhanced apoptosis, degeneration/regeneration cycles, massive inflammation and substantial connective tissue infiltration (fibrosis) [3]. Histological analyses of quadriceps femoris muscle sections from 3-week-old dy^{3K}/miR-21 mice revealed that dystrophic alterations were readily present, just like in dy^{3K}/dy^{3K} muscle (Fig 1B). Regenerating fibers with centrally located nuclei were in fact increased in dy^{3K}/miR-21 muscle compared to dy^{3K}/dy^{3K} muscle (Fig 1C). Measures of fibrosis (sirius red and fast green staining,

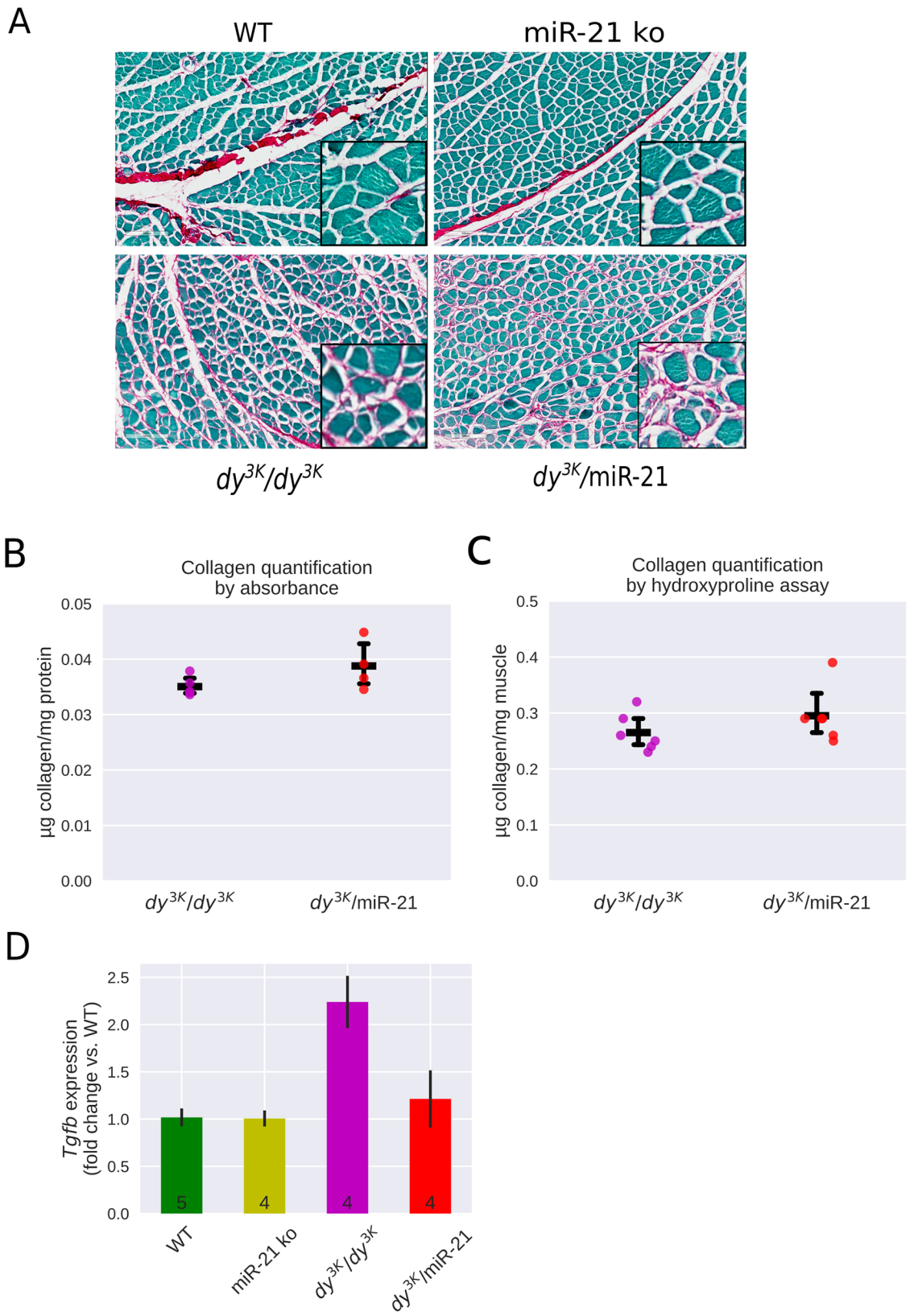

Fig 2. Fibrotic lesions are equally abundant in muscles from dy^{3K}/dy^{3K} and dy^{3K}/miR-21 mice. A. Picrosirius red/fast green stained sections demonstrate significant fibrosis (collagen deposition in pink) in dy^{3K}/dy^{3K} and dy^{3K}/miR-21

quadriceps muscle. **B**. Sirius red/fast green quantification of collagen content in dy^{3K}/dy^{3K} and dy^{3K}/miR-21 quadriceps muscle. **C.** Biochemical collagen quantification (hydroxyproline assay) in dy^{3K}/dy^{3K} and dy^{3K}/miR-21 quadriceps muscle. Please note that collagen content is very similar in dy^{3K}/dy^{3K} and dy^{3K}/miR-21 muscle. **D.** qPCR analysis of TGF-β transcript levels in WT, miR-21 ko, dy^{3K}/dy^{3K} and dy^{3K}/miR-21 quadriceps muscle.

https://doi.org/10.1371/journal.pone.0181950.g002

visualizing collagenous and non-collagenous tissue, respectively, as well as biochemical collagen quantification) demonstrated that a similar deposition of collagen was present in dy^{3K}/miR-21 and dy^{3K}/dy^{3K} muscle (Fig 2A–2C). Finally, expression of TGF-β (a master regulator of fibrosis) has been shown to be enhanced in LAMA2-CMD muscle [16; 36] but analysis of TGF-β gene expression revealed no reduction of TGF-β transcript levels upon miR-21 deletion in dy^{3K}/dy^{3K} muscle (Fig 2D).

In summary, our results indicated that removal of miR-21 has no beneficial effects in the severely affected dy^{3K}/dy^{3K} mouse model. Considering that inhibition of miR-21 expression reduced fibrosis in the mildly affected dystrophin-deficient *mdx* mouse model of Duchenne muscular dystrophy [21], we next investigated if removal of miR-21 would have propitious effects in the milder LAMA2-CMD dy^{2J}/dy^{2J} mouse model.

The phenotype of dy^{2J}/miR-21 double knock-out mice is not improved compared to dy^{2J}/dy^{2J} single knock-outs

We generated dy^{2J}/miR-21 mice expressing a polymerization-defective truncated laminin α2 chain with no miR-21 (by series of breeding; please see Materials and methods for further information). Similar to the dy^{3K}/miR-21 mouse, the overall health of 6-week-old dy^{2J}/miR-21 mice was not improved compared to that of dy^{2J}/dy^{2J} mice and dy^{2J}/miR-21 mice exhibited a similar reduction in body weight and hindleg paralysis (Fig 3A).

Dy^{2J}/dy^{2J} muscle is also characterized by enhanced apoptosis, degeneration/regeneration cycles, inflammation and connective tissue infiltration [3; 27]. Histological analyses of quadriceps muscle sections from 6-week-old dy^{2J}/miR-21 mice revealed that dystrophic alterations were readily present, just like in dy^{2J}/dy^{2J}mice (Fig 3B). Regenerating fibers with centrally located nuclei were present to a similar degree in dy^{2J}/miR-21 and dy^{2J}/dy^{2J} muscle (Fig 3C). Sirius red and fast green staining revealed a similar collagen deposition in dy^{2J}/miR-21 and dy^{2J}/dy^{2J} muscle (Fig 4A), but when quantified, a small but significant reduction in collagen deposition was noted in dy^{2J}/miR-21 muscle (Fig 4B). Biochemical collagen quantification (hydroxyproline assay), on the other hand, demonstrated similar collagen accumulation in dy^{2J}/dy^{2J} and dy^{2J}/miR-21 muscle (Fig 4C). Also, expression of TGF-β mRNA was comparable in dy^{2J}/dy^{2J} and dy^{2J}/miR-21 quadriceps muscle (Fig 4D). Finally, we assessed forelimb grip strength. It has previously been demonstrated that grip strength is significantly decreased in 6-week-old dy^{2J}/dy^{2J} mice, compared to wild-type animals [27]. We found that normalized grip strength (strength divided by body weight) was very similar in dy^{2J}/miR-21 and dy^{2J}/dy^{2J} mice (Fig 4E).

Altogether, our results indicate that removal of miR-21 has no beneficial effects in the severely affected dy^{3K}/dy^{3K} or in the mildly affected dy^{2J}/dy^{2J} mouse model of LAMA2-CMD.

Discussion

The present study aimed at investigating potential benefits of deleting miR-21, a known pro-fibrotic miRNA, in LAMA2-CMD. We present evidence that deleting miR-21 in two different LAMA2-CMD mouse models is insufficient to reduce fibrotic tissue build up and improve the skeletal muscle phenotype. In general, we did not observe any change or improvement due to miR-21 absence, neither on wild-type nor dy^{3K}/dy^{3K} and dy^{2J}/dy^{2J} backgrounds, apart from a possible minor reduction in collagen content in dy^{2J}/miR-21 muscle. This is in sharp contrast to

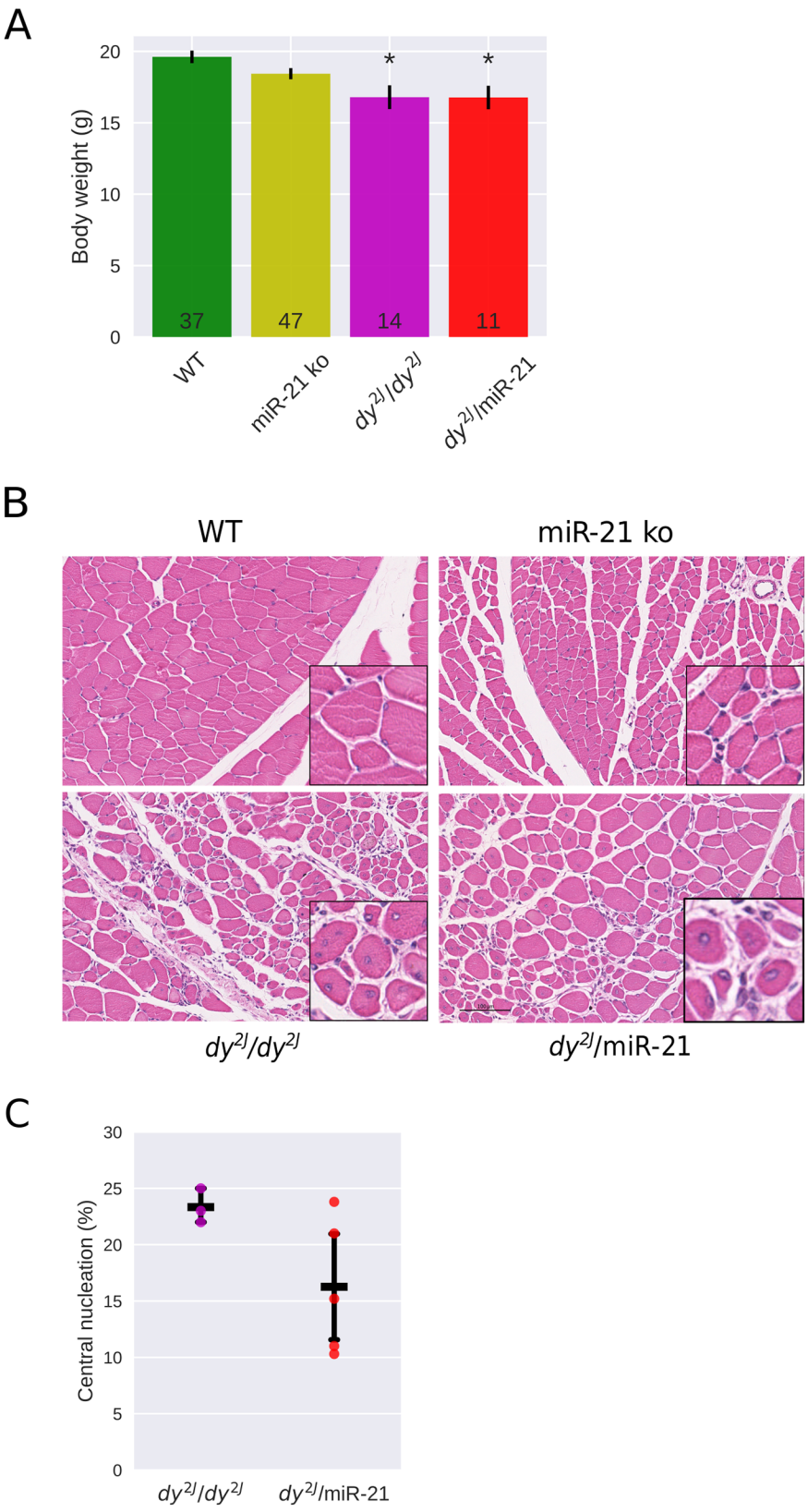

Fig 3. Muscular dystrophy hallmarks are not reduced in 6-week-old *dy*^{2J}/miR-21 mice. A. Body weight is significantly reduced in *dy*^{2J}/*dy*^{2J} and *dy*^{2J}/miR-21 compared to WT mice but is not significantly different

between dy^{2J}/dy^{2J} and dy^{2J}/miR-21 mice. **B**. Hematoxylin & eosin staining of quadriceps muscles shows similar muscular dystrophy histopathology in dy^{2J}/dy^{2J} and dy^{2J}/miR-21 muscle. **C**. Central nucleation is similar in dy^{2J}/dy^{2J} and dy^{2J}/miR-21 in quadriceps muscle. * $p < 0.05$.

https://doi.org/10.1371/journal.pone.0181950.g003

previous studies on *mdx* mice where inhibition of miR-21 significantly improved disease phenotype [22]. The differences to the aforementioned study could be due to the mouse strains used (*mdx* vs. $dy^{3K}/dy^{3K}$and dy^{2J}/dy^{2J}) and it is important to note that the *mdx* mouse has mild clinical symptoms in contrast to both dy^{3K}/dy^{3K} and dy^{2J}/dy^{2J} mice [2]. Also, the strategy for miR-21 inhibition was different. An antagomir for mir-21 was utilized to silence expression in *mdx* mice whereas a constitutive genetic deletion was used in dy^{3K}/dy^{3K} and dy^{2J}/dy^{2J} animals, possibly activating compensatory mechanisms over the course of development. We cannot entirely rule out the possibility that removal of miR-21 could have beneficial effects in older dy^{2J}/dy^{2J} animals. However, at 6 weeks of age dy^{2J}/dy^{2J} mice display a full-blown muscular dystrophy but dy^{2J}/dy^{2J} mice have an extended life span compared to $dy^{3K}dy^{3K}$ mice (more than 6 months vs. 3 weeks) suggesting that no major worsening of the skeletal muscle phenotype appears after 6 weeks of age.

Despite its bad reputation, inflammation and the ensuing immunological response, is actually fundamental for muscle homeostasis [26]. In healthy tissue there is a fine balance between pro- and anti-inflammatory cues in response to injury and the resolution of the inflammatory response allows for recovery of tissue morphology and function. In LAMA2-CMD, however, this balance is heavily tilted towards pro-inflammatory signals, leading to a state of chronic inflammation [31; 37] Interestingly, miR-21 is also involved in inflammation. Tissue damage leads to increased miR-21 expression through (p38) MAPK [26]. MiR-21 then targets PTEN, an inhibitor of Akt. Relieved from PTEN's inhibition Akt is free to promote fibroblast proliferation thus increasing collagen synthesis [19–21, 24, 37]. In macrophages the same pathway acts to transition the cells from a pro-inflammatory state into an anti-inflammatory one. In healthy tissue this transition allows the resolution of inflammation and tissue recovery. Under chronic inflammation, however, persistently elevated levels of miR-21 will lead to sustained Akt activity and thus prolonged fibroblast proliferation and delayed transition of macrophages, shortening their anti-inflammatory state [25; 26].

miR-21 has also been shown to promote kidney fibrosis and, in contrast to LAMA2-CMD mouse models, both genetic deletion of miR-21 and inhibition with an antagomir reduced fibrogenesis in mouse models [18]. One explanation to the different outcome in response to miR-21 removal is related to organ-specific aspects of fibrosis. Although various signalling pathways associated with the fibrotic process are conserved across different organs, it is well known that unique, organ-specific features of fibrosis exist [37]. It is also possible that the lack of response upon miR-21 removal in LAMA2-CMD mouse models is due to miRNA promiscuity. That is, one miRNA can target several genes and a single gene can be targeted by many miRNAs. Tarbase (v. 7.0) [38], a manually curated database of experimentally validated miRNA targets, lists 824 unique miR-21a-5p targets, although none in skeletal muscle tissue. MiR-21a-3p has 626 target genes, 160 in common with miR-21a-5p. Moreover, 399 different miRNAs have at least one common target with miR-21a-5p, with 137 having more than 50 common targets. In this scenario it seems very likely that other miRNAs may compensate for miR-21 deficiency. In summary, we have demonstrated that removing miR-21 is not sufficient to improve muscle morphology and function in LAMA2-CMD mouse models. Future research employing multiple miR KOs will have to investigate whether removing other miRNAs that work synergistically with miR-21 represents a better strategy and expanding the list of miR-21 validated targets to include skeletal muscle tissue would help us in that direction.

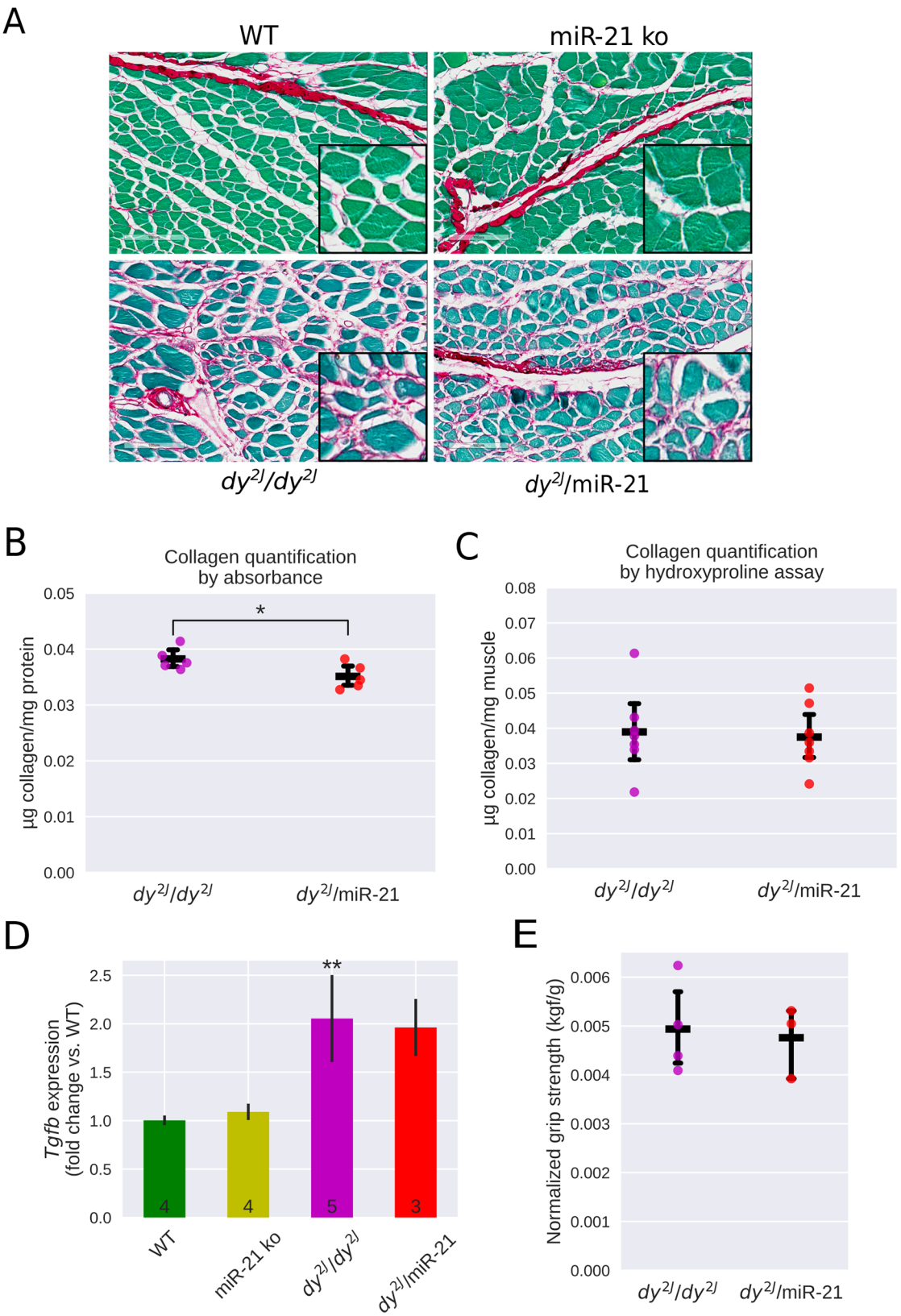

Fig 4. Fibrotic lesions and grip strength in dy^{2J}/dy^{2J} and dy^{2J}/miR-21 mice. A. Sirius red/fast green stained sections demonstrate significant fibrosis (collagen deposition in pink) in dy^{2J}/dy^{2J} and dy^{2J}/miR-21 quadriceps muscle. **B**. Sirius

red/fast green quantification of collagen content demonstrates slightly reduced fibrosis in dy^{2J}/miR-21 compared to dy^{2J}/dy^{2J} quadriceps muscle. **C**. Hydroxyproline assay reveals no difference in collagen content between dy^{2J}/dy^{2J} and dy^{2J}/miR-21 muscle. **D.** qPCR analysis of TGF-β transcript levels in WT, miR-21 ko, dy^{2J}/dy^{2J} and dy^{2J}/miR-21 quadriceps muscle. **E**. Grip strength testing uncovers similar forelimb muscle strength (normalized to body weight) in dy^{2J}/dy^{2J} and dy^{2J}/miR-21 mice. * $p < 0.05$.

https://doi.org/10.1371/journal.pone.0181950.g004

Supporting information

S1 Fig. miR-21 qPCR. Absence of miR-21 in dy^{3K}/miR-21 mice. Mice with the same miR-21 ko background were used to generate dy^{2J}/miR-21 mice.
(TIF)

Author Contributions

Conceptualization: Madeleine Durbeej, Johan Holmberg.

Data curation: Bernardo Moreira Soares Oliveira.

Formal analysis: Bernardo Moreira Soares Oliveira.

Funding acquisition: Madeleine Durbeej, Johan Holmberg.

Methodology: Bernardo Moreira Soares Oliveira, Johan Holmberg.

Project administration: Madeleine Durbeej, Johan Holmberg.

Software: Bernardo Moreira Soares Oliveira.

Supervision: Madeleine Durbeej, Johan Holmberg.

Visualization: Bernardo Moreira Soares Oliveira.

Writing – original draft: Bernardo Moreira Soares Oliveira, Madeleine Durbeej.

Writing – review & editing: Bernardo Moreira Soares Oliveira, Madeleine Durbeej, Johan Holmberg.

References

1. Holmberg J. and Durbeej M. (2013). Laminin-211 in skeletal muscle function, Cell Adhesion and Migration 7: 1–11. https://doi.org/10.4161/cam.22495
2. Allamand V. (2002). Animal models for muscular dystrophy: valuable tools for the development of therapies, Human Molecular Genetics 9: 2459–2467.
3. Gawlik K. I. and Durbeej M. (2011). Skeletal muscle laminin and MDC1A: pathogenesis and treatment strategies, Skeletal Muscle 1.
4. Kuang W.; Xu H.; Vachon P. H.; Liu L.; Loechel F.; Wewer U. M. et al. (1998). Merosin-deficient congenital muscular dystrophy. Partial genetic correction in two mouse models., The Journal of Clinical Investigation 102: 844–852. https://doi.org/10.1172/JCI3705 PMID: 9710454
5. Moll J.; Barzaghi P.; Lin S.; Bezakova G.; Lochmüller H.; Engvall E. et al. (2001). An agrin minigene rescues dystrophic symptoms in a mouse model for congenital muscular dystrophy, Nature 413: 302–307. https://doi.org/10.1038/35095054 PMID: 11565031
6. Gawlik K.; Miyagoe-Suzuki Y.; Ekblom P.; Takeda S. and Durbeej M. (2004). Laminin a1 chain reduces muscular dystrophy in laminin a2 chain deficient mice, Human Molecular Genetics 13: 1775–1784. https://doi.org/10.1093/hmg/ddh190 PMID: 15213105
7. Gawlik K. I. and Durbeej M. (2010). TRANSGENIC OVEREXPRESSION OF LAMININ a1 CHAIN IN LAMININ a2 CHAIN–DEFICIENT MICE RESCUES THE DISEASE THROUGHOUT THE LIFESPAN, Muscle Nerve 42: 30–37. https://doi.org/10.1002/mus.21616 PMID: 20544910
8. Rooney J. E.; Knapp J. R.; Hodges B. L.; Wuebbles R. D. and Burkin D. J. (2012). Laminin-111 Protein Therapy Reduces Muscle Pathology and Improves Viability of a Mouse Model of Merosin-Deficient

Congenital Muscular Dystrophy, The American Journal of Pathology 180: 1593–1602. https://doi.org/10.1016/j.ajpath.2011.12.019 PMID: 22322301

9. McKee K. K.; Crosson S. C.; Meinen S.; Reinhard J. R.; Rüegg M. A. and Yurchenco P. D. (2017). Chimeric protein repair of laminin polymerization ameliorates muscular dystrophy phenotype, The Journal of Clinical Investigation 127: 1075–1089. https://doi.org/10.1172/JCI90854 PMID: 28218617
10. Girgenrath M.; Dominov J. A.; Kostek C. A. and Miller J. B. (2004). Inhibition of apoptosis improves outcome in a model of congenital muscular dystrophy, The Journal of Clinical Investigation 114: 1635–1639. https://doi.org/10.1172/JCI22928 PMID: 15578095
11. Erb M.; Meinen S.; Barzaghi P.; Sumanovski L. T.; Courdier-Früh I.; Rüegg M. A. et al. (2009). Omigapil Ameliorates the Pathology of Muscle Dystrophy Caused by Laminin-α2 Deficiency, Journal of Pharmacology and Experimental Therapeutics 331: 787–795. https://doi.org/10.1124/jpet.109.160754 PMID: 19759319
12. Carmignac V.; Quéré R. and Durbeej M. (2011). Proteasome inhibition improves the muscle of laminin a2 chain-deficient mice, Human Molecular Genetics 20: 541–552. https://doi.org/10.1093/hmg/ddq499 PMID: 21084425
13. Carmignac V.; Svensson M.; Körner Z.; Elowsson L.; Matsumura C.; Gawlik K. I. et al. (2011). Autophagy is increased in laminin a2 chain-deficient muscle and its inhibition improves muscle morphology in a mouse model of MDC1A, Human Molecular Genetics 20: 4891–4902. https://doi.org/10.1093/hmg/ddr427 PMID: 21920942
14. Kumar A.; Yamauchi J.; Girgenrath T. and Girgenrath M. (2011). Muscle-specific expression of insulin-like growth factor 1 improves outcome in Lama2Dy-w mice, a model for congenital muscular dystrophy type 1A, Human Molecular Genetics 20: 2333. https://doi.org/10.1093/hmg/ddr126 PMID: 21441569
15. Elbaz M.; Yanay N.; Aga-Mizrachi S.; Brunschwig Z.; Kassis I.; Ettinger K. et al. (2012). Losartan, a therapeutic candidate in congenital muscular dystrophy: Studies in the dy2J/dy2J Mouse, Annals of Neurology 71: 1531-8249699-708.
16. Meinen S.; Lin S. and Ruegg M. A. (2012). Angiotensin II type 1 receptor antagonists alleviate muscle pathology in the mouse model for laminin-α2-deficient congenital muscular dystrophy (MDC1A), Skeletal Muscle 2.
17. Accorsi A.; Kumar A.; Rhee Y.; Miller A. and Girgenrath M. (2016). IGF-1/GH axis enhances losartan treatment in Lama2-related muscular dystrophy, Human Molecular Genetics 25.
18. Chau B. N.; Xin C.; Hartner J.; Ren S.; Castano A. P.; Linn G. et al. (2012). MicroRNA-21 Promotes Fibrosis of the Kidney by Silencing Metabolic Pathways, Science Translational Medicine 4.
19. Lorenzen J. M.; Schauerte C.; Hübner A.; Kölling M.; Martino F.; Scherf K. et al. (2015). Osteopontin is indispensible for AP1-mediated angiotensin II-related miR-21 transcription during cardiac fibrosis, Eur Heart J 36: 2184–2196. https://doi.org/10.1093/eurheartj/ehv109 PMID: 25898844
20. Zanotti S.; Gibertini S.; Curcio M.; Savadori P.; Pasanisi B.; Morandi L. et al. (2015). Opposing roles of miR-21 and miR-29 in the progression of fibrosis in Duchenne muscular dystrophy, Biochimica et Biophysica Acta 1852: 1451–1464. https://doi.org/10.1016/j.bbadis.2015.04.013 PMID: 25892183
21. Ardite E.; Perdiguero E.; Vidal B.; Gutarra S.; Serrano A. L. and Muñoz-Cánoves P. (2012). PAI-1–regulated miR-21 defines a novel age-associated fibrogenic pathway in muscular dystrophy, The Journal of Cell Biology 196: 163–175. https://doi.org/10.1083/jcb.201105013 PMID: 22213800
22. Acuna M. J.; Pessina P.; Olguin H.; Cabrera D.; Vio C. P.; Bader M. et al. (2013). Restoration of muscle strength in dystrophic muscle by angiotensin-1-7 through inhibition of TGF-β signalling, Human Molecular Genetics 23: 1237–1249. https://doi.org/10.1093/hmg/ddt514 PMID: 24163134
23. Tonevitsky A.; Maltseva D.; Abbasi A.; Samatov T.; Sakharov D.; Shkurnikov M. et al. (2013). Dynamically regulated miRNA-mRNA networks revealed by exercise, BMC Physiology 13: 9. https://doi.org/10.1186/1472-6793-13-9 PMID: 24219008
24. Thum T.; Gross C.; Fiedler J.; Fischer T.; Kissler S.; Bussen M. et al. (2008). MicroRNA-21 contributes to myocardial disease by stimulating MAP kinase signalling in fibroblasts, Nature 456: 980–984. https://doi.org/10.1038/nature07511 PMID: 19043405
25. Perdiguero E.; Sousa-Victor P.; Ruiz-Bonilla V.; Jard M.; Caelles C.; Serrano A. L. et al. (2011). p38/MKP-1textendashregulated AKT coordinates macrophage transitions and resolution of inflammation during tissue repair, J Cell Biol 195: 307–322. https://doi.org/10.1083/jcb.201104053 PMID: 21987635
26. Perdiguero E.; Kharraz Y.; Serrano A. L. and Muñoz-Cánoves P. (2012). MKP-1 coordinates ordered macrophage-phenotype transitions essential for stem cell-dependent tissue repair, Cell Cycle 11: 877–886. https://doi.org/10.4161/cc.11.5.19374 PMID: 22361726
27. Holmberg J.; Alajbegovic A.; Gawlik K. I.; Elowsson L. and Durbeej M. (2014). Laminin α2 Chain-Deficiency is Associated with microRNA Deregulation in Skeletal Muscle and Plasma, Frontiers in Aging Neuroscience 6.

28. Miyagoe Y.; Hanaoka K.; Nonaka I.; Hayasaka M.; Nabeshima Y.; Arahata K. et al. (1997). Laminin α2 chain-null mutant mice by targeted disruption of the Lama2 gene: a new model of merosin (laminin 2)-deficient congenital muscular dystrophy, FEBS Letters 415: 33–39. PMID: 9326364

29. Sunada Y.; Bernier S. M.; Kozak C. A.; Yamada Y. and Campbell K. P. (1994). Deficiency of merosin in dystrophic dy mice and genetic linkage of laminin M chain gene to dy locus., Journal of Biological Chemistry 269: 13729–13732. PMID: 8188645

30. Xu H.; Wu X.-R.; Wewer U. M. and Engvall E. (1994). Murine muscular dystrophy caused by a mutation in the laminin upalpha2 (Lama2) gene, Nature Genetics 8: 297–302. https://doi.org/10.1038/ng1194-297 PMID: 7874173

31. Ma X.; Kumar M.; Choudhury S. N.; Becker Buscaglia L. E.; Barker J. R.; Kanakamedala K. et al. (2011). Loss of the miR-21 allele elevates the expression of its target genes and reduces tumorigenesis, Proceedings of the National Academy of Sciences 108: 10144–10149.

32. Gawlik K. I.; Holmberg J. and Durbeej M. (2014). Loss of Dystrophin and b-Sarcoglycan Significantly Exacerbates the Phenotype of Laminin a2 Chain-Deficient Animals, The American Journal of Pathology 184: 740–752. https://doi.org/10.1016/j.ajpath.2013.11.017 PMID: 24393714

33. Leon A. L.-D. and Rojkind M. (1985). A simple micromethod for collagen and total protein determination in formalin-fixed paraffin-embedded sections., Journal of Histochemistry & Cytochemistry 33: 737–743.

34. Perez F. and Granger B. E. (2007). IPython: A System for Interactive Scientific Computing, Computing in Science & Engineering 9: 21–29.

35. Jones, E.; Oliphant, T.; Peterson, P. and others (2001). *SciPy: Open source scientific tools for Python*,.

36. Gawlik K. I.; Holmberg J.; Svensson M.; Einerborg M.; Oliveira B. M. S.; Deierborg T. et al. (2017). Potent pro-inflammatory and pro-fibrotic molecules, osteopontin and galectin-3, are not major disease modulators of laminin upalpha2 chain-deficient muscular dystrophy, Scientific Reports 7: 44059. https://doi.org/10.1038/srep44059 PMID: 28281577

37. Zeisberg M. and Kalluri R. (2013). Cellular Mechanisms of Tissue Fibrosis. 1. Common and organ-specific mechanisms associated with tissue fibrosis, American Journal of Physiology—Cell Physiology 304: C216–C225. https://doi.org/10.1152/ajpcell.00328.2012 PMID: 23255577

38. Vlachos I. S.; Paraskevopoulou M. D.; Karagkouni D.; Georgakilas G.; Vergoulis T.; Kanellos I. et al. (2014). DIANA-TarBase v7.0: indexing more than half a million experimentally supported miRNA: mRNA interactions, Nucleic Acids Research 43: D153–D159. https://doi.org/10.1093/nar/gku1215 PMID: 25416803

Exploratory profiling of urine microRNAs in the *dy^{2J}/dy^{2J}* mouse model of LAMA2-CMD: relation to disease progression

Bernardo Moreira Soares Oliveira*, Kinga I Gawlik, Madeleine Durbeej[#] and Johan Holmberg[#]

Muscle Biology Unit, Department of Experimental Medical Science, Lund University.

BMC C12, 221 84, Lund, Sweden

[#]Equal contribution

*Corresponding author: bernardo.moreira_soares_oliveira@med.lu.se, +46462220679

BMC C12
221 84 Lund
Sweden

Conflict of interests: the authors declare that no competing interests exist.
Data availability: all data and access information is contained in the article.

Funding:
CNPq, Association Française contre les Myopathies, Crafoord foundation, Greta and Johan Kock foundation, Lars Hierta foundation, Olle Engkvist Byggmästare foundation, Royal Physiographic Society in Lund, Swedish Research Council, Thelma Zoéga foundation, Österlund foundation, Anna and Edwin Berger foundation. The funders had no role in study design, data collection and analysis, decision to publish, or preparation of the manuscript.

ABSTRACT

Circulating microRNAs (miRNAs) are being considered as non-invasive biomarkers for disease progression and clinical trials. Congenital muscular dystrophy with deficiency of laminin α2 chain (LAMA2-CMD) is a very severe form of muscular dystrophy, for which no treatment is available. In order to identify LAMA2-CMD biomarkers we have profiled miRNAs in urine from the *dy*^{2J}/*dy*^{2J} mouse model of LAMA2-CMD at three distinct time points (representing asymptomatic, initial and established disease). We demonstrate that unique groups of miRNAs are differentially expressed at each time point. To our knowledge, this is the first time that a urine miRNA profile for muscular dystrophy has been presented. We suggest that urine miRNAs can be sensitive biomarkers for different stages of LAMA2-CMD.

INTRODUCTION

Laminin α2 chain-deficient congenital muscular dystrophy, or LAMA2-CMD, is a severe form of muscular dystrophy caused by mutations in the *LAMA2* gene. Genotype-phenotype analyses have demonstrated that complete deficiency of laminin α2 chain leads to a more severe phenotype whereas partial absence leads to a milder disease course. The clinical manifestations of complete laminin α2 chain-deficiency include profound hypotonia at birth, widespread muscle weakness, proximal joint contractures, scoliosis and delayed motor milestones. Patients may achieve unsupported sitting but very few children acquire independent ambulation. Individuals with partial deficiency often have later onset of proximal muscle weakness and delayed motor milestones but achieve independent ambulation [1].

There are several mouse models for laminin α2 chain-deficiency that adequately represent the clinical heterogeneity of LAMA2-CMD and phenocopy the skeletal muscle changes. The dy^{3K}/dy^{3K} mouse completely lacks laminin α2 chain and displays a very severe muscular dystrophy with a median survival of three weeks whilst the dy^{2J}/dy^{2J} mouse model has slightly reduced expression and shows a relatively mild muscular dystrophy with a life span of several months. In both models, skeletal muscle is characterized by repeated cycles of degeneration/regeneration and pathological fibrosis. Consequently, dy^{3K}/dy^{3K} and dy^{2J}/dy^{2J} mice weigh less and display impaired skeletal muscle function [2]. Diagnosis of LAMA2-CMD and knowledge of underlying pathogenetic mechanisms have greatly improved due to advances in clinical and pre-clinical studies involving LAMA2-CMD patient material and the above mentioned mouse models (as well as other animal models). However, early detection, assessment of disease progression and response to treatment are still major challenges. Hence, it would be important to find novel biomarkers that could facilitate diagnosis and prognosis and aid in evaluating preclinical as well as clinical trial results. The traditional biomarker for muscular dystrophy is creatine kinase (CK), coupled with histological inspection of muscle biopsies. Unfortunately, CK is not very reliable as it is sensitive to age, sex, physical exertion, stress and diet [3], and muscle biopsies are invasive. Therefore, there is an urgent need for more reliable and less invasive biomarkers for LAMA2-CMD and muscular dystrophies in general.

After their discovery in the early nineties, microRNAs (also called miRNAs or miRs) have been extensively studied for their biological roles and biomarker potential. miRNAs are short (18-24 nt) non-coding RNAs that post-transcriptionally regulate protein synthesis by complementary-binding messenger RNA, which leads to degradation of the latter or translation inhibition [4]. Their presence in extracellular fluids, such as blood and urine, along with miRNA dysregulation in various diseases, including muscular dystrophy [5], has spurred extensive biomarker research [6-

10]. Indeed, we have previously demonstrated that laminin α2 chain-deficiency is associated with miRNA dysregulation in skeletal muscle and plasma [11]. In this study we aimed at profiling miRNA expression in urine from *dy^{2J}/dy^{2J}* mice to assess their potential for monitoring disease progression. Three distinct time points (three, four and six weeks of age) were chosen to represent asymptomatic, initial symptoms and established disease, respectively. Here we show that distinct sets of miRNA characterise each time point whilst CK fails to differentiate between them.

MATERIALS AND METHODS

Animals

Wild-type and dy^{2J}/dy^{2J} (B6.WK-$Lama^{2dy\text{-}2J}$/J) mice were purchased from Jackson laboratory and bred in the Biomedical Center according to institutional animal care guidelines. Permission was given by the Malmö/Lund (Sweden) ethical committee for animal research (ethical permit number M152-14).

Tissue collection

Three-, four- and six-week-old control and dy^{2J}/dy^{2J} mice (n = 5 per group) were sacrificed by cervical dislocation. Quadriceps muscles were dissected for histology and embedded in paraffin.

Histology and morphometric analysis

Muscle sections were stained with haematoxylin & eosin [12] or picro sirius red/fast green [11]. Stained cross-sections were scanned using Aperio's Scanscope CS2 (with Scanscope console v. 8.2.0.1263) and representative images were created using Aperio software.

Centrally nucleated muscle fibres representing regenerating muscle cells and peripherally nucleated non-regenerating muscle cells were counted in quadriceps femoris using ImageJ software version 1.45i (NIH, Bethesda, MD). The whole area of each muscle cross section was considered.

Creatine kinase assay

Blood was collected from heart puncture and transferred to anticoagulant tubes (EDTA) and centrifuged at 1100 × g for 10 min. at 4°C. Plasma was analysed at Clinical Chemistry Laboratory at Skåne University Hospital. The CK_P_S Cobas method was used to quantify enzyme activity.

Fast green/sirius red quantification

Collagen content was quantified by a colorimetric method as described [13]. Briefly, approximately 15 paraffin sections of 15 µm were placed in a plastic tube. Paraffin removal was accomplished by immersing the sections in the following solutions: 5 min. xylene, 5 min. xylene/ethanol (1:1), 5 min. ethanol, 5 min. ethanol/water (1:1), 5 min. water. The sections were then stained with fast green/sirius red for 30 min. (rotating). The tissue was washed with distilled water until excess dye was removed and the solution was clear. One ml of 0.1 N NaOH was added to elute colours. The

eluted fraction was analysed at 560 nm and 605 nm to estimate collagen and non-collagenous protein content, respectively.

Grip strength

Forelimb grip strength was measured on a grip-strength meter (Columbus Instruments, Columbus, OH) as previously described [14]. In short, the mouse was held by the base of the tail and allowed to grasp the flat wire mesh of the pull bar with its forepaws. When the mouse got a good grip it was slowly pulled away by its tail until it released the pull bar. Each mouse was allowed to pull the pull bar five times. The two lowest values were rejected and the mean of the three remaining values was counted. Animals were not subjected to any training prior to the experiment.

Urine collection

Individual mice were manually handled on top of a grid placed above a collection plate. The mouse was grabbed by the neck and tail and placed in an upright position. When stressed by the handling the mouse would urinate onto the plate. The urine was pipetted into a tube and stored at -80°C.

Isolation of RNA and RNA sequencing

Total RNA from urine was extracted with Qiagen miRNeasy Mini Kit following the manufacturer's instructions. One hundred and twenty microliters of urine were pooled from two or three animals into one sample.

Total RNA isolated from urine was sent to the Uppsala Genome Centre for high-throughput sequencing on the IonTorrent platform (ThermoFisher Scientific). The raw sequencing data is deposited in the European Nucleotide Archive under accession number PRJEB23307.

Bioinformatics analyses

Bioinformatics analyses were performed in conjunction with the Bioinformatics Long-term Support (WABI – SciLifeLab). Shortly, raw reads between 18 and 24 nt were kept for further analyses. These were mapped to the mouse hairpin miRNA sequences (miRBase, v 22) using bowtie [15] (v. 1.2, Johns Hopkins University). Read counts were calculated with HTSeq [16] and miRBase annotation (v. 21). Differential expression analysis was performed in the R statistical environment (v. 3.3.2, R Foundation for Statistical Computing) with the Bioconductor package DESeq2 [17] (v. 1.12.3), with significance set at adjusted p lower than 5%.

Statistical analysis

The statistical analysis of next-generation sequencing data was done as described above. The remaining analyses were performed in the IPython [18] environment using the SciPy (v. 0.18.1) [19] and statsmodels packages (v. 0.61). Difference between groups was assessed by one-way analysis of variance. Significance was set at the 5% level. Data are presented as mean ± SEM.

RESULTS

Characterization of disease stages

Figure 1. Experimental overview. The arrows (upper part) indicate the different time points when analyses (lower left) were performed.

In order to profile miRNA expression in urine from *dy^{2J}/dy^{2J}* mice at asymptomatic, initial and established stages of the disease, we first assessed body weight, muscle function, muscle histology, and creatine kinase levels in three-, four- and six-week-old *dy^{2J}/dy^{2J}* and wild-type (WT) littermate mice (Figure 1). Independent of age, *dy^{2J}/dy^{2J}* male mice weighed less than wild-type mice. This reduction in body weight was only significant at six weeks of age among female *dy^{2J}/dy^{2J}* mice (Figure 2A). Grip strength to body weight ratio is an indicator of muscle function that allows comparison of animals with different body weights. It is also an indicator of muscle mass change as skeletal muscle is the main tissue that produces force. At three weeks of age there was no difference in normalised grip strength, indicating no functional decline at this age, which is in accordance with the lack of overt symptoms (Figure 2B). At four and six weeks of age the *dy^{2J}/dy^{2J}* groups had lower normalised grip strength (Figure 2B). A similar result was found by McKee et al. (2017), where *dy^{2J}/dy^{2J}* mice had similar normalised forelimb grip-strength to wild-type mice at 3 weeks of age, with a sharp decline thereafter [20].

Figure 2. Male *dy^{2J}/dy^{2J}* mice weight less than WT and display impaired muscle function. A: Body weight for males and females WT and *dy^{2J}/dy^{2J}*; B: Normalised grip strength at indicated time points. * $p < 0.05$, ** $p < 0.01$, *** $p < 0.001$.

In order to assess if impaired muscle function was reflected by abnormal histology, we inspected haematoxylin-eosin and picro-sirius red/fast green stained sections. We found that the first visual signs of muscle pathology appeared at four weeks of age and two weeks later the diseased phenotype was evident (Figure 3A). The only indication of disease at 3 weeks of age was a low degree of inflammation (data not shown). Central nucleation was measured as an index of muscle regeneration. At three weeks of age we did not observe any signs of regeneration in *dy^{2J}/dy^{2J}* muscle. However, at subsequent time points there was a dramatic increase in the number of regenerating fibres in *dy^{2J}/dy^{2J}* muscle (Figure 3B). A hallmark of muscular dystrophies is the progressive replacement of skeletal muscle by fibrous tissue. At three and four weeks of age, there

was no difference in collagen content (assessed by picro-sirius red absorbance) between *dy^{2J}/dy^{2J}* and wild-type muscle (Figure 3, C and D). However, at six weeks of age there was a significant increase in collagen content in *dy^{2J}/dy^{2J}* muscle (Figure 3, C and D).

CK, a classical biomarker for skeletal muscle disease, was elevated in *dy^{2J}/dy^{2J}* serum at all time points (Figure 3E). Furthermore, CK levels in *dy^{2J}/dy^{2J}* serum did not differ between three and six weeks of age (not shown).

Figure 3: Progressive muscle deterioration and collagen accumulation as evidenced by histology and CK concentration. A: Haematoxylin and eosin staining; B: Central nucleation quantification (as percentage of fibres with central nuclei); C: Fast green/sirius red staining: collagen is coloured red; D: Quantification of collagen as percentage of total protein; E: CK. Scale bars = 100 µm; * $p < 0.05$, ** $p < 0.01$, *** $p < 0.001$.

In summary, these data revealed that there are no signs of pathology in three-week-old *dy^{2J}/dy^{2J}* mice, but subsequently a gradual disease progression occurs. Hence, we decided to profile urine miRNAs in three-, four- and six-week-old animals.

MiRNA profiling in urine

We detected more than 700 miRNAs in mouse urine at each time point: 773 at three weeks, 764 at four weeks and 703 at six weeks of age. Among these, the number of differentially expressed miRNAs also varied. Five, 18 and 17 miRNAs, respectively, were differentially expressed at three, four and six weeks of age (Table 1, supplemental figures). We also found that distinct miRNA profiles were associated with each time point, i.e. there was minimal overlap between differentially expressed miRNAs at three, four and six weeks of age. Only miR-1957a and miR-675 were differentially expressed both at three and six weeks of age, and miR-181 was differentially expressed at four and six weeks of age. However, miRNA-181 was down-regulated at four weeks but up-regulated at six weeks of age (Table 1). Furthermore, we found that myomiRs (miR-1, miR-133 and miR-206) and muscle-enriched miRNAs (miR-181a and miR-486) dominate the differentially expressed miRNA panel at six weeks of age.

DISCUSSION

For the past couple of decades miRNAs have been extensively studied for their biomarker potential. However, most investigations use biopsies or blood samples for this purpose, which are invasive. CK assessment (along with morphological analysis) is often part of the standard diagnostic protocols for muscle wasting diseases. The reliability of this method has long been questioned as CK is responsive to age, sex, stress, physical exertion and diet [3]. It is largely a binary analysis, indicating recent muscle damage but not cause or severity. Here, we show that CK measurement cannot be used to distinguish disease severity as it was elevated in dy^{2J}/dy^{2J} mice already from three weeks onwards. Furthermore, CK levels did not differ between three- and six-week-old dy^{2J}/dy^{2J} mice. We also observed higher variability in the diseased group compared to controls, making it difficult to establish a cut-off value. Considering the aforementioned limitations, we have opted for a less invasive intervention and profiled miRNAs in urine from a LAMA2-CMD mouse model at three distinct time points (asymptomatic, initial symptoms and established disease). We found that distinct miRNA profiles are associated with each time point. Specifically, we demonstrated that: 1) Some miRNAs are differentially expressed in urine from dy^{2J}/dy^{2J} mice at three weeks of age although skeletal muscles appear histologically and functionally normal at that age with no obvious signs of muscle regeneration or fibrosis; 2) The highest number of differentially expressed miRNAs is seen in urine from four-week-old dy^{2J}/dy^{2J} mice, a time point when these mice display dystrophic characteristics including increased myofibre regeneration (but no fibrosis) and functional decline, and finally: 3) Differentially expressed miRNAs in urine from six-week-old animals are predominantly myomiRs (i.e. miRNAs that are specific for or enriched in skeletal muscle) corresponding to fully developed muscle pathology with a high degree of muscle fibre regeneration and fibrosis. Thus, we suggest that urine miRNAs can be sensitive biomarkers for different stages of LAMA2-CMD.

Our analysis showed that at three weeks of age the miRNA with the largest fold change is miR-675-3p, followed closely by its -5p counterpart. Both miRNA are derived from exon 1 of the long non-coding RNA H19. H19 is highly expressed during embryonic phases but strongly repressed after birth, with significant expression remaining only in skeletal and cardiac muscle [21; 22]. H19 acts through miR-675 to influence regeneration and differentiation [21-23]. miR-15b was down-regulated in myasthenia gravis patients and was found to regulate IL-15 expression in a mouse model of the disease [8]. It also stimulated cardiomyocyte apoptosis in response to ischaemia/reperfusion injury [24].

The highest number of differentially expressed miRNAs was found at four weeks of age and it is the only time point with down-regulated miRNAs. It is also the first time point with a differentially expressed muscle-enriched miRNA, i.e. miR-181a-1 and miR-181a-2, both of which are down-regulated at four weeks of age. Mir-181a was previously associated with the degree of muscle wasting following high-risk cardiothoracic surgery, with a high predictive value of 91%, despite some limitations in study design and low sensitivity (56%) [9]. Apart from being a myomiR, miR-181a is also one of the mitochondria-associated miRNAs, also called mitomiRs. They bind to the mitochondrial outer membrane to regulate its metabolism, gene expression and function [25]. Besides taking part in energy metabolism, mitochondria also have prominent roles in cell longevity and apoptosis. In line with this our group has previously shown that most differentially expressed proteins in dy^{3K}/dy^{3K} (a severely affected LAMA2-CMD mouse model) muscle are coupled to energy and calcium metabolism/signalling [26]. The most up-regulated miRNA at four weeks of age was miR-495, which is also up-regulated in various cardiac diseases, including cardiomyopathies associated with muscular dystrophies [27]. Another differentially expressed miRNA involved in cardiopathy is miR-154, which is associated with increased fibrosis and reduced apoptosis [28]. With an almost 6-fold increased expression in dystrophic muscle, miR-182 is involved in skeletal muscle atrophy [29], myocardial hypertrophy [30], muscle glucose utilisation [31] and the response to hormone replacement therapy in women [32]. The most down-regulated miRNA at this time point was miR-155. It was reported to be involved in various processes in skeletal and cardiac muscle, such as pathological cardiac hypertrophy [33], skeletal muscle differentiation [34] and regeneration [35]. Moreover, miR-155 regulates macrophage transition from a pro- to an anti-inflammatory state in skeletal muscle [35], which is an important step in muscle regeneration.

At six weeks of age myomiRs dominate the differentially expressed miRNA panel. It may suggest that compensatory mechanisms are at play and degeneration/regeneration cycles are intensified. Our lab has previously shown that miR-1, miR-133 and miR-206 are altered in quadriceps and plasma of dy^{2J}/dy^{2J} and dy^{3K}/dy^{3K} mice [6]. Levels of miR-1 and miR-133 changed in opposite directions in muscle and plasma, i.e. both were down-regulated in quadriceps whilst up-regulated in blood plasma. MiR-206 was up-regulated in both muscle and plasma. MiR-1 and miR-133 are involved in differentiation and proliferation, respectively [31-33]. MiR-206 on the other hand seems to be an important hub in gene networks in skeletal muscle given its involvement in fundamental processes such as muscle cell differentiation [32; 34] and regeneration [35]. Interestingly, work by Böttger et al. [36] presented evidence that the miR-206/133b cluster is in fact dispensable for skeletal muscle development and regeneration. MiR-486, a muscle-enriched miRNA, is also involved in various processes relevant for LAMA2-CMD. Hitachi et al. [37] showed that myostatin, a well-known

negative regulator of muscle mass, acts via miR-486 to regulate the IGF-1/Akt/mTOR pathway; others have found similar results [38; 39]. MiR-486 also affects myoblast differentiation along with miR-206 [34]. One of the most interesting findings at six weeks of age is that miR-181a is up-regulated, given that it was down-regulated at four weeks. This makes it an interesting target for further investigation, coupled with its purported role in ageing, inflammation, and muscle and mitochondrial metabolism. Validating its targets in skeletal muscle would provide valuable insight into its function in this tissue.

Despite our interesting findings care must be taken when interpreting NGS results. NGS library preparation is known to induce biases that may favour certain sequences and thus compromise further analyses. For this reason, ideally, biomarkers should be validated with an orthogonal method, such as qPCR for example. We must also bear in mind that the clinical reality is quite different from a laboratory one. Our mice had standardised housing, diet, light-cycle, genetic background, etc., all of which differ amongst patients. Future work with clinical samples will have to deal with much higher data variability. Considering the low incidence of LAMA2-CMD it will be very difficult to run clinical trials with age- and sex-matched subjects. One of our goals was to match disease severity to miRNA profile. In the clinical setting this goal is likely to be hampered by the lack of standardised clinical outcomes for muscular dystrophies, another limitation in the field.

In summary, we were able to follow disease progression in LAMA2-CMD by analysing three distinct time points. Three-week-old dy^{2J}/dy^{2J} muscle appears histologically normal with no functional deficit. Yet, CK is elevated and a few miRNAs are differentially expressed. At four weeks of age, muscles are histologically abnormal and show increased regeneration and functional decline (but no fibrosis). CK is increased and several differentially expressed miRNAs are detected. Finally, six-week-old dy^{2J}/dy^{2J} muscle displays histological and functional impairment along with increased CK and the differentially expressed myomiRs. To our knowledge, this is the first time urine miRNAs are profiled in muscular dystrophy. We would like to propose that miRNAs have the potential to distinguish disease stages and should be further investigated as biomarkers for LAMA2-CMD.

References

[1] Sparks, SE; Quijano-Roy, S; Harper, A and et al.Pagon, R. A.; Adam, M. P.; Ardinger, H. H. & et al. (Ed.), **2001**. *Congenital Muscular Dystrophy Overview.. , .*

[2] **Gawlik, K. I. and Durbeej, M.** (**2011**). *Skeletal muscle laminin and MDC1A: pathogenesis and treatment strategies*, Skeletal Muscle 1.

[3] **Spurney, C. F.; Gordish-Dressman, H.; Guerron, A. D.; Sali, A.; Pandey, G. S.; Rawat, R.; Meulen, J. H. V. D.; Cha, H.-J.; Pistilli, E. E.; Partridge, T. A.; Hoffman, E. P. and Nagaraju, K.** (**2009**). *Preclinical drug trials in the mdx mouse: Assessment of reliable and sensitive outcome measures*, Muscle & Nerve 39 : 591-602.

[4] **Brown, D. M. and Goljanek-Whysall, K.** (**2015**). *microRNAs: modulators of the underlying pathophysiology of sarcopenia?*, Ageing Research Reviews .

[5] **Morlando, M.; Rosa, A.; Caffarelli, E.; Fatica, A. and Bozzoni, I.** (**2013**). *Non Coding RNA in Muscle Differentiation and Disease*, MicroRNA 2 : 91-101.

[6] **Gupta, S. K.; Bang, C. and Thum, T.** (**2010**). *Circulating MicroRNAs as Biomarkers and Potential Paracrine Mediators of Cardiovascular Disease*, Circulation: Cardiovascular Genetics 3 : 484-488.

[7] **Roberts, T. C.; Godfrey, C.; McClorey, G.; Vader, P.; Briggs, D.; Gardiner, C.; Aoki, Y.; Sargent, I.; Morgan, J. E. and Wood, M. J.** (**2013**). *Extracellular microRNAs are dynamic non-vesicular biomarkers of muscle turnover*, Nucleic Acids Research 1.

[8] **Zaharieva, I. T.; Calissano, M.; Scoto, M.; Preston, M.; Cirak, S.; Feng, L.; Collins, J.; Kole, R.; Guglieri, M.; Straub, V.; Bushby, K.; Ferlini, A.; Morgan, J. E. and Muntoni, F.** (**2013**). *Dystromirs as Serum Biomarkers for Monitoring the Disease Severity in Duchenne Muscular Dystrophy*, PLoS ONE 8 : e80263.

[9] **Bloch, S. A.; Donaldson, A. V.; Lewis, A.; Banya, W. A.; Polkey, M. I.; Griffiths, M. J. and Kemp, P. R.** (**2015**). *MiR-181a: a potential biomarker of acute muscle wasting following elective high-risk cardiothoracic surgery*, Critical Care 19.

[10] **Perfetti, A.; Greco, S.; Cardani, R.; Fossati, B.; Cuomo, G.; Valaperta, R.; Ambrogi, F.; Cortese, A.; Botta, A.; Mignarri, A.; Santoro, M.; Gaetano, C.; Costa, E.; Dotti, M. T.; Silvestri, G.; Massa, R.; Meola, G. and Martelli, F.** (**2016**). *Validation of plasma microRNAs as biomarkers for myotonic dystrophy type 1*, Scientific Reports 6.

[11] **Holmberg, J.; Alajbegovic, A.; Gawlik, K. I.; Elowsson, L. and Durbeej, M.** (**2014**). *Laminin α2 Chain-Deficiency is Associated with microRNA Deregulation in Skeletal Muscle and Plasma*, Frontiers in Aging Neuroscience 6.

[12] **Gawlik, K. I.; Holmberg, J. and Durbeej, M.** (**2014**). *Loss of Dystrophin and β-Sarcoglycan Significantly Exacerbates the Phenotype of Laminin α2 Chain-Deficient Animals*, The American Journal of Pathology 184 : 740-752.

[13] **Leon, A. L.-D. and Rojkind, M.** (**1985**). *A simple micromethod for collagen and total protein determination in formalin-fixed paraffin-embedded sections.*, Journal of Histochemistry & Cytochemistry 33 : 737-743.

[14] **Gawlik, K. I. and Durbeej, M.** (**2010**). *TRANSGENIC OVEREXPRESSION OF LAMININ α1 CHAIN IN LAMININ α2 CHAIN–DEFICIENT MICE RESCUES THE DISEASE THROUGHOUT THE LIFESPAN*, Muscle Nerve 42 : 30-37.

[15] **Langmead, B.; Trapnell, C.; Pop, M. and Salzberg, S. L.** (**2009**). *Ultrafast and memory-efficient alignment of short DNA sequences to the human genome*, Genome Biology 10 : R25.

[16] **Anders, S.; Pyl, P. T. and Huber, W.** (**2014**). *HTSeq--a Python framework to work with high-throughput sequencing data*, Bioinformatics 31 : 166–169.

[17] **Love, M. I.; Huber, W. and Anders, S.** (**2014**). *Moderated estimation of fold change and dispersion for RNA-seq data with DESeq2*, Genome Biology 15.

[18] **Perez, F. and Granger, B. E.** (**2007**). *IPython: A System for Interactive Scientific Computing*, Computing in Science & Engineering 9 : 21-29.

[19] Jones, E.; Oliphant, T.; Peterson, P. and others (**2001**). *SciPy: Open source scientific tools for Python*, .

[20] **McKee, K. K.; Crosson, S. C.; Meinen, S.; Reinhard, J. R.; Rüegg, M. A. and Yurchenco, P. D.** (**2017**). *Chimeric protein repair of laminin polymerization ameliorates muscular dystrophy phenotype*, The Journal of Clinical Investigation 127 : 1075-1089.

[21] **Dey, B. K.; Pfeifer, K. and Dutta, A.** (**2014**). *The H19 long noncoding RNA gives rise to microRNAs miR-675-3p and miR-675-5p to promote skeletal muscle differentiation and regeneration*, Genes & Development 28 : 491–501.

[22] **Liu, L.; An, X.; Li, Z.; Song, Y.; Li, L.; Zuo, S.; Liu, N.; Yang, G.; Wang, H.; Cheng, X.; Zhang, Y.; Yang, X. and Wang, J.** (**2016**). *The H19 long noncoding RNA is a novel negative regulator of cardiomyocyte hypertrophy*, Cardiovascular Research 111 : 56-65.

[23] **Martinet, C.; Monnier, P.; Louault, Y.; Benard, M.; Gabory, A. and Dandolo, L.** (**2016**). *H19 controls reactivation of the imprinted gene network during muscle regeneration*, Development 143 : 962-971.

[24] **Shi, L.; Liu, T.; Zhang, M.; Guo, Y.; Song, C.; Song, D. and Liu, H.** (**2015**). *miR-15b is Downregulated in Myasthenia Gravis Patients and Directly Regulates the Expression of Interleukin-15 (IL-15) in Experimental Myasthenia Gravis Mice*, Medical Science Monitor 21 : 1774-1780.

[25] **Rippo, M. R.; Olivieri, F.; Monsurrò, V.; Prattichizzo, F.; Albertini, M. C. and Procopio, A. D.** (**2014**). *MitomiRs in human inflamm-aging: A hypothesis involving miR-181a, miR-34a and miR-146a*, Experimental Gerontology 56 : 154-163.

[26] **de Oliveira, B. M.; Matsumura, C. Y.; Fontes-Oliveira, C. C.; Gawlik, K. I.; Acosta, H.; Wernhoff, P. and Durbeej, M.** (**2014**). *Quantitative Proteomic Analysis Reveals Metabolic Alterations, Calcium Dysregulation, and Increased Expression of Extracellular Matrix Proteins in Laminin α2 Chaintextendashdeficient Muscle*, Mol Cell Proteomics 13 : 3001-3013.

[27] **Clark, A. L.; Maruyama, S.; Sano, S.; Accorsi, A.; Girgenrath, M.; Walsh, K. and Naya, F. J.** (**2016**). *miR-410 and miR-495 Are Dynamically Regulated in Diverse Cardiomyopathies and Their Inhibition Attenuates Pathological Hypertrophy*, PLOS ONE 11 : e0151515.

[28] **Sun, L.-Y.; Bie, Z.-D.; Zhang, C.-H.; Li, H.; Li, L.-D. and Yang, J.** (**2016**). *MiR-154 directly suppresses DKK2 to activate Wnt signaling pathway and enhance activation of cardiac fibroblasts*, Cell Biology International 40 : 1271-1279.

[29] **Hudson, M. B.; Rahnert, J. A.; Zheng, B.; Woodworth-Hobbs, M. E.; Franch, H. A. and Price, S. R.** (**2014**). *miR-182 attenuates atrophy-related gene expression by targeting FoxO3 in skeletal muscle*, AJP: Cell Physiology 307 : C314-C319.

[30] **Li, N.; Hwangbo, C.; Jaba, I. M.; Zhang, J.; Papangeli, I.; Han, J.; Mikush, N.; Larrivée, B.; Eichmann, A.; Chun, H. J.; Young, L. H. and Tirziu, D.** (**2016**). *miR-182 Modulates Myocardial Hypertrophic Response Induced by Angiogenesis in Heart*, Scientific Reports 6 : 21228.

[31] **Zhang, D.; Li, Y.; Yao, X.; Wang, H.; Zhao, L.; Jiang, H.; Yao, X.; Zhang, S.; Ye, C.; Liu, W.; Cao, H.; Yu, S.; Wang, Y.-c.; Li, Q.; Jiang, J.; Liu, Y.; Zhang, L.; Liu, Y.; Iwai, N.; Wang, H.; Li, J.; Li, J.; Li, X.; Jin, Z.-B. and Ying, H.** (**2016**). *miR-182 Regulates Metabolic Homeostasis by Modulating Glucose Utilization in Muscle*, Cell Reports 16 : 757-768.

[32] **Olivieri, F.; Ahtiainen, M.; Lazzarini, R.; Pöllänen, E.; Capri, M.; Lorenzi, M.; Fulgenzi, G.; Albertini, M. C.; Salvioli, S.; Alen, M. J.; Kujala, U. M.; Borghetti, G.; Babini, L.; Kaprio, J.; Sipilä, S.; Franceschi, C.; Kovanen, V. and Procopio, A. D.** (**2014**). *Hormone replacement therapy enhances IGF-1 signaling in skeletal muscle by diminishing miR-182 and miR-223 expressions: a study on postmenopausal monozygotic twin pairs*, Aging Cell 13 : 850-861.

[33] **Seok, H. Y.; Chen, J.; Kataoka, M.; Huang, Z.-P.; Ding, J.; Yan, J.; Hu, X. and Wang, D.-Z.** (**2014**). *Loss of MicroRNA-155 Protects the Heart From Pathological Cardiac Hypertrophy*, Circulation Research 114 : 1585-1595.

[34] **Seok, H. Y.; Tatsuguchi, M.; Callis, T. E.; He, A.; Pu, W. T. and Wang, D.-Z.** (**2011**). *miR-155 Inhibits Expression of the MEF2A Protein to Repress Skeletal Muscle Differentiation*, Journal of Biological Chemistry 286 : 35339-35346.

[35] **Nie, M.; Liu, J.; Yang, Q.; Seok, H. Y.; Hu, X.; Deng, Z.-L. and Wang, D.-Z.** (**2016**). *MicroRNA-155 facilitates skeletal muscle regeneration by balancing pro- and anti-inflammatory macrophages*, Cell Death and Disease 7 : e2261.

[36] **Boettger, T.; Wüst, S.; Nolte, H. and Braun, T.** (**2014**). *The miR-206/133b cluster is dispensable for development, survival and regeneration of skeletal muscle*, Skeletal Muscle 4.

[37] **Hitachi, K.; Nakatani, M. and Tsuchida, K.** (**2014**). *Myostatin signaling regulates Akt activity via the regulation of miR-486 expression*, The International Journal of Biochemistry & Cell Biology 47 : 93-103.

[38] **Huang, M.-B.; Xu, H.; Xie, S.-J.; Zhou, H. and Qu, L.-H.** (**2011**). *Insulin-Like Growth Factor-1 Receptor Is Regulated by microRNA-133 during Skeletal Myogenesis*, PLoS One 6 : e29173.

[39] **Roberts, T. C.; Blomberg, K. E. M.; McClorey, G.; Andaloussi, S. E.; Godfrey, C.; Betts, C.; Coursindel, T.; Gait, M. J.; Edvard Smith, C. and Wood, M. J.** (**2012**). *Expression Analysis in Multiple Muscle Groups and Serum Reveals Complexity in the MicroRNA Transcriptome of the mdx Mouse with Implications for Therapy*, Mol Ther Nucleic Acids 1 : e39.

TABLES

Table 1

mirna	log2FoldChange	padj	time
mmu-miR-675-3p	4.4063	0.0005	3wk
mmu-miR-675-5p	4.1857	0.0003	3wk
mmu-miR-1957a	2.9201	0.0022	3wk
mmu-miR-15b-5p	2.4532	0.0001	3wk
mmu-miR-320-5p	2.4024	0.0063	3wk
mmu-miR-495-3p	3.8713	0.0052	4wk
mmu-miR-369-3p	3.6786	0.0108	4wk
mmu-miR-337-3p	3.6545	0.0028	4wk
mmu-miR-154-3p	3.6308	0.0028	4wk
mmu-miR-376b-3p	2.9790	0.0028	4wk
mmu-miR-182-5p	2.7268	0.0031	4wk
mmu-miR-127-3p	2.7131	0.0489	4wk
mmu-miR-148a-3p	2.5092	0.0028	4wk
mmu-miR-31-5p	2.1256	0.0012	4wk
mmu-miR-1839-5p	1.8521	0.0167	4wk
mmu-miR-21a-5p	1.3860	0.0108	4wk
mmu-miR-155-5p	-2.4041	0.0389	4wk
mmu-miR-615-3p	-2.1658	0.0028	4wk
mmu-miR-204-5p	-1.7558	0.0389	4wk
mmu-miR-187-3p	-1.7246	0.0477	4wk
mmu-miR-181a-1-5p	-1.3911	0.0389	4wk
mmu-miR-181a-2-5p	-1.3911	0.0389	4wk
mmu-miR-378c	-1.1433	0.0389	4wk
mmu-miR-486a-5p	4.7623	0.0002	6wk
mmu-miR-486b-5p	4.7524	0.0002	6wk
mmu-miR-5108	4.5049	0.0076	6wk
mmu-miR-206-3p	4.1917	0.0031	6wk
mmu-miR-8101	4.0483	0.0127	6wk
mmu-miR-675-5p	3.9570	0.0031	6wk
mmu-miR-133b-3p	3.7315	0.0221	6wk
mmu-miR-1a-2-3p	3.5710	0.0103	6wk
mmu-miR-1a-1-3p	3.5710	0.0103	6wk
mmu-miR-133a-1-3p	2.8598	0.0103	6wk
mmu-miR-133a-2-3p	2.8598	0.0103	6wk
mmu-miR-1957a	2.5676	0.0401	6wk
mmu-miR-5100	1.9848	0.0127	6wk
mmu-miR-7a-2-5p	1.7627	0.0204	6wk
mmu-miR-7a-1-5p	1.7603	0.0204	6wk
mmu-miR-181a-1-5p	1.5137	0.0190	6wk
mmu-miR-181a-2-5p	1.5137	0.0190	6wk

Table 1. Differentially expressed miRNAs at the selected time points. Adjusted $p < 0.05$ and log2FoldChange > 1.

FIGURE LEGENDS

Fig1. Experimental overview. The arrows (upper part) indicate the different time points when analyses (lower left) were performed.

Fig2. Male dy /dy mice weight less than WT and display impaired muscle function. A: Body weight for males and females WT and dy /dy ; B: Normalised grip strength at indicated time points. * $p < 0.05$, ** $p < 0.01$, *** $p < 0.001$.

Fig3. Progressive muscle deterioration and collagen accumulation as evidenced by histology and CK concentration. A: Haematoxylin and eosin staining; B: Central nucleation quantification (as percentage of fibres with central nuclei); C: Fast green/sirius red staining: collagen is coloured red; D: Quantification of collagen as percentage of total protein; E: CK. Scale bars = 100 μm; * $p < 0.05$, ** $p < 0.01$, *** $p < 0.001$.

Sup1. Diagnostic plots: principal component analysis (PCA) shows how well samples group based on global gene expression; heatmaps are color-coded values from an expression matrix, which may or may not include all the genes. A: PCA of three-week-old samples; B: Heatmap of the 20 mostly expressed miRNAs at three weeks of age; C: Heatmap of differentially expressed miRNAs at three weeks of age.

Sup2. A: PCA of four-week-old samples; B: Heatmap of the 20 mostly expressed miRNAs at four weeks of age; C: Heatmap of differentially expressed miRNAs at four weeks of age.

Sup3. A: PCA of six-week-old samples; B: Heatmap of the 20 mostly expressed miRNAs at six weeks of age; C: Heatmap of differentially expressed miRNAs at six weeks of age.

453 **FIGURE 1**

454

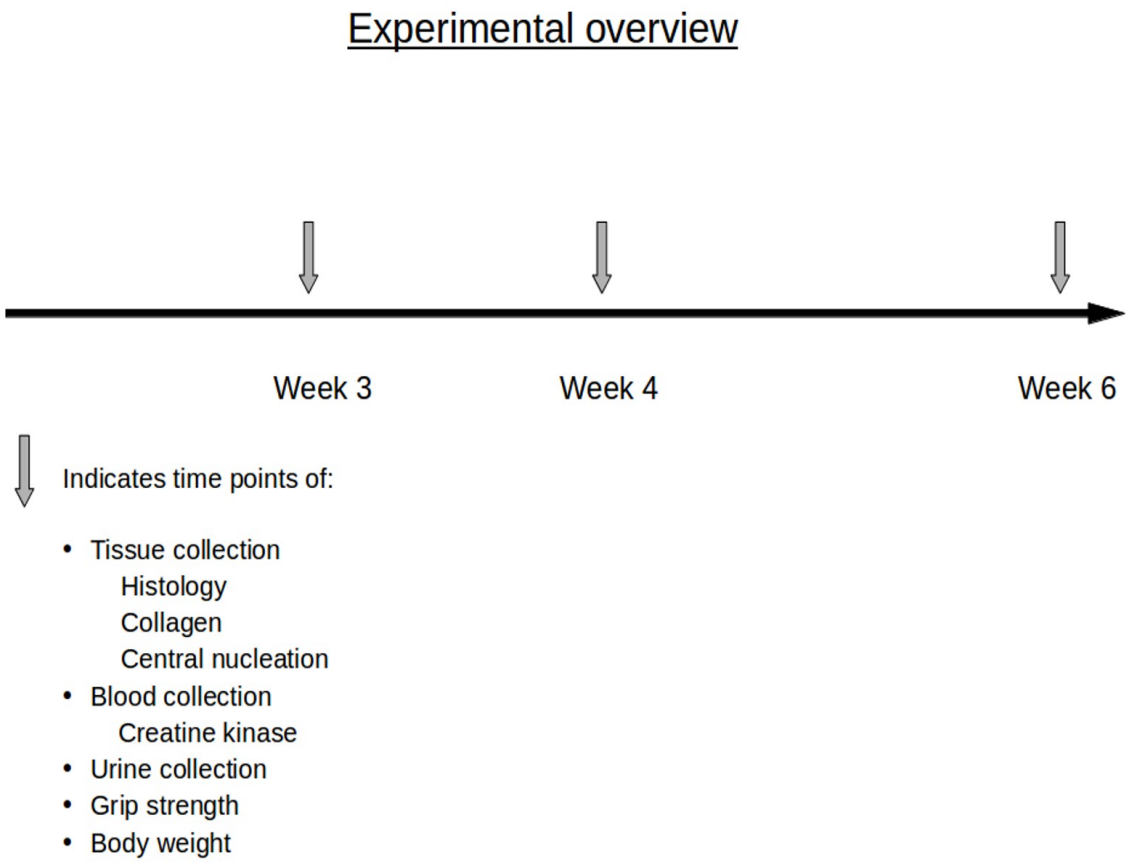

456 **FIGURE 2**

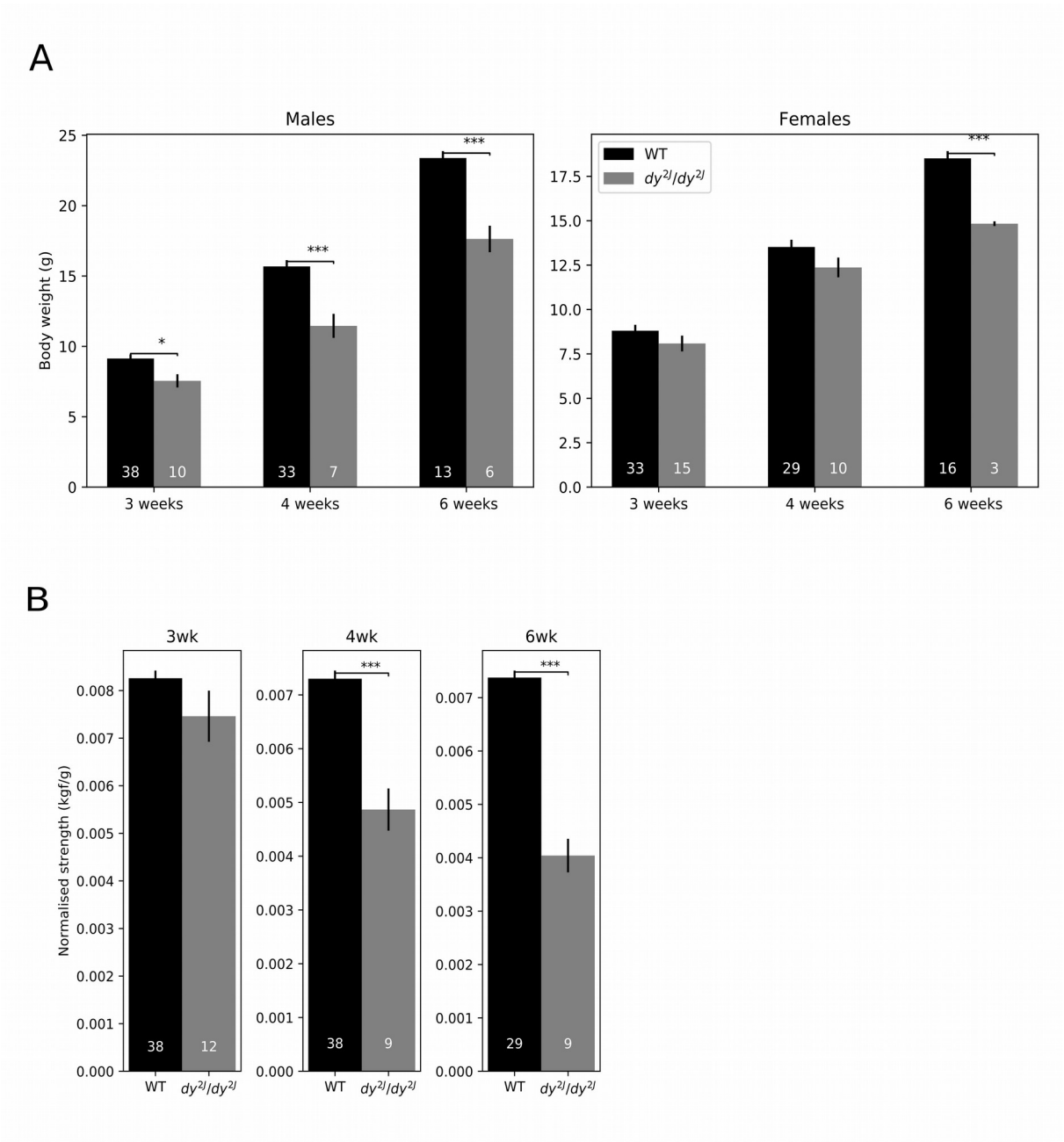
A
Males
Females
Body weight (g)
WT
dy2J/dy2J
3 weeks
4 weeks
6 weeks
38
10
33
7
13
6
33
15
29
10
16
3
*
***
B
3wk
4wk
6wk
Normalised strength (kgf/g)
38
12
38
9
29
9
WT
dy2J/dy2J

457 **FIGURE 3**

458

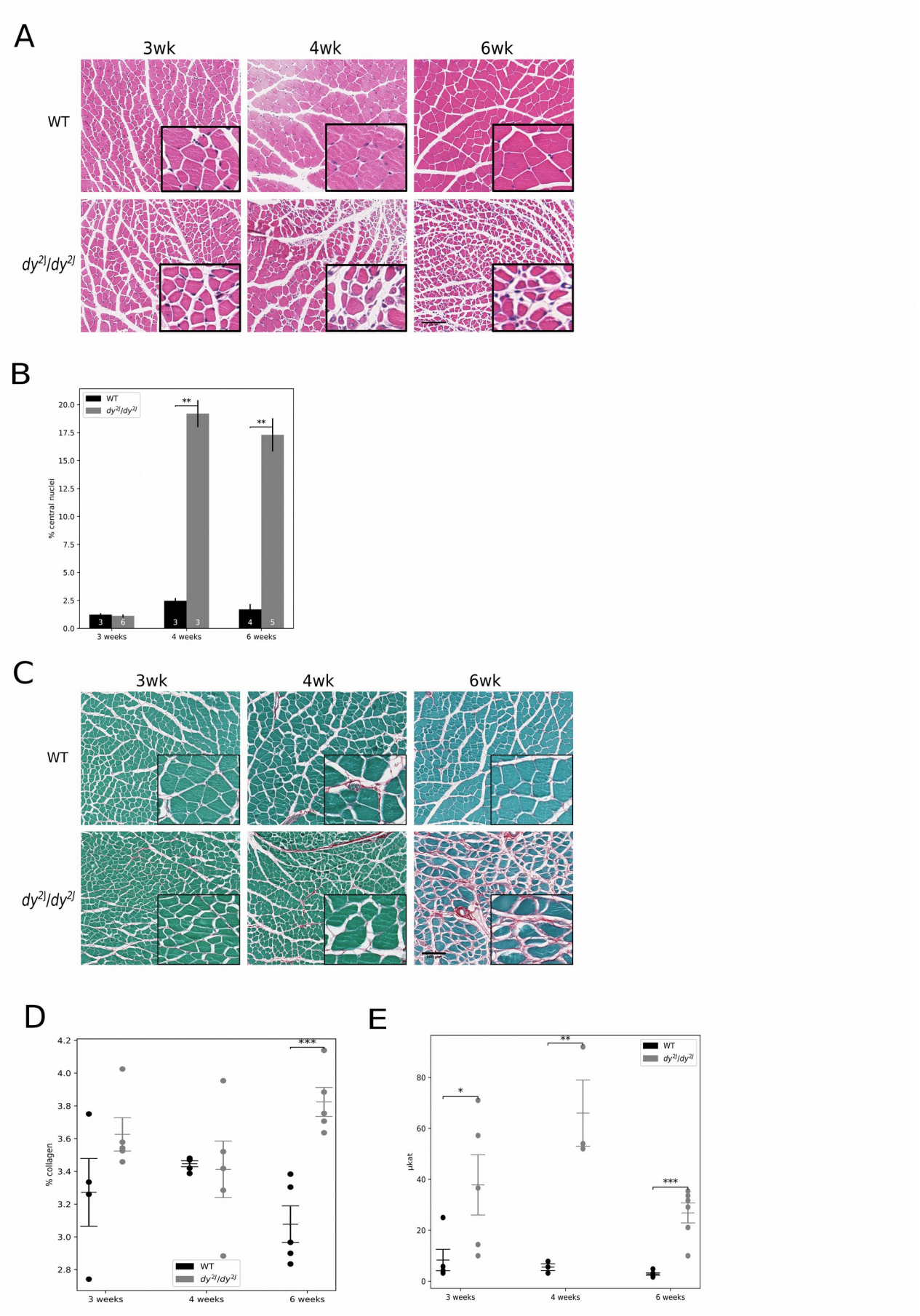

459 **SUP. FIGURE 1**

460

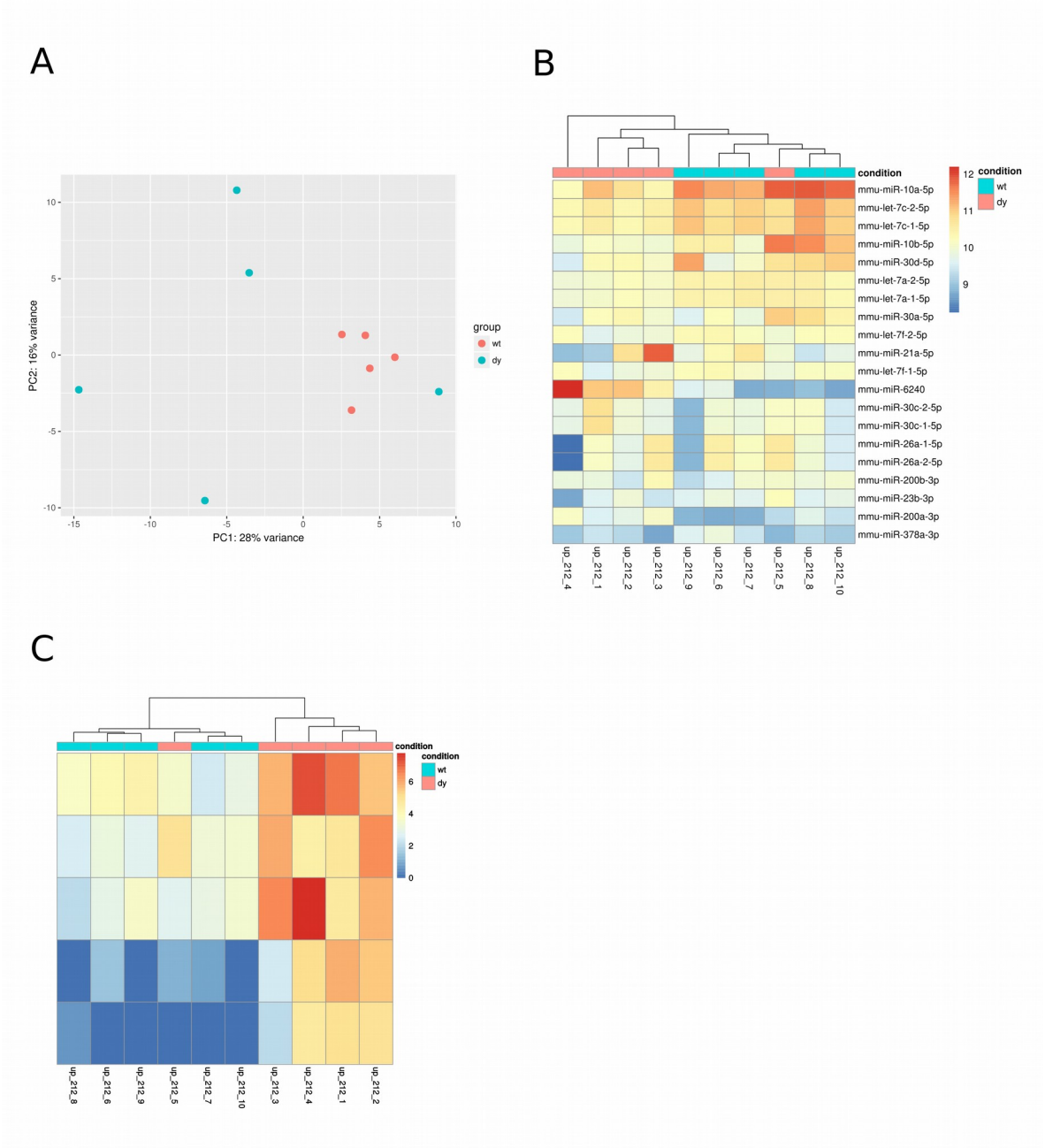

SUP. FIGURE 2

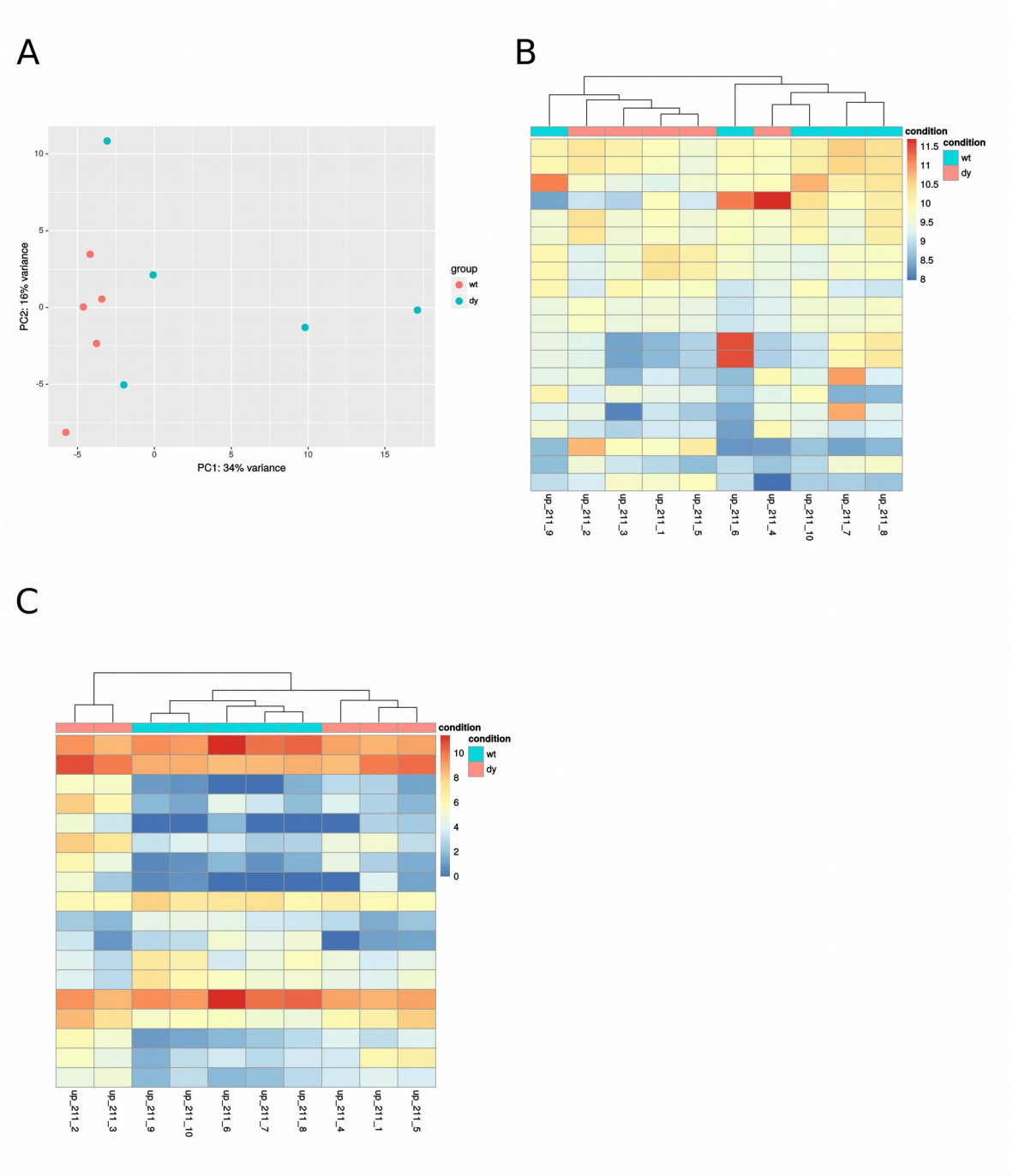
A
PC2: 16% variance
PC1: 34% variance
group
wt
dy
B
condition
condition
wt
dy
up_211_9
up_211_2
up_211_3
up_211_1
up_211_5
up_211_6
up_211_4
up_211_10
up_211_7
up_211_8
C
condition
condition
wt
dy
up_211_2
up_211_3
up_211_9
up_211_10
up_211_6
up_211_7
up_211_8
up_211_4
up_211_1
up_211_5

463 **SUP. FIGURE 3**

464

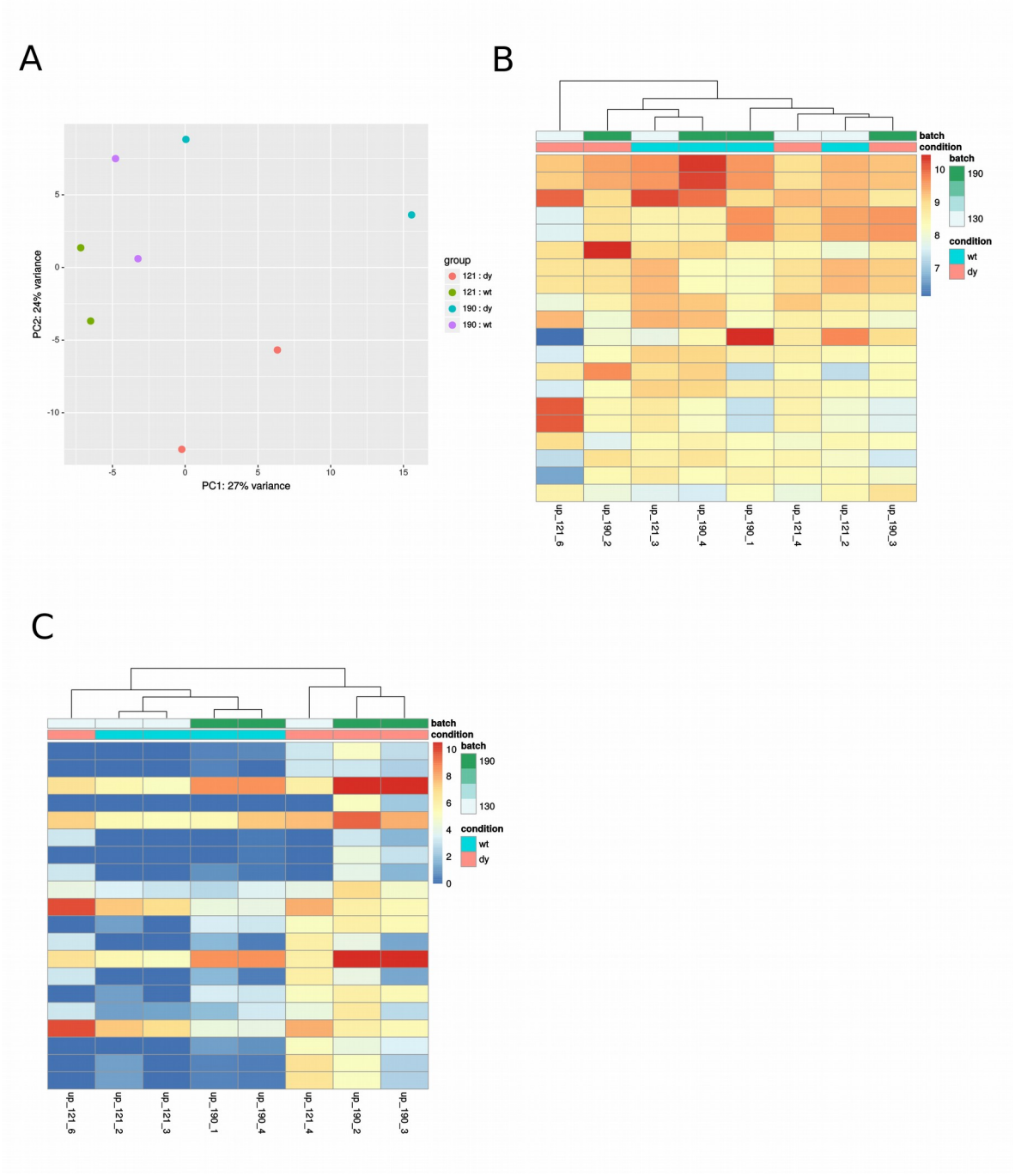

Effects of metformin on congenital muscular dystrophy type 1A disease progression in mice: a gender impact study

Cibely C. Fontes-Oliveira*, Bernardo Moreira Soares Oliveira, Zandra Körner,

Vahid M. Harandi and Madeleine Durbeej*

Unit of Muscle Biology, Department of Experimental Medical Science,

Lund University, Lund, Sweden

*Corresponding authors
Madeleine Durbeej and Cibely C. Fontes-Oliveira
Department of Experimental Medical Science
Unit of Muscle Biology
Lund University
BMC C12
221 84 Lund, Sweden
Tel : +46 46 2220812
Email: madeleine.durbeej-hjalt@med.lu.se or cibely.fontes_oliveira@med.lu.se

Congenital muscular dystrophy with laminin α2 chain-deficiency (LAMA2-CMD) is a severe muscle disorder with complex underlying pathogenesis. We have previously employed profiling techniques to elucidate molecular patterns and demonstrated significant metabolic impairment in skeletal muscle from LAMA2-CMD patients and mouse models. Thus, we hypothesize that skeletal muscle metabolism may be a promising pharmacological target to improve muscle function in LAMA2-CMD. Here, we have investigated whether the multifunctional medication metformin could be used to reduce disease in the *dy^{2J}/dy^{2J}* mouse model of LAMA2-CMD. First, we show gender disparity for several pathological hallmarks of LAMA2-CMD. Second, we demonstrate that metformin treatment significantly increases weight gain and energy efficiency, enhances muscle function and improves skeletal muscle histology in female *dy^{2J}/dy^{2J}* mice (and to a lesser extent in *dy^{2J}/dy^{2J}* males). Thus, our current data suggest that metformin may be a potential future supportive treatment that improves many of the pathological characteristics of LAMA2-CMD.

INTRODUCTION

Mutations in the *LAMA2* gene encoding laminin α2 chain cause congenital muscular dystrophy with laminin α2 chain-deficiency (LAMA2-CMD), a very severe muscle disorder. Under normal conditions, laminin α2 chain forms the heterotrimeric protein laminin-211 (together with laminin β1 and γ1 chains) and this extracellular matrix protein is highly expressed in the basement membranes of muscle and Schwann cells. Laminin α2 chain is either completely or partially absent in LAMA2-CMD and the clinical manifestations include profound hypotonia at birth, widespread muscle weakness, proximal joint contractures, inability to stand and walk, scoliosis, dysmyelinating neuropathy and white matter abnormalities [1]. At the histological level the skeletal muscle pathology comprises muscle fiber size variation, the presence of regenerating and necrotic fibers, vast inflammation and extensive proliferation of connective tissue [2].

In order to obtain novel insights into the molecular mechanisms underlying LAMA2-CMD, we previously performed transcriptional and proteomic profiling of affected skeletal muscles from LAMA2-CMD mice. A majority of the differentially expressed genes and proteins were found to be involved in various metabolic processes [3,4]. Subsequently, we demonstrated functional bioenergetic impairment, with decreased *PGC-1α* expression, reduced mitochondrial respiration and a compensatory upregulation of glycolysis in human LAMA2-CMD muscle cells [5]. Thus, from these studies, we concluded that skeletal muscle metabolism may be a promising pharmacological target to improve muscle function in LAMA2-CMD patients.

Metformin, a biguanide derived from *Galega officinalis*, has been used for more than 50 years to treat type II diabetes [6]. Despite long clinical use, its mechanisms of action still

remain obscure but several studies have demonstrated the effectiveness of metformin in skeletal muscle. For example, it was recently demonstrated that six weeks of metformin treatment increased expression of non-metabolic and metabolic-related genes in adipose and muscle tissue in old humans [7]. Furthermore, positive non-metabolic effects in exercised *mdx* mice (a mouse model of Duchenne muscular dystrophy) were observed after 20 weeks of metformin treatment, with improved skeletal muscle histopathology and force [8]. Moreover, metformin has been shown to protect skeletal muscle from cardiotoxin-induced degeneration [9], increase physical performance in sedentary mice [10] and enhance *PGC-1α* in dystrophin-deficient *mdx* muscle [11]. Also, an open-label proof-of-concept study demonstrated improved muscle function in four out of five ambulatory Duchenne muscular dystrophy patients treated with L-arginine and metformin [12]. Therefore, we reasoned that metformin might improve muscle function and delay disease progression in LAMA2-CMD. Hence, in this study, we have treated dy^{2J}/dy^{2J} mice with metformin. Dy^{2J}/dy^{2J} mice exhibit a mutation in the N-terminal domain of laminin α2 chain causing a laminin polymerization defect and a slight reduction of laminin α2 chain expression [13]. Consequently, dy^{2J}/dy^{2J} mice present a relatively mild muscular dystrophy with the first symptoms appearing at around 3-4 weeks of age and dy^{2J}/dy^{2J} mice typically live more than 6 months [2,13,14]. We demonstrate that dy^{2J}/dy^{2J} mice treated with metformin display improved muscle structure and function. Importantly, we also analyzed the gender factor in the progression of the disease and demonstrate sex differences.

RESULTS

Weight gain differences in male and female *dy^{2J}/dy^{2J}* mice

To analyze the gender factor in the progression of the disease, males and females were separated in WT and *dy^{2J}/dy^{2J}* groups. As expected, the initial body weight was significantly different between males and females in both WT and *dy^{2J}/dy^{2J}* groups (Fig. 1). The same trend was observed for the final body weight, with gender and disease significantly different when analyzed by two-way ANOVA (Figure 1). Notably, male *dy^{2J}/dy^{2J}* mice displayed similar weights as female WT mice (Figure 1). When weight gain was compared between *dy^{2J}/dy^{2J}* males and females, we noted that *dy^{2J}/dy^{2J}* males gain around 85% more weight than *dy^{2J}/dy^{2J}* females (Figure 1). Bearing this data in mind, metformin treatment was performed in males and females separately.

Metformin treatment increases water intake and weight gain in female *dy^{2J}/dy^{2}* mice

We treated mice with metformin (250 mg/kg, daily oral gavage) during four weeks. The dose was chosen based on a small pilot study in which metformin at 100 mg/kg (daily oral gavage for four weeks) enhanced grip strength in female *dy^{2J}/dy^{2J}* mice but the increase was not statistically different from untreated *dy^{2J}/dy^{2J}* mice (data not shown).

We first assessed the effects of metformin administration on water intake, food intake and weight gain. In *dy^{2J}/dy^{2J}* females, we observed a 34% reduction of water intake compared with WT females (Figure 2). In contrast, water intake was not significantly different between *dy^{2J}/dy^{2J}* and WT males (Figure 2). Interestingly, metformin treatment slightly increased water intake in *dy^{2J}/dy^{2J}* females and also in WT males (Figure 2). Food intake was not

significantly different between WT and dy^{2J}/dy^{2J} mice, neither in males nor in females and metformin did not alter food intake in any of the groups (Figure 2).

An 87% reduction in weight gain was observed in dy^{2J}/dy^{2J} females when compared with WT females whereas the reduction in males was around 54% (Figure 2). Metformin treatment had a positive effect in both dy^{2J}/dy^{2J} females and males, but was more explicit in dy^{2J}/dy^{2J} females, with levels statistically indistinguishable from those of WT mice (Figure 2). Accordingly, energy efficiency (calculated based on the weight gain and energy intake along the experimental period [15]) was positively affected by metformin with a six-fold increase (statistically significant) in dy^{2J}/dy^{2} females and a 1.7-fold increase (non-significant) in dy^{2J}/dy^{2J} males (Figure 2).

Metformin treatment does not enhance muscle weight but augments grip strength in female dy^{2J}/dy^{2J} mice

Next, we evaluated if the weight gain was associated with larger skeletal muscles in metformin-treated dy^{2J}/dy^{2J} mice. A significant decrease in the weight of gastrocnemius (41% in females and 38% in males), tibialis anterior (23% in females and 36% in males) and quadriceps (30% in females and 37% in males) was seen in dy^{2J}/dy^{2J} mice (Figure 3). Also, heart weight was declined in dy^{2J}/dy^{2J} mice (32% in females and 14% in males). In contrast, there was no difference in the weight of dy^{2J}/dy^{2J} soleus muscle (neither in males nor females) compared to WT soleus. However, metformin treatment had no major effect in improving muscle mass in female and male dy^{2J}/dy^{2J} mice (Figure 3), except for a slightly increased heart weight in dy^{2J}/dy^{2J} females. Yet, metformin significantly enhanced grip strength in dy^{2J}/dy^{2J} mice. Grip strength was significantly reduced (about 70%) in dy^{2J}/dy^{2J}

females compared to WT females and metformin treatment approximately doubled the muscle strength (Figure 4). Following this pattern, a 30% decrease in grip strength was observed in dy^{2J}/dy^{2J} males when compared with WT (but this reduction was not statistically different). Furthermore, metformin treatment marginally improved grip strength in both WT and dy^{2J}/dy^{2J} males (but again, the increase was not statistically different).

Parameters such as exploratory locomotion and stand-ups were evaluated but metformin did not confer any beneficial effect in dy^{2J}/dy^{2J} females or males (data not shown).

Skeletal muscle histology is improved in female dy^{2J}/dy^{2J} mice

A microscopic evaluation of H&E-stained quadriceps sections revealed typical muscular dystrophy characteristics with fiber degeneration/regeneration (evidenced by central nucleation) and fiber size variability in dy^{2J}/dy^{2J} mice (Figure 5). Central nucleation was significantly amplified in both dy^{2J}/dy^{2J} females and males and metformin treatment reduced the number of fibers with centrally located nuclei to levels statistically indiscernible from those of WT mice (Figure 5). In dy^{2J}/dy^{2J} female muscle, the percentage of fibers with cross sectional areas in the range of 500 to 1000 mm^2 was increased compared to WT counterparts. In contrast, the percentage of fibers between 2000 to 2500 mm^2 was decreased (Figure 5). A similar trend was noted in male dy^{2J}/dy^{2J} muscle but the differences were not statistically significant (Figure 5). Notably, metformin treatment caused a shift of fiber-size distribution and normalized the fiber size and proportion in dy^{2J}/dy^{2J} females (Figure 5) whereas metformin did not affect fiber-size distribution in dy^{2J}/dy^{2J} males (Figure 5).

To analyze whether metformin-treatment affected fiber type composition, we analyzed the expression of skeletal muscle slow myosin. The number of fibers with positive staining was reduced in dy^{2J}/dy^{2J} mice (both females and males) compared to WT and metformin seemed to increase the percentage of positive slow fibers in both WT and dy^{2J}/dy^{2J} animals. However, there were no significant differences between any four studied groups (Figure 6).

Metformin treatment enhances the weight of white adipose tissue in dy^{2J}/dy^{2J} mice

Finally, to investigate whether metformin influenced non-muscle organs we analyzed the weights of white adipose tissue, brown adipose tissue, liver, spleen and kidney. In dy^{2J}/dy^{2J} mice we noted a 54% and 60% decrease of white adipose tissue weight in males and females, respectively, and metformin treatment enhanced dy^{2J}/dy^{2J} white adipose tissue weight in both females and males but did not impact WT white adipose tissue weight (Figure 7). The weight of brown adipose tissue was not affected in dy^{2J}/dy^{2J} females but was significantly reduced in dy^{2J}/dy^{2J} males. Metformin did not alter the weight of brown adipose tissue in female mice but marginally increased the brown adipose tissue weight in dy^{2J}/dy^{2J} males (Figure 7). Neither liver nor kidney weights were affected in dy^{2J}/dy^{2J} females and males. Spleen weight, on the other hand, was reduced by 20% in dy^{2J}/dy^{2J} females (a non-significant reduction was also noted in dy^{2J}/dy^{2J}males) and metformin slightly increased spleen weight in dy^{2J}/dy^{2J} females (Figure 7).

DISCUSSION

LAMA2-CMD, the second-most common form of congenital muscular dystrophy, remains incurable despite the development of successful genetic and pharmacological preclinical treatment strategies [1,2]. Metformin is FDA approved for treatment of type II diabetes in children over 10 years of age but is also used off-label to treat obesity in adolescents [16]. In this study, we show that metformin enhances weight gain, restores energy efficiency, augments muscle function and improves morphological features of muscular dystrophy in dy^{2J}/dy^{2J} females (and to a lesser extent in dy^{2J}/dy^{2J} males). Some features were not improved, such as exploratory locomotion and stand-ups but this may be due to the fact that metformin only had little effect on hindleg lameness. Peripheral neuropathy is particularly evident in dy^{2J}/dy^{2J} mice but is not a clinical manifestation in patients [17]. Another therapeutic candidate for LAMA2-CMD is losartan that was demonstrated to confer clinical improvement and reduce fibrosis in the dy^{2J}/dy^{2J} mouse model [18]. The anti-apoptotic compound omigapil also provided beneficial effects in dy^{2J}/dy^{2J} mice [19] as well as in the dy^{W}/dy^{W} mouse [20] (another mouse model of LAMA2-CMD). Losartan and omigapil are expected to target fibrosis and apoptosis, respectively, but neither compound has been shown to regulate metabolism, which is significantly altered in LAMA2-CMD as well as in other muscular dystrophies [5,21,22].

Metformin has been described to control metabolism, for example by decreasing lipogenesis and gluconeogenesis and modulating mitochondrial function [23]. Studies demonstrate that metformin increases healthspan and lifespan in mice [24] and in elderly patients, improving glucose tolerance and regulating expression not only of metabolic genes but also collagen and DNA repair-related-genes in muscle and adipose tissue [7]. Moreover, it

was recently described that metformin treatment attenuated fibrosis and insulin resistance in adipose tissue caused by doxorubicin treatment in rats [25]. In skeletal muscle, metformin treatment improved the oxidative metabolism in gastrocnemius muscle from mice and reduced muscle injury induced by cardiotoxin [9]. In the same study, reduction of cell damage and necrosis was demonstrated *in vitro* using C2C12 myotubes subjected to metformin treatment [9]. Finally, in tumor-bearing animals metformin was shown to increase protein synthesis and reduces protein degradation in gastrocnemius muscle [26]. It is tempting to speculate that metformin improves oxidative metabolism, which is significantly impaired in LAMA2-CMD cells [5]. On the other hand, while metformin conferred positive effects in *mdx* skeletal muscle, no clear protective actions on dystrophic metabolism were observed [8]. Hence, the mechanisms of metformin action in dy^{2J}/dy^{2J} mice are still to be clarified. Yet, it is interesting to note that another compound (N-acetyl-cysteine), which affects metabolism by reducing the formation of reactive oxygen species that may arise through insufficient mitochondrial respiration, also improves muscle function and structure in dy^{2J}/dy^{2J} mice (Harandi et al., unpublished data). Nevertheless, there are some other limitations of this study. For example, treatment was initiated at 6-weeks of age when muscle impairment is already readily detected in dy^{2J}/dy^{2J} mice [14]. It would be interesting to start metformin treatment sooner and continue over a longer period of time (as no overt side effects of metformin were noted). Moreover, we have only analysed histology of one skeletal muscle (quadriceps).

It is well known that gender affects a wide variety of physiological functions including cardiovascular and autoimmune systems and influences a broad range of diseases such as

gastrointestinal, liver, kidney, endocrine, blood and neurological disorders. Moreover, gender also impacts pharmacokinetics and pharmacodynamics [27]. Duchenne muscular dystrophy is an X-linked recessive muscular dystrophy, thus affecting only boys, but apart from gender differences due to the genetic inheritance pattern, there is only little data available regarding gender differences in disease progression of muscular dystrophy [28-30]. Bearing this in mind, we monitored the disease progression during four weeks in 6-week-old dy^{2J}/dy^{2J} females and males. We found several important gender differences (at least in this age range). Weight gain was lower in dy^{2J}/dy^{2J} female mice compared to dy^{2J}/dy^{2J} males; water intake was significantly reduced in dy^{2J}/dy^{2J} females compared to WT females (not in corresponding males); a larger decrease of relative grip strength was noted in dy^{2J}/dy^{2J} females compared to dy^{2J}/dy^{2J} males and the shift in fiber size distribution was much more pronounced in dy^{2J}/dy^{2J} females compared to males. Thus, to our knowledge, this is the first time gender differences are reported in LAMA2-CMD.

In conclusion, this study shows that metformin treatment significantly reduces muscular dystrophy in dy^{2J}/dy^{2J} females. Importantly, metformin is already approved for use in humans, which is advantageous from a clinical point of view. Nevertheless, metformin treatment does not target the primary genetic defect and is not expected to completely cure LAMA2-CMD. Yet, metformin could be used as a supportive treatment that may improve many of the pathological symptoms in LAMA2-CMD.

MATERIALS AND METHODS

Animals

Heterozygous dy^{2J}/dy^{2J} (B6.WK-Lama2dy-2J/J) were obtained from Jackson Laboratory and bred and maintained in our animal facility according to institutional animal care guidelines. All experimental procedures involving animals were approved by the Malmö/Lund (Sweden) ethical committee for animal research (ethical permit number 5.8.18-02255/2017) in accordance with guidelines issues by the Swedish Board of Agriculture. The animals were maintained at 22 ± 2°C with a regular light-dark cycle (light on from 6:00 am to 6:00 pm) and had free access to food and water. The diet consisted of 51.2% carbohydrate, 22% protein and 4.25% fat (Special Diet Services). Six-week-old mice were separated according to gender and into wild-type (WT) and dystrophic (dy^{2J}/dy^{2J}) groups and further subdivided into WT control, WT metformin-treated, dy^{2J}/dy^{2J} control and dy^{2J}/dy^{2J} metformin-treated.

Treatment

Metformin (CAS 1115-70-4, Calbiochem) diluted in filtered water was administrated by oral gavage once a day at 250 mg/kg body weight during four weeks. Control animals received filtered water by oral gavage. Initial and final bodyweight and weight gain were analyzed. Food and water intake were estimated twice-a-week (by weight measurements). The energy efficiency ratio was calculated as the weight gain (g) during the experimental period divided by the cumulative energy intake over the same period (kcal), according to Jung et al. [15].

Locomotor activity and grip strength

After four weeks of treatment, animals were subjected to exploratory locomotion testing

and grip strength analysis. Exploratory locomotion was evaluated in an open-field test, as previously described [31]. In each experiment, a mouse was placed into a new cage and allowed to explore the cage for five minutes. The time that the mouse spent moving around was measured, as well as number of stand-ups on hindlimbs.

Forelimb grip strength was measured using a grip-strength meter (Columbus Instruments) as previously described [31]. In brief, the mouse was held by the base of the tail and allowed to grasp the flat wire mesh of the pull bar with its forepaws. When the mouse got a good grip, it was slowly pulled away by its tail until it released the pull bar. Each mouse was allowed to pull the pull bar five times. The two lowest values were rejected and the mean of the three remaining values was counted. Animals were not subjected to any training prior to the experiment. Grip strength was calculated as force divided by final body weight [32].

Tissue collection

Mice were sacrificed by cervical dislocation. Tissues were rapidly excised, carefully dissected, and weighed. Skeletal muscles isolated were soleus, gastrocnemius, tibialis anterior and quadriceps. Heart, white adipose tissue (perigenital), brown adipose tissue (intercostal), liver, spleen and kidney were isolated and weighed as well.

Histology and immunohistochemistry

For morphometric analyses, quadriceps muscles were either embedded in OCT compound (Tissue-Tek) and frozen in liquid nitrogen or embedded in paraffin. Paraffin-embedded specimens were sectioned using a microtome (5 µm) (Microm H355) and OCT embedded sections were sectioned using a cryostat (7 µm) (Microm HM 560). Paraffin sections were

stained with hematoxylin and eosin (H&E) staining and cryosections were subjected to immunostaining (see further down). H&E stained sections were scanned using an Aperio ScanScope CS2 scanner with ScanScope console version 8.2.0.1263. Central nucleation was quantified using ImageJ software version 1.43u, Cell Counter plug-in (NIH). The whole quadriceps cross-section muscle was used for quantification and the percentage of central nuclei was subsequently calculated. The fiber area of biotinylated wheat germ agglutinin (WGA) stained muscle fibers was measured and quantified using Adobe Photoshop CS5 extended version (Adobe System) and ImageJ.

Immunohistochemistry was performed as previously described [33] using a monoclonal antibody against anti-myosin (skeletal, slow; M8421, Sigma Aldrich). In addition, biotinylated WGA was used as a membrane marker. The secondary antibody was goat anti-mouse IgG 546 (Thermo Fisher Scientific) together with avidin. The slides were analyzed by Zeiss Axioplan fluorescence microscope (Zeiss) and images were captured using an ORCA 1394 ER digital camera (Hamamatsu Photonics) and Openlab software version 4 (Improvision). The whole quadriceps cross-section muscle was used for quantification and the percentage of fibers with positive staining of type I slow fibers was subsequently calculated.

Statistical analysis

All data are shown as mean ± S.E.M. Statistical analysis of the data was performed by means of two-way analysis of variance (ANOVA) with Bonferroni *post hoc* test for comparison of gender and disease effect and one-way analysis of variance (ANOVA) with Bonferroni *post hoc* test for comparison of treatment effect. $p<0.05$ values were considered as significant.

Data availability

The datasets generated during and/or analyzed during the current study are available from the corresponding author on reasonable request.

ACKNOWLEDGEMENTS

This work was generously supported by Anna and Edwin Berger Foundation, Anna-Greta Crafoord Foundation for Rheumatology Research, Association Française contre les Myopathies, Conselho Nacional de Desenvolvimento Científico e Tecnológico, Crafoord Foundation, Fanny Ekdahl Foundation, Greta and Johan Kock Foundation, Jane and Dan Olsson Foundation, Lisa and Johan Grönberg Foundation, Olle Engkvist Byggmästare Foundation, Royal Physiographic Society in Lund, The Swedish Research Council, Tore Nilsson Foundation and Österlund Foundation. We dedicate this work in the memory of our friend and colleague Bruno Menezes de Oliveira, Ph.D.

AUTHOR CONTRIBUTIONS

CCFO and MD designed research; CCFO, BMSO, ZK and VH performed research and analyzed data; CCFO and MD wrote the paper.

ADDITIONAL INFORMATION

The authors declare no competing interests.

REFERENCES

1 Yurchenco, P. D., McKee, K. K., Reinhard, J. R. & Ruegg, M. A. Laminin-deficient muscular dystrophy: Molecular pathogenesis and structural repair strategies. *Matrix Biol*, doi:10.1016/j.matbio.2017.11.009 (2017).

2 Durbeej, M. Laminin-alpha2 Chain-Deficient Congenital Muscular Dystrophy: Pathophysiology and Development of Treatment. *Curr Top Membr* **76**, 31-60, doi:10.1016/bs.ctm.2015.05.002 (2015).

3 de Oliveira, B. M. *et al.* Quantitative proteomic analysis reveals metabolic alterations, calcium dysregulation, and increased expression of extracellular matrix proteins in laminin alpha2 chain-deficient muscle. *Mol Cell Proteomics* **13**, 3001-3013, doi:10.1074/mcp.M113.032276 (2014).

4 Hager, M. *et al.* Cib2 binds integrin alpha7Bbeta1D and is reduced in laminin alpha2 chain-deficient muscular dystrophy. *J Biol Chem* **283**, 24760-24769, doi:10.1074/jbc.M801166200 (2008).

5 Fontes-Oliveira, C. C., Steinz, M., Schneiderat, P., Mulder, H. & Durbeej, M. Bioenergetic Impairment in Congenital Muscular Dystrophy Type 1A and Leigh Syndrome Muscle Cells. *Sci Rep* **7**, 45272, doi:10.1038/srep45272 (2017).

6 Fujita, Y. & Inagaki, N. Metformin: New Preparations and Nonglycemic Benefits. *Curr Diab Rep* **17**, 5, doi:10.1007/s11892-017-0829-8 (2017).

7 Kulkarni, A. S. *et al.* Metformin regulates metabolic and nonmetabolic pathways in skeletal muscle and subcutaneous adipose tissues of older adults. *Aging Cell* **17**, doi:10.1111/acel.12723 (2018).

8 Mantuano, P. *et al.* Effect of a long-term treatment with metformin in dystrophic mdx mice: a reconsideration of its potential clinical interest in Duchenne muscular dystrophy. *Biochem Pharmacol*, doi:10.1016/j.bcp.2018.04.022 (2018).

9 Langone, F. *et al.* Metformin protects skeletal muscle from cardiotoxin induced degeneration. *PLoS One* **9**, e114018, doi:10.1371/journal.pone.0114018 (2014).

10 Senesi, P. *et al.* Metformin Treatment Prevents Sedentariness Related Damages in Mice. *J Diabetes Res* **2016**, 8274689, doi:10.1155/2016/8274689 (2016).

11 Ljubicic, V. & Jasmin, B. J. Metformin increases peroxisome proliferator-activated receptor gamma Co-activator-1alpha and utrophin a expression in dystrophic skeletal muscle. *Muscle Nerve* **52**, 139-142, doi:10.1002/mus.24692 (2015).

12 Hafner, P. *et al.* Improved Muscle Function in Duchenne Muscular Dystrophy through L-Arginine and Metformin: An Investigator-Initiated, Open-Label, Single-Center, Proof-Of-Concept-Study. *PLoS One* **11**, e0147634, doi:10.1371/journal.pone.0147634 (2016).

13 Gawlik, K. I. & Durbeej, M. Skeletal muscle laminin and MDC1A: pathogenesis and treatment strategies. *Skelet Muscle* **1**, 9, doi:10.1186/2044-5040-1-9 (2011).

14 Pasteuning-Vuhman, S. *et al.* Natural disease history of the dy2J mouse model of laminin alpha2 (merosin)-deficient congenital muscular dystrophy. *PLoS One* **13**, e0197388, doi:10.1371/journal.pone.0197388 (2018).

15 Jung, H. W., Kang, A. N., Kang, S. Y., Park, Y. K. & Song, M. Y. The Root Extract of Pueraria lobata and Its Main Compound, Puerarin, Prevent Obesity by Increasing the Energy Metabolism in Skeletal Muscle. *Nutrients* **9**, doi:10.3390/nu9010033 (2017).

16 McDonagh, M. S., Selph, S., Ozpinar, A. & Foley, C. Systematic review of the benefits and risks of metformin in treating obesity in children aged 18 years and younger. *JAMA Pediatr* **168**, 178-184, doi:10.1001/jamapediatrics.2013.4200 (2014).
17 Bonnemann, C. G. *et al.* Diagnostic approach to the congenital muscular dystrophies. *Neuromuscul Disord* **24**, 289-311, doi:10.1016/j.nmd.2013.12.011 (2014).
18 Elbaz, M. *et al.* Losartan, a therapeutic candidate in congenital muscular dystrophy: studies in the dy(2J) /dy(2J) mouse. *Ann Neurol* **71**, 699-708, doi:10.1002/ana.22694 (2012).
19 Yu, Q. *et al.* Omigapil treatment decreases fibrosis and improves respiratory rate in dy(2J) mouse model of congenital muscular dystrophy. *PLoS One* **8**, e65468, doi:10.1371/journal.pone.0065468 (2013).
20 Erb, M. *et al.* Omigapil ameliorates the pathology of muscle dystrophy caused by laminin-alpha2 deficiency. *J Pharmacol Exp Ther* **331**, 787-795, doi:10.1124/jpet.109.160754 (2009).
21 Turk, R. *et al.* Common pathological mechanisms in mouse models for muscular dystrophies. *FASEB J* **20**, 127-129, doi:10.1096/fj.05-4678fje (2006).
22 Groh, S. *et al.* Sarcoglycan complex: implications for metabolic defects in muscular dystrophies. *J Biol Chem* **284**, 19178-19182, doi:10.1074/jbc.C109.010728 (2009).
23 Nasri, H. & Rafieian-Kopaei, M. Metformin: Current knowledge. *J Res Med Sci* **19**, 658-664 (2014).
24 Martin-Montalvo, A. *et al.* Metformin improves healthspan and lifespan in mice. *Nat Commun* **4**, 2192, doi:10.1038/ncomms3192 (2013).
25 Biondo LA, B. H., Souza C, Teixeira ASA, Silveira LA, Alonso-Vale MI, Oyama LM, Alves MJ, Seelaender M, Neto JCR. Metformin Mitigates Fibrosis and Glucose Intolerance Induced byDoxorubicin in Subcutaneous Adipose Tissue. *Frontriers in Pharmacology* **9**, doi:doi: 10.3389/fphar.2018.00452 (2018).
26 Oliveira, A. G. & Gomes-Marcondes, M. C. Metformin treatment modulates the tumour-induced wasting effects in muscle protein metabolism minimising the cachexia in tumour-bearing rats. *BMC Cancer* **16**, 418, doi:10.1186/s12885-016-2424-9 (2016).
27 Regitz-Zagrosek, V. Sex and gender differences in health. Science & Society Series on Sex and Science. *EMBO Rep* **13**, 596-603, doi:10.1038/embor.2012.87 (2012).
28 Fanin, M., Nascimbeni, A. C. & Angelini, C. Gender difference in limb-girdle muscular dystrophy: a muscle fiber morphometric study in 101 patients. *Clin Neuropathol* **33**, 179-185, doi:10.5414/np300728 (2014).
29 Hakim, C. H. & Duan, D. Gender differences in contractile and passive properties of mdx extensor digitorum longus muscle. *Muscle Nerve* **45**, 250-256, doi:10.1002/mus.22275 (2012).
30 Salimena, M. C., Lagrota-Candido, J. & Quirico-Santos, T. Gender dimorphism influences extracellular matrix expression and regeneration of muscular tissue in mdx dystrophic mice. *Histochem Cell Biol* **122**, 435-444, doi:10.1007/s00418-004-0707-8 (2004).
31 Korner, Z., Fontes-Oliveira, C. C., Holmberg, J., Carmignac, V. & Durbeej, M. Bortezomib partially improves laminin alpha2 chain-deficient muscular dystrophy. *Am J Pathol* **184**, 1518-1528, doi:10.1016/j.ajpath.2014.01.019 (2014).

32 Leiter, J. R., Peeler, J. & Anderson, J. E. Exercise-induced muscle growth is muscle-specific and age-dependent. *Muscle Nerve* **43**, 828-838, doi:10.1002/mus.21965 (2011).
33 Gawlik, K. I., Harandi, V. M., Cheong, R. Y., Petersen, A. & Durbeej, M. Laminin alpha1 reduces muscular dystrophy in dy(2J) mice. *Matrix Biol*, doi:10.1016/j.matbio.2018.02.024 (2018).

FIGURE LEGENDS

Figure 1. Differences between males and females in disease progression. Body weights were recorded when the animals were 6-weeks-old and monitored during four weeks. Results are expressed as mean ± SEM in 13 WT males, 10 WT females, 4 dy^{2J}/dy^{2J} males and 6 dy^{2J}/dy^{2J} females. Initial body weight (IBW) and final body weight (FBW) values are significantly different by two-way ANOVA for disease and gender both with $p<0.0001$. Weight gain values are significantly different by two-way ANOVA for disease ($p<0.01$) and gender ($p<0.001$). Letters a, b and c were used to express the differences among groups and columns with the same letter are not significantly different.

Figure 2. Differences between males and females in disease progression and response to metformin treatment. Water intake is expressed in milliliter (mL) and food intake in grams. The measurements refer to ingestion during the period of treatment. Weight gain is expressed in grams. Energy efficiency is expressed in percentage comparative to WT control group, which is considered 100% efficient. WT control: females=7, males=13; WT metformin: females=10, males=6; dy^{2J}/dy^{2J} control: females=5, males=4; dy^{2J}/dy^{2J} metformin: females=5, males=5. Results are expressed as mean ± SEM. Statistical significance was assessed by one-way ANOVA followed by Bonferroni *post hoc* test. $p<0.05$ values were considered as statistically significantly different. Letters a, b and c were used to express the differences among groups and columns with the same letter are not significantly different.

Figure 3. Muscle and heart weights. Values are expressed in grams (weights collected after four weeks of treatment). WT control: females=7, males=13; WT metformin: females=10, males=6; dy^{2J}/dy^{2J} control: females=5, males=4; dy^{2J}/dy^{2J} metformin: females=5, males=5. Results are expressed as mean ± SEM. Statistical significance was assessed by one-way ANOVA followed by Bonferroni *post hoc* test. $p<0.05$ values were considered as statistically significantly different. Letters a, b and c were used to express the differences among groups and columns with the same letter are not significantly different.

Figure 4. Relative forelimb grip strength. Calculations were done as force (KgF) divided by final body weight in grams. Results are expressed as % relative grip strength. WT control: females=7, males=13; WT metformin: females=10, males=6; dy^{2J}/dy^{2J} control: females=5, males=4; dy^{2J}/dy^{2J} metformin: females=5, males=5. Results are expressed as mean ± SEM. Statistical significance was assessed by one-way ANOVA followed by Bonferroni *post hoc* test. $p<0.05$ values were considered as statistically significantly different. Letters a, b and c were used to express the differences among groups and columns with the same letter are not significantly different.

Figure 5. A) Representative hematoxylin and eosin stained sections. B) Central nucleation in quadriceps muscle. C) Cross-sectional area of quadriceps muscle cells. WT control: females=6, males=10; WT metformin: females=9, males=5; dy^{2J}/dy^{2J} control: females=5, males=3; dy^{2J}/dy^{2J} metformin: females=4, males=4. Results are expressed as mean ± SEM. Statistical significance was assessed by one-way ANOVA followed by Bonferroni *post hoc* test. $p<0.05$ values were considered as statistically significantly different. Letters a, b and c

were used to express the differences among groups and columns with the same letter are not significantly different. (Bar=50 µm, Magnification=4.9X).

Figure 6. A) Labelling against slow quadriceps muscle fibers. B) Values are expressed in percentage of positive slow muscle fibers (analyzed after four weeks of treatment). WT control: females=3, males=3; WT metformin: females=3, males=2; dy^{2J}/dy^{2J} control: females=3, males=3; dy^{2J}/dy^{2J} metformin: females=4, males=3. Results are expressed as mean ± SEM. Statistical significance was assessed by one-way ANOVA followed by Bonferroni *post hoc* test (Bar=100 µm).

Figure 7. Tissue weights. WAT: white (perigenital) adipose tissue, BAT: brown (intercostal) adipose tissue. Values are expressed in grams (collected after four weeks of treatment). WT control: females, males=13; WT metformin: females=10, males=6; dy^{2J}/dy^{2J} control: females=5, males=4; dy^{2J}/dy^{2J} metformin: females=5, males=5. Results are expressed as mean ± SEM. Statistical significance was assessed by one-way ANOVA followed by Bonferroni *post hoc* test. $p<0.05$ values were considered as statistically significantly different. Letters a, b and c were used to express the differences among groups and columns with the same letter are not significantly different.

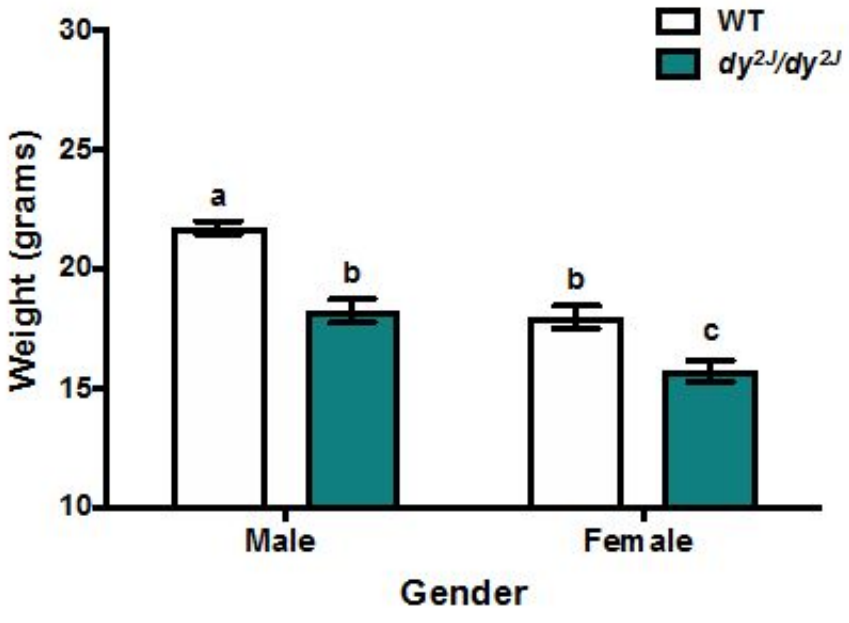
IBW
WT
dy2J/dy2J
Weight (grams)
30
25
20
15
10
a
b
b
c
Male
Female
Gender

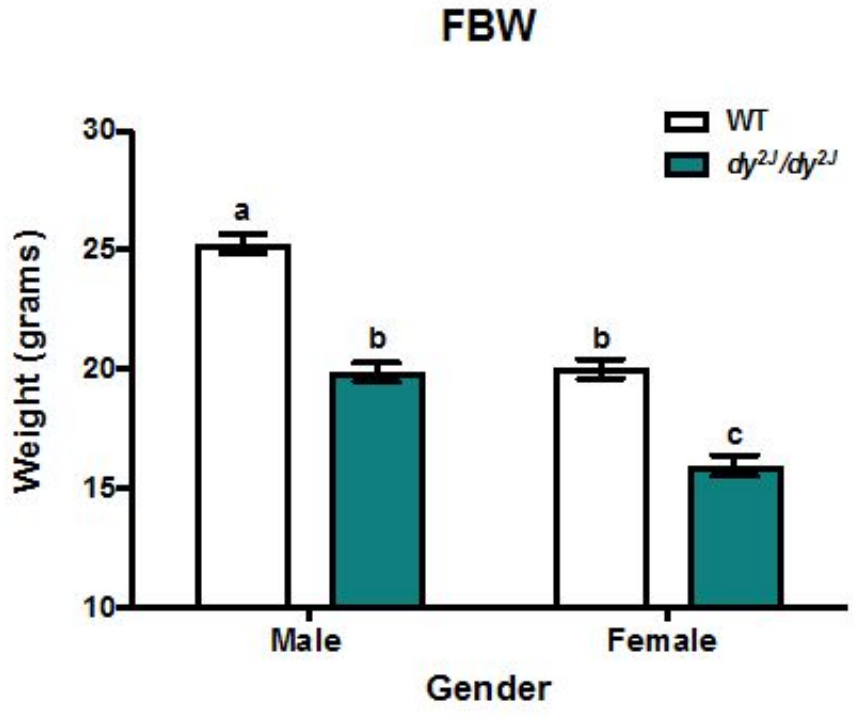
FBW
WT
dy2J/dy2J
Weight (grams)
30
25
20
15
10
a
b
b
c
Male
Female
Gender

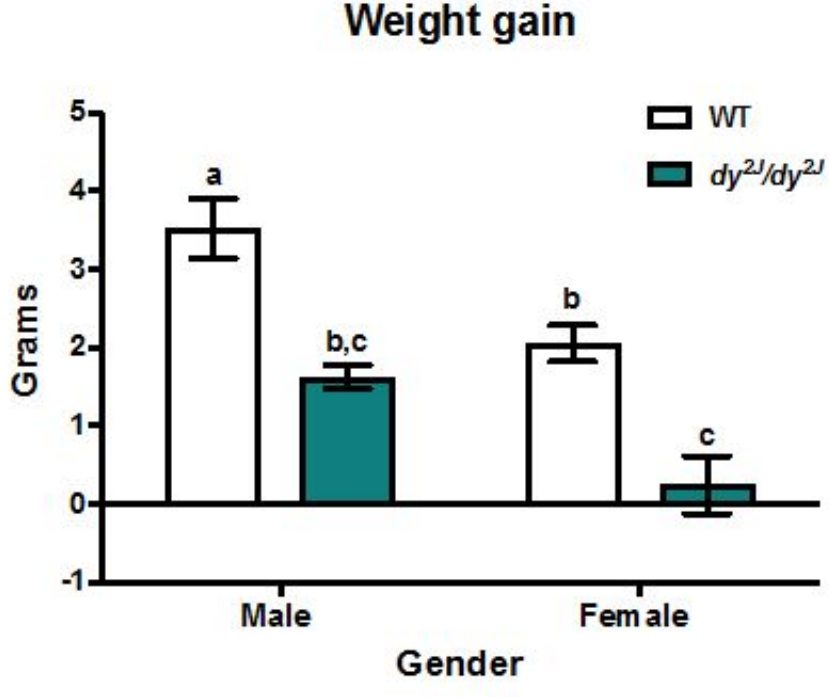
Weight gain
WT
dy2J/dy2J
Grams
5
4
3
2
1
0
-1
a
b,c
b
c
Male
Female
Gender

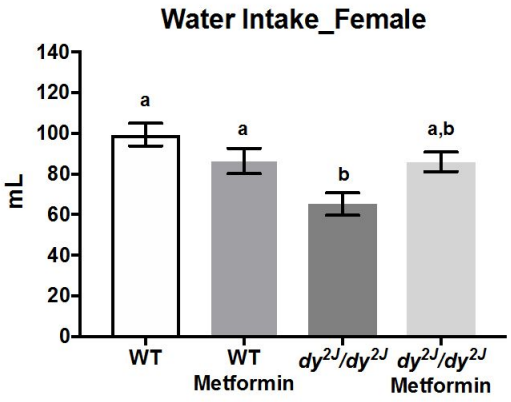
Water Intake_Female
mL
140
120
100
80
60
40
20
0
a
a
b
a,b
WT
WT Metformin
dy2J/dy2J
dy2J/dy2J Metformin

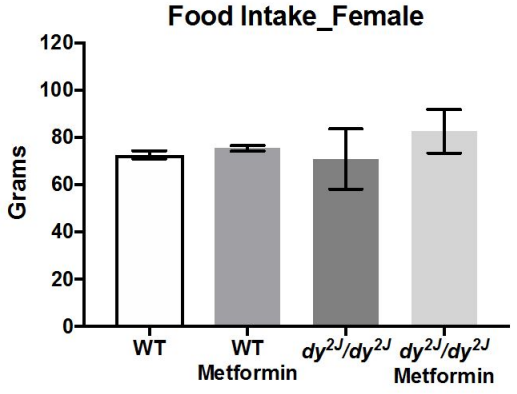
Food Intake_Female
Grams
120
100
80
60
40
20
0
WT
WT Metformin
dy2J/dy2J
dy2J/dy2J Metformin

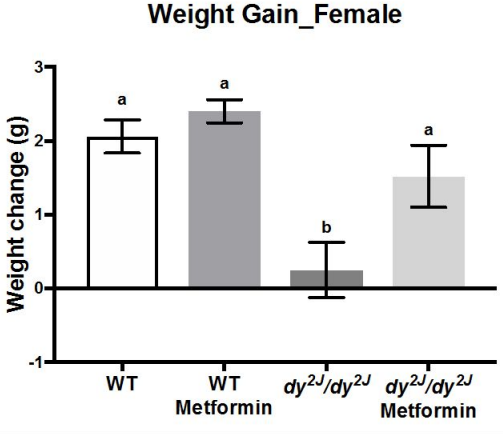
Weight Gain_Female
Weight change (g)
3
2
1
0
-1
a
a
b
a
WT
WT Metformin
dy2J/dy2J
dy2J/dy2J Metformin

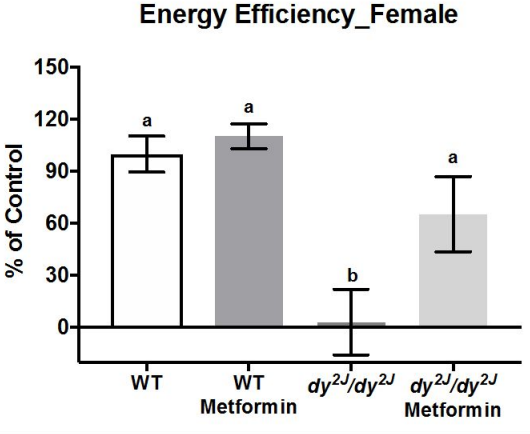
Energy Efficiency_Female
% of Control
150
120
90
60
30
0
a
a
b
a
WT
WT Metformin
dy2J/dy2J
dy2J/dy2J Metformin

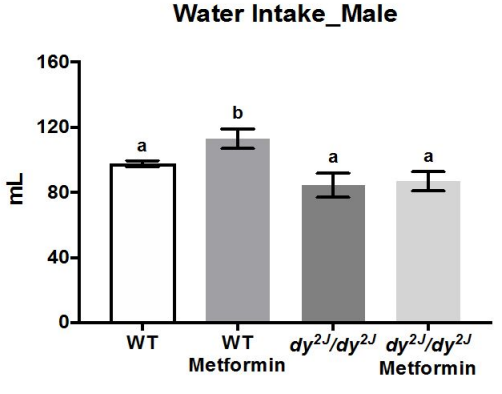
Water Intake_Male
mL
160
120
80
40
0
a
b
a
a
WT
WT Metformin
dy2J/dy2J
dy2J/dy2J Metformin

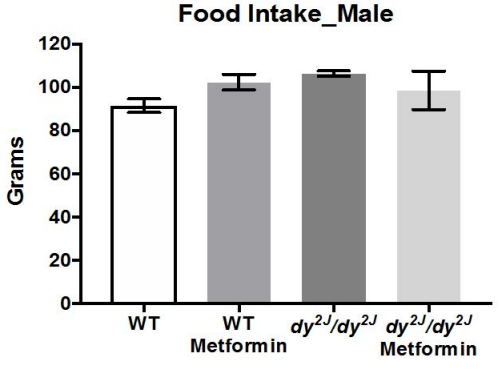
Food Intake_Male
Grams
120
100
80
60
40
20
0
WT
WT Metformin
dy2J/dy2J
dy2J/dy2J Metformin

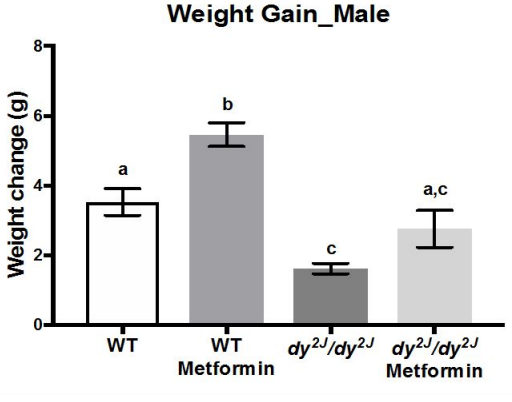
Weight Gain_Male
Weight change (g)
8
6
4
2
0
a
b
c
a,c
WT
WT Metformin
dy2J/dy2J
dy2J/dy2J Metformin

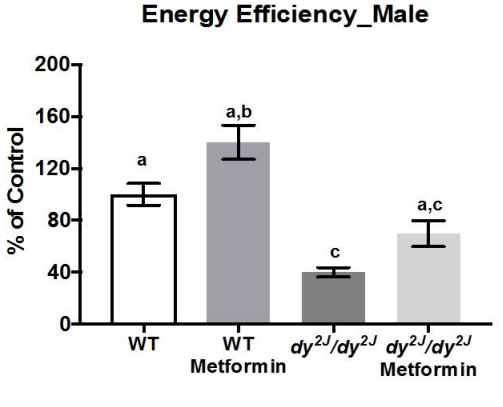
Energy Efficiency_Male
% of Control
200
160
120
80
40
0
a
a,b
c
a,c
WT
WT Metformin
dy2J/dy2J
dy2J/dy2J Metformin

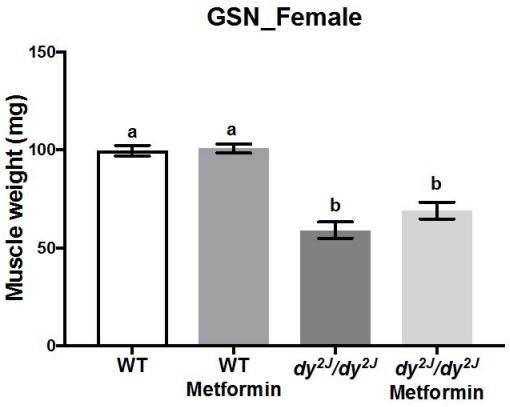
GSN_Female
Muscle weight (mg)
150
100
50
0
a
a
b
b
WT
WT Metformin
dy2J/dy2J
dy2J/dy2J Metformin

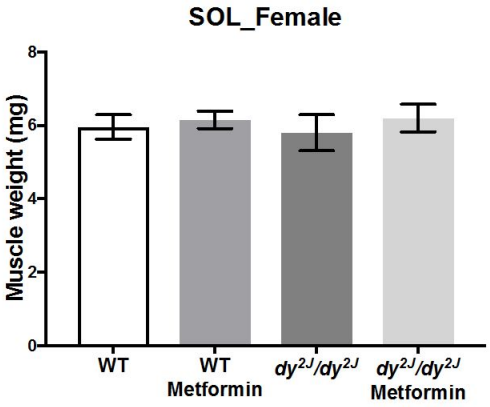
SOL_Female
Muscle weight (mg)
8
6
4
2
0
WT
WT Metformin
dy2J/dy2J
dy2J/dy2J Metformin

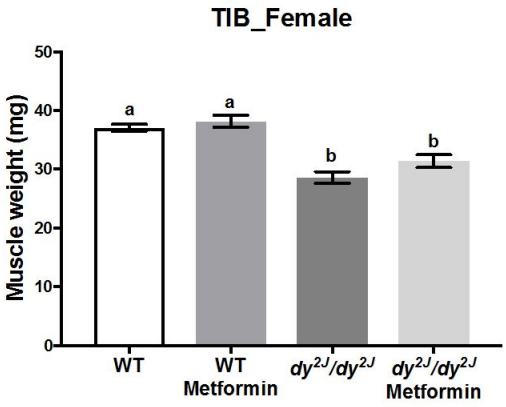
TIB_Female
Muscle weight (mg)
50
40
30
20
10
0
a
a
b
b
WT
WT Metformin
dy2J/dy2J
dy2J/dy2J Metformin

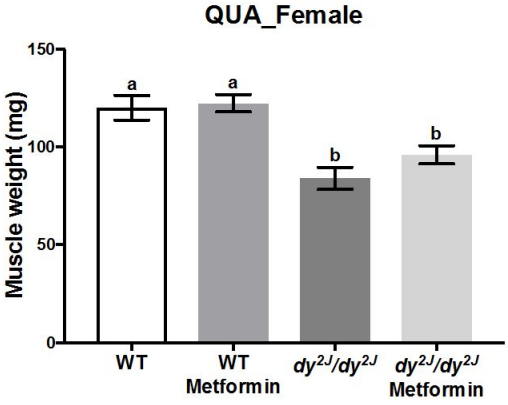
QUA_Female
Muscle weight (mg)
150
100
50
0
a
a
b
b
WT
WT Metformin
dy2J/dy2J
dy2J/dy2J Metformin

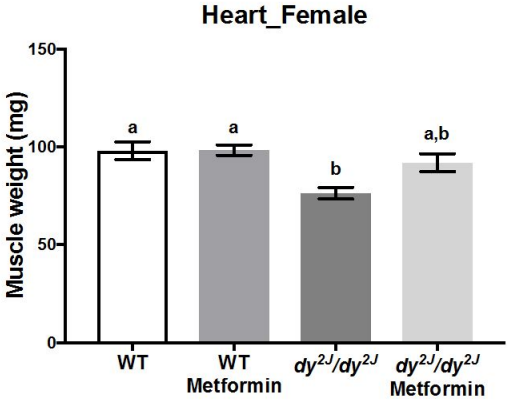
Heart_Female
Muscle weight (mg)
150
100
50
0
a
a
b
a,b
WT
WT Metformin
dy2J/dy2J
dy2J/dy2J Metformin

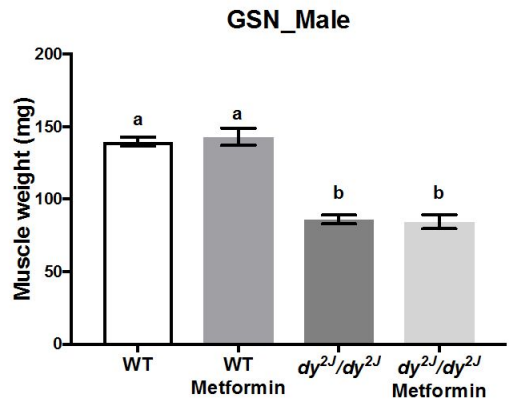
GSN_Male
Muscle weight (mg)
200
150
100
50
0
a
a
b
b
WT
WT Metformin
dy2J/dy2J
dy2J/dy2J Metformin

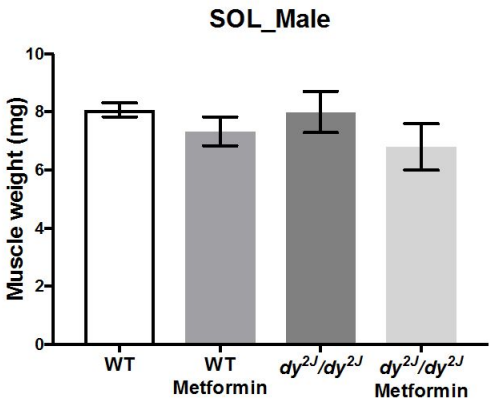
SOL_Male
Muscle weight (mg)
10
8
6
4
2
0
WT
WT Metformin
dy2J/dy2J
dy2J/dy2J Metformin

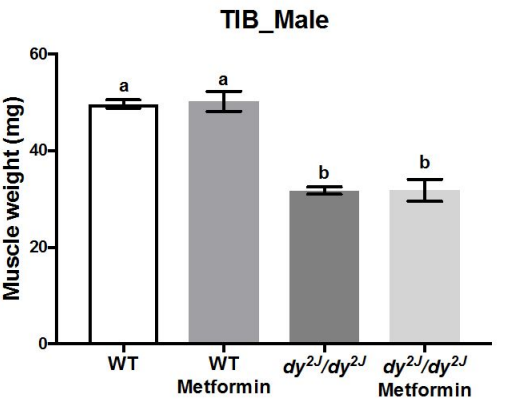
TIB_Male
Muscle weight (mg)
60
40
20
0
a
a
b
b
WT
WT Metformin
dy2J/dy2J
dy2J/dy2J Metformin

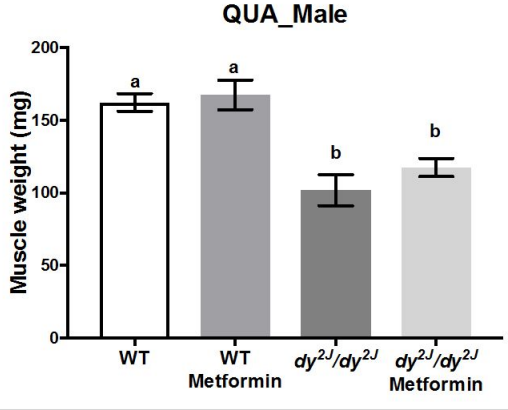
QUA_Male
Muscle weight (mg)
200
150
100
50
0
a
a
b
b
WT
WT Metformin
dy2J/dy2J
dy2J/dy2J Metformin

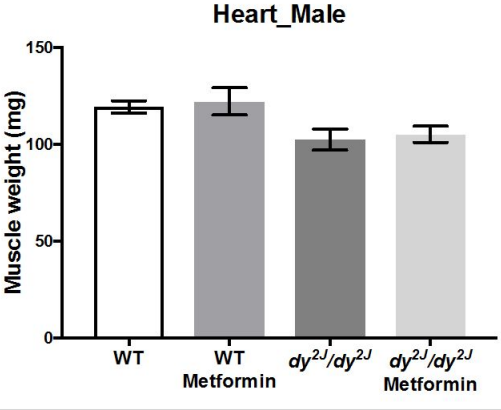
Heart_Male
Muscle weight (mg)
150
100
50
0
WT
WT Metformin
dy2J/dy2J
dy2J/dy2J Metformin

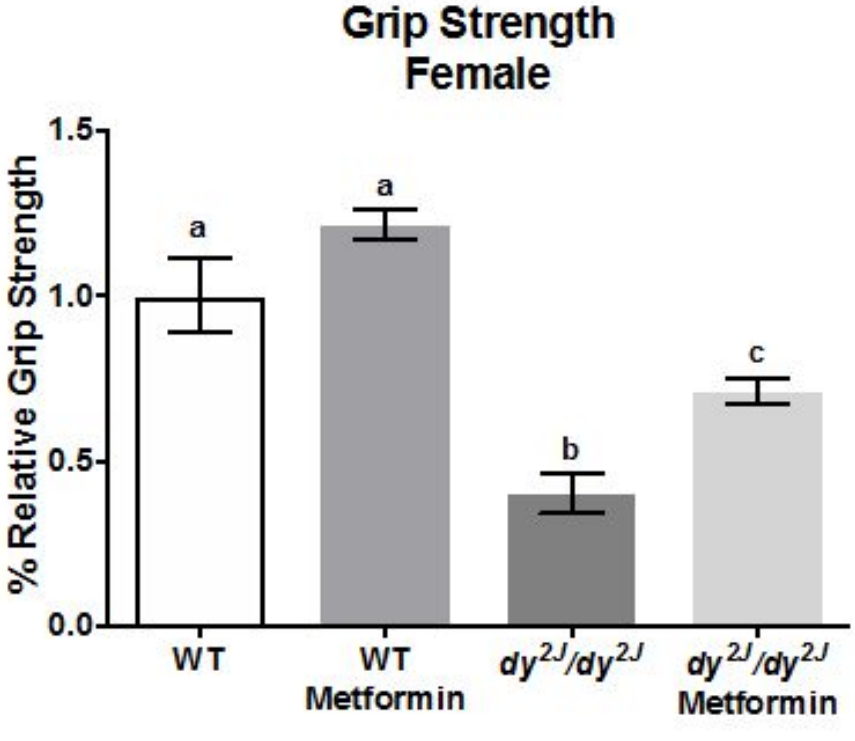
Grip Strength
Female
% Relative Grip Strength
1.5
1.0
0.5
0.0
a
a
b
c
WT
WT
Metformin
dy2J/dy2J
dy2J/dy2J
Metformin

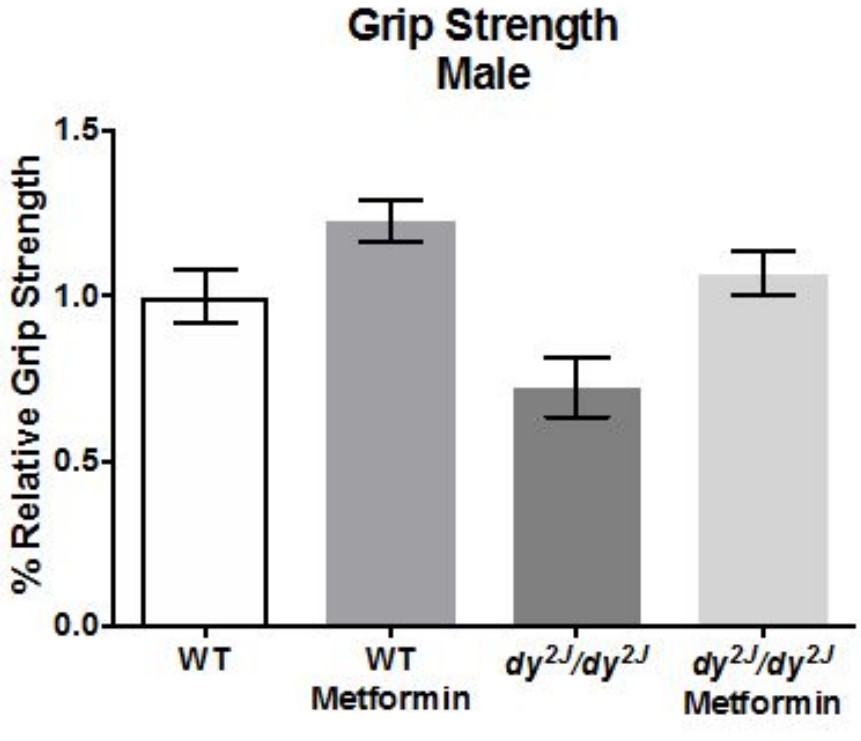
Grip Strength
Male
% Relative Grip Strength
1.5
1.0
0.5
0.0
WT
WT
Metformin
dy2J/dy2J
dy2J/dy2J
Metformin

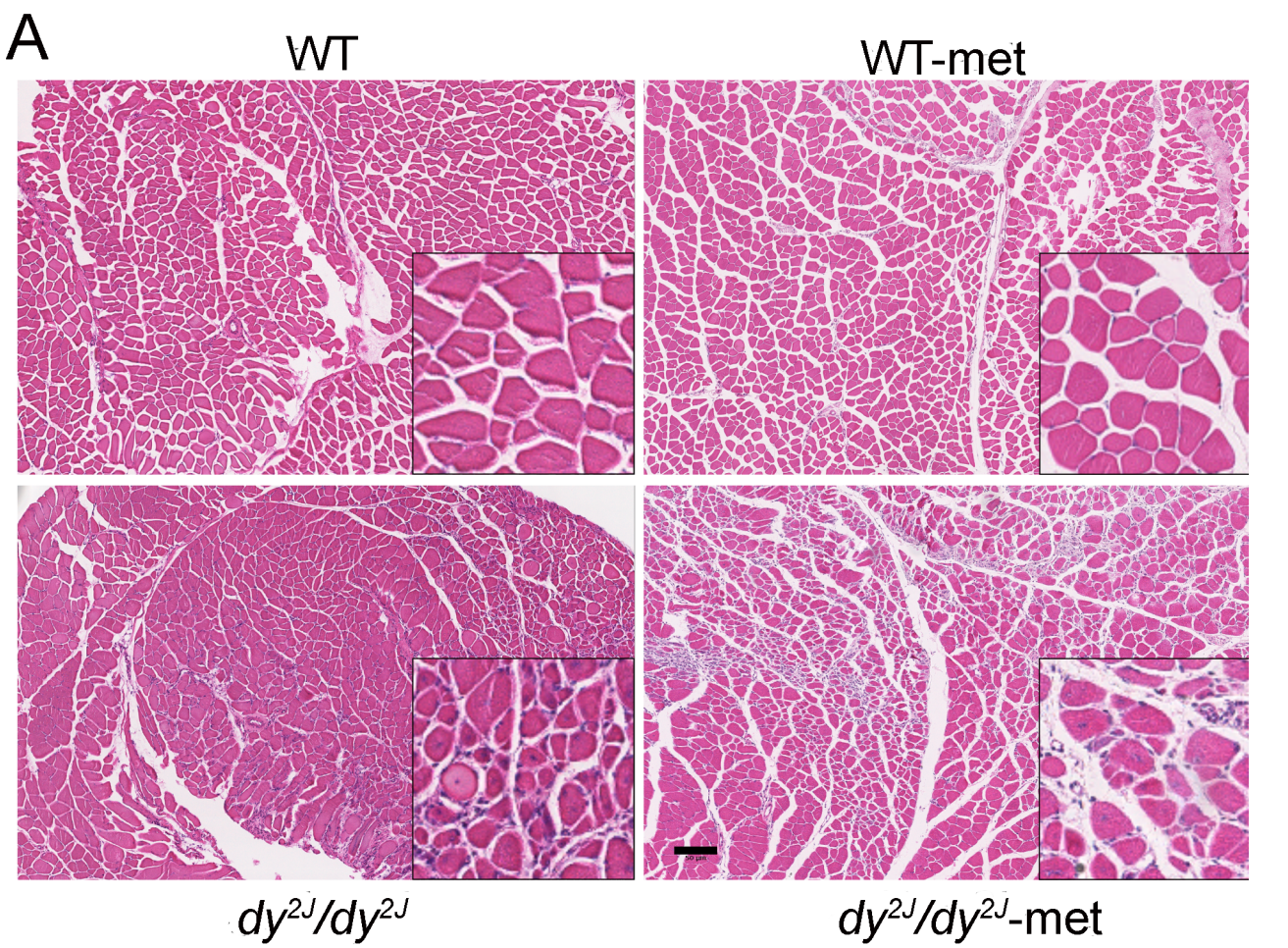
A
WT
WT-met
dy2J/dy2J
dy2J/dy2J-met

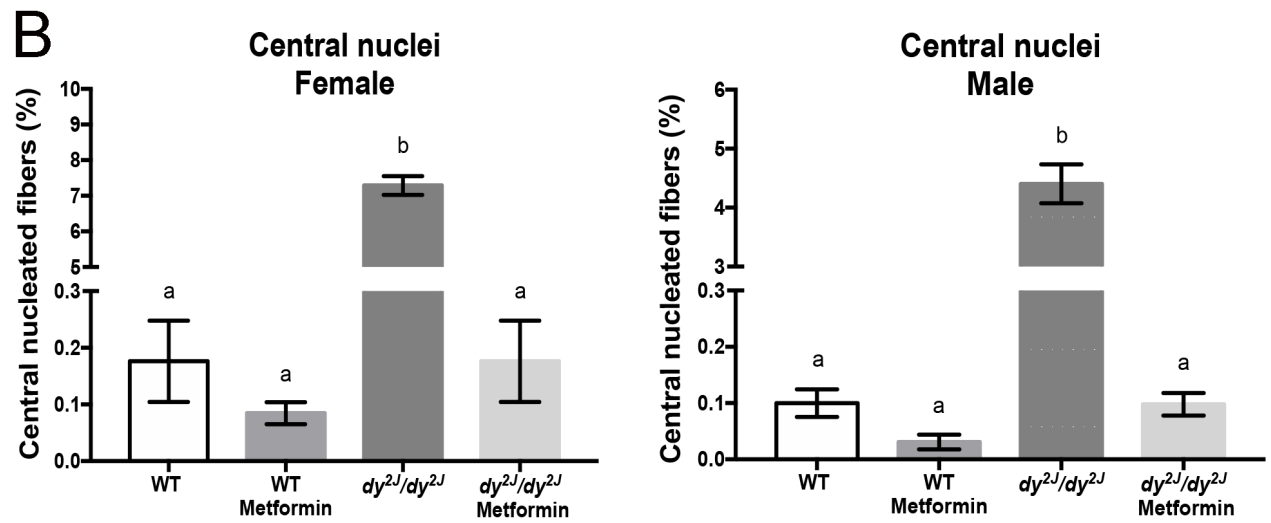
B
Central nuclei
Female
Central nucleated fibers (%)
WT
WT Metformin
dy2J/dy2J
dy2J/dy2J Metformin
Central nuclei
Male
Central nucleated fibers (%)
WT
WT Metformin
dy2J/dy2J
dy2J/dy2J Metformin

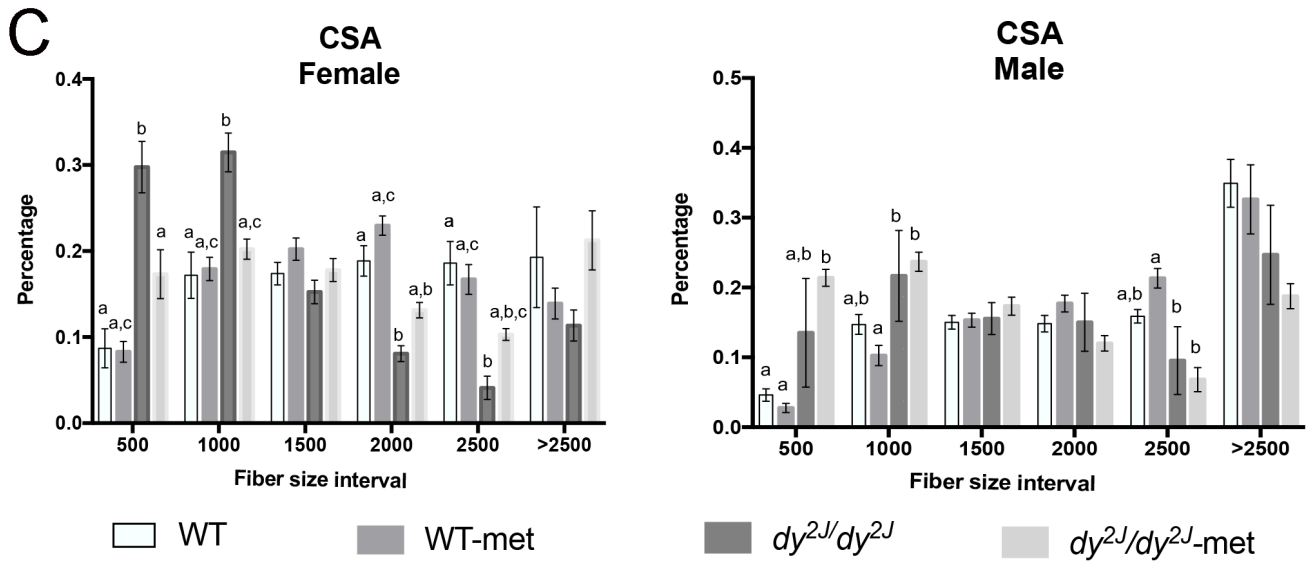
C
CSA
Female
Percentage
Fiber size interval
500
1000
1500
2000
2500
>2500
CSA
Male
Percentage
Fiber size interval
WT
WT-met
dy2J/dy2J
dy2J/dy2J-met

A

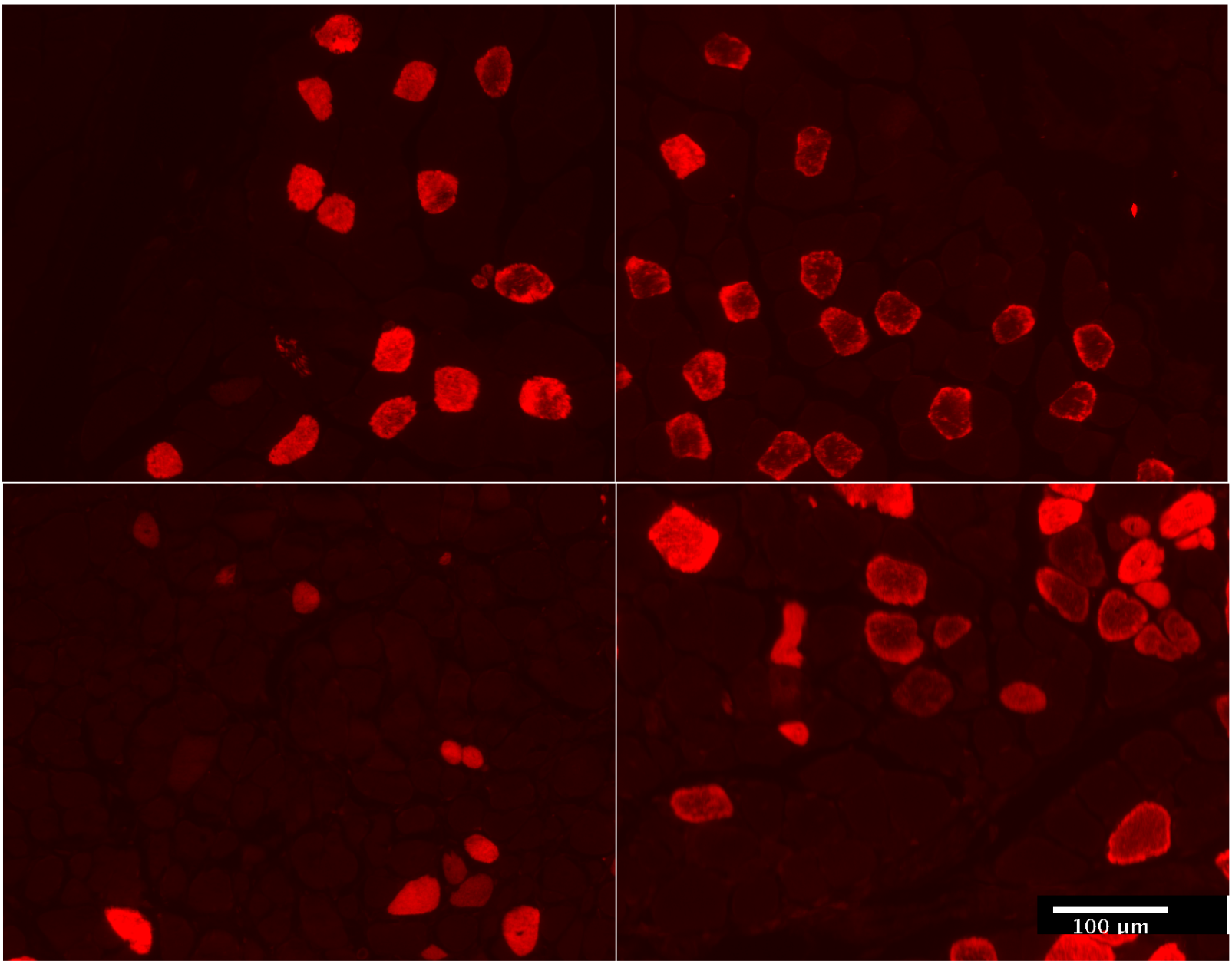
WT
WT-met
100 µm
dy2J/dy2J
dy2J/dy2J-met

B

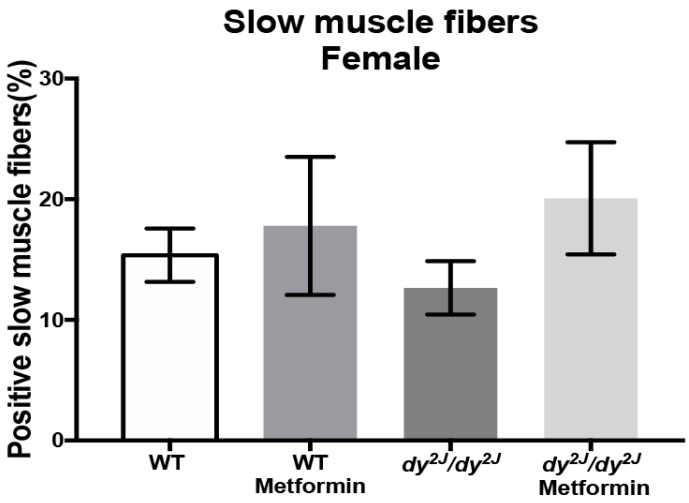
Slow muscle fibers
Female
Positive slow muscle fibers(%)
0
10
20
30
WT
WT Metformin
dy2J/dy2J
dy2J/dy2J Metformin

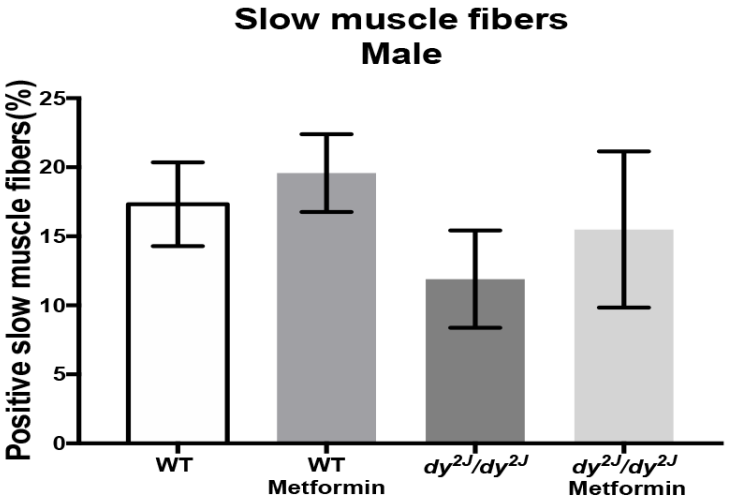
Slow muscle fibers
Male
Positive slow muscle fibers(%)
0
5
10
15
20
25
WT
WT Metformin
dy2J/dy2J
dy2J/dy2J Metformin

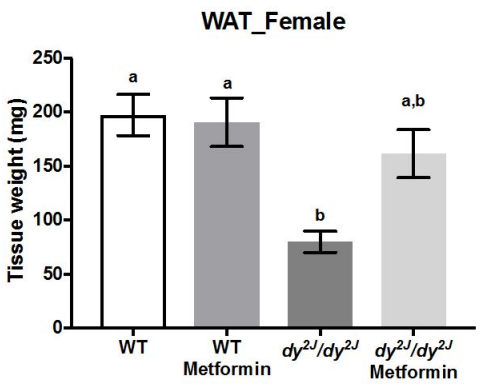
WAT_Female
Tissue weight (mg)
250
200
150
100
50
0
a
a
b
a,b
WT
WT Metformin
dy2J/dy2J
dy2J/dy2J Metformin

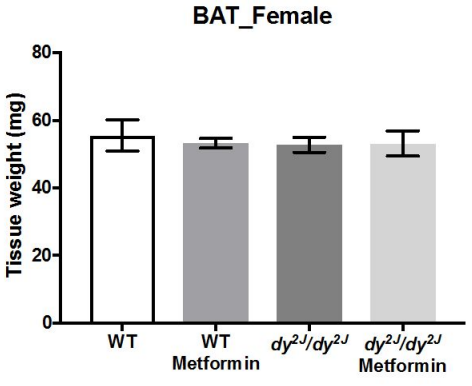
BAT_Female
Tissue weight (mg)
80
60
40
20
0
WT
WT Metformin
dy2J/dy2J
dy2J/dy2J Metformin

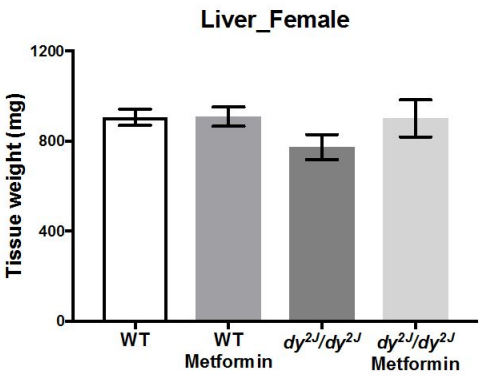
Liver_Female
Tissue weight (mg)
1200
800
400
0
WT
WT Metformin
dy2J/dy2J
dy2J/dy2J Metformin

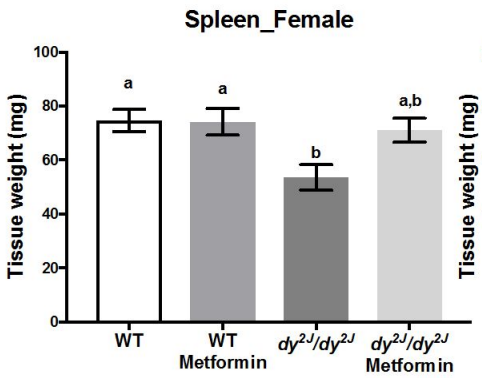
Spleen_Female
Tissue weight (mg)
100
80
60
40
20
0
a
a
b
a,b
WT
WT Metformin
dy2J/dy2J
dy2J/dy2J Metformin

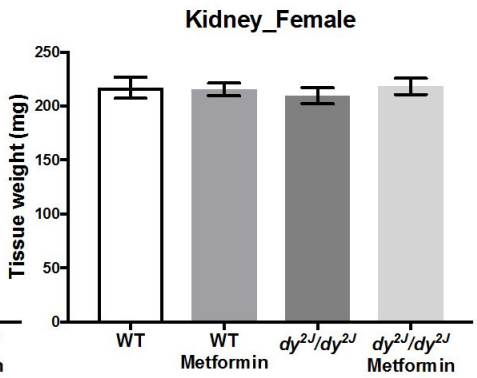
Kidney_Female
Tissue weight (mg)
250
200
150
100
50
0
WT
WT Metformin
dy2J/dy2J
dy2J/dy2J Metformin

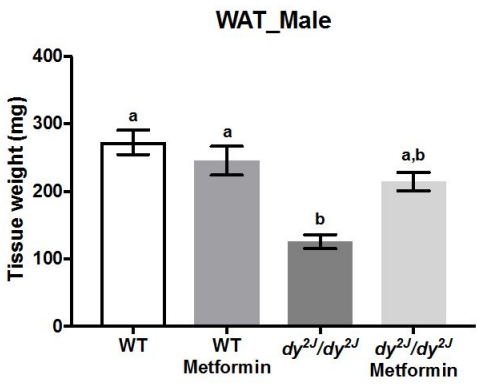
WAT_Male
Tissue weight (mg)
400
300
200
100
0
a
a
b
a,b
WT
WT Metformin
dy2J/dy2J
dy2J/dy2J Metformin

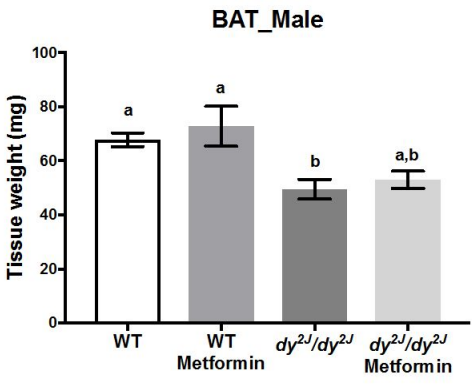
BAT_Male
Tissue weight (mg)
100
80
60
40
20
0
a
a
b
a,b
WT
WT Metformin
dy2J/dy2J
dy2J/dy2J Metformin

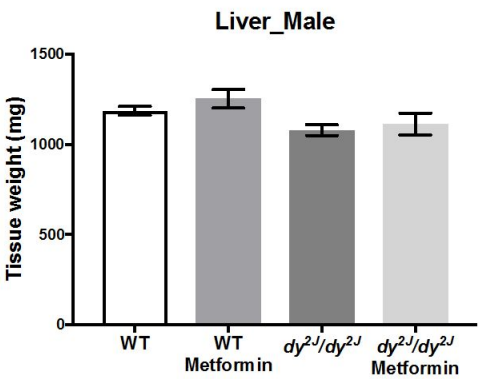
Liver_Male
Tissue weight (mg)
1500
1000
500
0
WT
WT Metformin
dy2J/dy2J
dy2J/dy2J Metformin

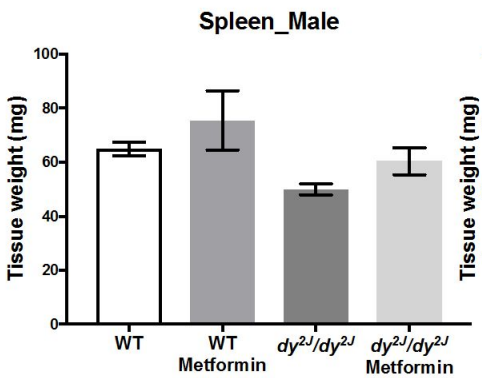
Spleen_Male
Tissue weight (mg)
100
80
60
40
20
0
WT
WT Metformin
dy2J/dy2J
dy2J/dy2J Metformin

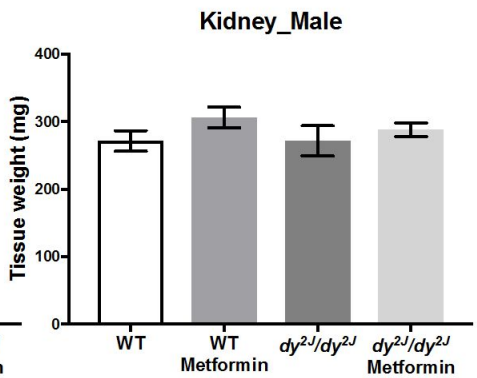
Kidney_Male
Tissue weight (mg)
400
300
200
100
0
WT
WT Metformin
dy2J/dy2J
dy2J/dy2J Metformin